Navigational Assistance for Visually Impaired Shoppers (NAVIS)
Group 10 - Spring 2025 / Summer 2025

Review Committee:
Dr. Mike Borowczak - *Associate Professor, UCF ECE*
Dr. Stephen Eikenberry - *Professor, UCF CREOL*
Dr. Justin Phelps - *Post doctorate Researcher, UCF ECE*

Advisors:
Dr. ChungYong Chan
Dr. Aravinda Kar

Group Members:
Matias Barzallo - *BSPSE*
Michael Castiglia - *BSCpE (VLSI Digital Circuits Track)*
Aden McKinney - *BSCpE (Comprehensive Track)*
Pavan Senthil - *BSEE (Comprehensive Track), BSBS (Neuroscience Track)*

UCF Electrical and Computer Engineering
UNIVERSITY OF CENTRAL FLORIDA

UCF CREOL, The College of Optics and Photonics
UNIVERSITY OF CENTRAL FLORIDA

Contents

List of Figures

List of Tables

Chapter 1 Executive Summary

It is estimated that at least 2.2 billion people globally suffer from a visual impairment. While the vast majority of these people can have their vision corrected using artificial lenses such as contacts and glasses, there are many that have such poor vision that these techniques are not largely successful. Many health problems, including but not limited to those caused by poor vision, negatively affect the person's freedom to pursue daily activities that many take for granted to a substantial degree. One of these tasks is that of grocery shopping. The VIRAS project aims to assist those with about a 3 foot / 1 meter effective visual acuity and return much of their ability to shop for grocieries without assistance from other people. While in the past few years there have been a great increase in grocery delivery services, allowing the user to gain freedom and independence, while having a small amount of physical activity may be able to increase their quality of life. The VIRAS project prototype is developed and assembled entirely by a group of one Electrical Engineering one Photonics Science and Engineering, and two Computer Engineering students at the University of Central Florida's College of Engineering and Computer Science. As such, this project is split into two main systems which are then integrated together: optical and electrical.

The optical system contains an active stereo vision system. This system is comprised of the emission system where the output of an 850nm pigtailed laser diode is split through a FBT splitter and then collimated and transmitted through a diffractive optical element, transforming the beam of light into a grid-like structure of light. This grid-like structure is captured by both cameras where the disparity of the position of structured light in the sensors is calculated in order to get a depth map allowing the operator to be notified of objects in front of the shopping cart.

The electrical system contains the power supply and distribution for all of the components in both systems. In addition, it includes necessary input and output peripheral equipment along with a microcontroller, all of which communicate with each other. Finally, the system contains a single board computer which is running the mapping and navigational algorithms, utilizing the peripherals, including the cameras as inputs provided by the optical system, to make decisions about where to instruct the user to move next.

This document is the record of the complete project design process, including more detailed reasoning behind the project, research for all design theories and technologies to be used, and further moving onto parts / software selection, and finally the design and implementation of the prior selected components. Additionally, there is supporting administrative processes throughout the document.

Chapter 2 Project Description

2.1 Project Background and Motivation

The World Health Organization estimates that at least 2.2 billion people globally are affected by some type of visual impairment [1]. While a large percent of these impairments is due to refractive errors, which can be corrected by visual aids such as glasses and contact lenses, a portion is also uncorrectable by glasses, medicine, or surgery [2, 3]. The National Institute of Health categorizes these impairments as 'low vision' [4]. Low vision is commonly caused by visual disorders such as age-related macular degeneration, cataracts, diabetic retinopathy, and glaucoma, with many of these disorders being linked to aging [4]. In the United States, the Centers for Disease Control and Prevention predicts that the number of low vision individuals over the age of 40 will more than double by 2050 from 2012's estimate of 4.2 million, largely due to America's aging population [3, 5]. 3% of children under the age of 18 in America also experience low vision even with wearable visual aids [3].

There are several ways to categorize the range of visual acuity for individuals with low vision; for the purposes of this project, we are focusing on individuals with visual acuity ranging from 6/18 to 3/60, as defined by the International Classification of Diseases [6]. Comfortable vision within this range is between one to six meters with potential challenges in central vision, peripheral vision, and light perception [6]. On the more severe end of this range, objects or signs beyond an arm's length away may be difficult to perceive or recognize. This introduces challenges in activities of daily living, necessitating assistance from a caregiver in order to complete many tasks. While caregivers offer valuable support, the need for constant assistance may diminish autonomy and impact quality of life by reducing an individual's independence.

The aim of this project is to improve on current assistive technology to promote autonomy of individuals with low vision by creating a portable device tailored to help independently navigate grocery stores. More specifically, this device will guide them to within half a meter of requested items and offer directions and object avoidance along their path. By reducing the need for caregiver assistance for this instrumental activity of daily living, we hope to foster greater self-sufficiency and empowerment, enhancing quality of life and supporting the autonomy of individuals with low vision.

2.2 Current Commercial Technologies and Existing Projects

2.2.1 VIRAS: Visually Impaired Robot-Assisted Shopping

The VIRAS project was developed by the Institute for Lab Automation and Mechatronics (ILT) at the Eastern Switzerland University of Applied Sciences with the goal of aiding blind and visually impaired individuals with grocery shopping [7]. The device is comprised of the entire shopping cart, which has a navigation system composed of a stereo camera for 3D mapping the store environment and mapping the user's hand for more precise object location [7]. The system takes in speech input from the user to generate the item list and provides audio instructions to direct the user's hand when they attempt to make contact with the object [7]. AI-based object detection is used along with the stereo camera to determine the identity of objects rather than requiring users to scan barcodes [7]. The cart is motorized and self-driving, which allows it to guide the user to the object location and checkout.

This technology has the same goal of improving user autonomy and minimizing caretaker dependency in the use case of grocery shopping. This technology is not only meant for users with low vision but can also be used by those with more severe visual impairments and even certain mobility issues. However, the system comprises of the entire shopping cart, which requires the stores to already have these devices in place. Our project aims to create a similar system but make the device portable, so that the user may be able to use it in stores that do not already have this device in place.

2.2.2 The Augmented Cane

The Augmented Cane is a similar assistive device which builds on the traditional white cane to enhance independence and mobility for individuals with visual impairments [8]. It integrates information from multiple added sensors, including LiDAR, a camera, GPS, and IMU to aid users with environment navigation both indoor and outdoor [8]. A microcontroller processes the sensor information to plan navigational routes and provide real-time feedback to the user through audio instructions, steering assistance, and kinesthetic haptic feedback from the ground to the user's hand [8]. An omni-wheel at the base of the cane supplements the user's movement by providing additional steering in the case of avoiding certain objects or making navigational changes [8].

This device facilitates several tasks that may be more difficult with just a traditional white cane. It improves walking speed for individuals with visual impairments through its motorized guidance system, and it serves to effectively map the user's surroundings through camera-based object detection and LiDAR and GPS-based localization to promote more confident navigation [8]. Our project's scope aims to translate some of the successes of this project to the more specific application of grocery shopping. Although compared to the VIRAS project this device is much more portable by the user and can be applied in several locations, it may be difficult to maneuver a traditional shopping cart in tandem with the Augmented Cane; therefore, our device addresses both portability and usability within a grocery store environment compared to the Augmented Cane.

2.2.3 Summary

Existing assistive devices for individuals with visual impairments have made significant progress in augmenting existing technology to enhance the user's confidence in navigating their environment, which by extension supports their autonomy in performing several tasks. Two examples of these devices, the VIRAS project and the Augmented Cane, both employ several sensors to improve on a shopping cart and white cane, respectively, to map the users environment and provide valuable information to the user to allow them to navigate their surroundings [7, 8].

Our developed device addresses the gap of a user-portable navigation-assistive device specific for streamlining shopping for individuals with low vision. It draws on several hardware and software features of both the aforementioned projects, including Depth camera sensing and IMU for mapping, a camera for object detection, and audio and haptic cues for feedback. Our device also aims to minimize cost in comparison to the two devices to make the technology more accessible; the VIRAS project requires stores to already have several of these shopping carts available for users, and the Augmented Cane has a total component cost of $400.

2.3 Goals and Objectives

This project's aim is to build a portable and mountable supplement for a shopping cart to aid individuals with visual impairments navigate stores and reach within 0.5 meter of the requested item.

Basic Goals

- Create a portable navigation device that users can mount onto a shopping cart
- Guide visually impaired users to within 0.5 meter of the items in the users shopping list
- Detect obstacles in front of the shopping cart to warn users of potential collisions

Advanced Goals

- Create an optimized route through the grocery store after the user provides the item list
- Assist users with locating the position of the object on the shelf
- Incorporate additional feedback systems to avoid collisions with other shoppers, walls, and obstacles

Stretch Goals

- Extend application to more severe visual impairments (total blindness)
- Expand to other locations (different store types such as libraries, hardware stores, etc.)

- Modulate IR depth camera system in order to be unaffected by different sources of IR

The basic, advanced, and stretch goals are further elaborated into their respective objectives.

Basic Objectives

- Design a lightweight mounting system that is simple to setup and teardown
- Integrate a rechargeable power source with sufficient battery life for the average shopping trip
- Recognize text inputs from the user through a user interface to create the item list
- Determine item locations using a store database with detailed inventory information
- Assess cart speed and direction with Inertial Measurement Unit (IMU) data
- Detect obstacles within a few meters with IR depth camera system
- Provide directions through audio commands

Advanced Objectives

- Path plan based on localization estimates and user inputted item list to calculate an efficient path through the store
- Include haptic cues in addition to audio commands for guidance and collision avoidance in noisy environments or for individuals with hearing impairments
- Build and incorporate an IR depth camera system capable of at least 100° of field of view (FOV) and 2 meters of object detection

Stretch Objectives

- Integrate a camera to identify and indicate shelf level upon reaching the requested object
- Incorporate real-time updates if users change the item list or obstacles require route changes
- Train a speech-to-text algorithm to recognizes verbal user input to generate the shopping list
- Track the user's hand position with a camera when attempting to grab an object and provide additional precise audio commands to direct the user
- Expand the store map database to support multiple locations and integrate with external mapping APIs
- Test the system in diverse lighting conditions to ensure the optical Citation & Abstract system can filter out other interferences

2.3.1 Hardware

2.3.1.1 Hardware for Basic and Advanced Goals

The primary hardware components for navigation and object avoidance include an IMU, an IR depth camera system, and a microcontroller for data processing. The IMU tracks the cart's speed and direction, allowing the system to understand its movement and adjust guidance accordingly. The active stereo system uses emission of IR constructed light and IR cameras to measure depth with a FOV of 100° and a longitudinal range of 2 meters in front of the cart which is essential for detecting objects in real time, whether those be walls, aisles, other shoppers, or obstacles or warnings such as displays or wet floor signs. This system serves to scan the path ahead outside the user's comfortable visual range and send signals to the microcontroller to process the data for distance. The system utilizes constructed light with the aid of diffractive optical elements (DOE) to emit a series of evenly spaced vertical and horizontal lines which are then detected by an IR camera with a similar FOV to the emission system and later calculate the disparity between the structure observed by the two cameras, where a greater disparity between features (the lines of light) indicate a shorter depth. The gathered data is processed to construct an environment map, which aids in detecting the user's position relative to their surroundings. This data is translated into cues for the users, signaled by audio through onboard speakers and haptic motors placed along the shopping cart's handlebars. The cues provide directional information to the user along with warnings and alerts to stop the cart in the event of an obstacle to ensure safe navigation through the store.

The item requests are handled by the app subsystem, which integrates user text input for the items list with a touchscreen device, such as a smartphone or tablet. The device processes inputs with an onboard computer containing the store's inventory database to determine the order of navigation for the listed items and the necessary directional cues to reach each item.

To ensure that the device is portable and easy to setup and takedown, power will be supplied through rechargeable LiPo batteries capable of powering for the duration of an average shopping session. Overall, the combined hardware setup, featuring the camera, depth camera, IMU, microcontroller, single-board computer, and app interface, ensures that the user is able to request items to shop and receive cues to safely navigate within range to those items.

2.3.1.2 Hardware for Stretch Goals

The primary stretch goal condition is to expand the system to individuals with more severe forms of visual impairments, including total blindness. This requires more robust navigation and object identification abilities. Some applications of this more advanced system include voice-recognition hardware for the user item input for individuals who may not be able to type to input this information. The optical subsystem would also undergo improvements to guide users to a more precise range within the object. This includes a active stereo vision system with a higher FOV and a detector with higher resolution to increase detection ranges and be able to detect objects with a higher resolution.

2.3.2 Software

2.3.2.1 Software for Basic and Advanced Goals

The software system is divided into various modules to support navigation, object detection, and user interaction. The user interface operates to take the text inputs from the user to generate the grocery list. The list order is determined through communication with the store's database for item location, which allows the items to be categorized by sections of the store to optimize the path the user would take to reach all requested items. This information is communicated to the navigation module to provide real-time navigational cues to the user.

The navigation module is comprised of a simultaneous localization and mapping (SLAM) algorithm fusing the incoming data streams from the IMU, active stereo vision system to determine the user's position in the grocery store and gather information about the surrounding environment. This data, along with the item list from the user interface module, is used to direct the user to items on the list in sequence. Continuous localization allows the system to adjust the planned route dynamically based on the user's movement and any objects and obstacles the active stereo vision system detect. This information is conveyed to the user through the audio cues, which provide details about which direction to move or turn and when to stop, along with haptic feedback which acts as secondary cues to indicate turns and alert the user of obstacles.

For object detection, the camera scans the shelves once the user is within range of the requested item; the captured information is processed to confirm the user has been brough to the requested object and determine its relative location, which is communicated to the user through audio cues to indicate the shelf direction the object can be found in.

To summarize, the workflow begins with the user inputting their grocery list into the app, which maps and categorizes the items using the store's inventory database. The navigation module generates an optimized route and tracks the cart's movement through the fused sensor information. As the cart navigates to waypoints within 0.5 meter of the requested item, directional information and item confirmation is communicated to the user, which obstacle alerts also provided if needed. Once all items in the list have been collected, the system guides the user to checkout and exit the store.

2.3.2.2 Software for Stretch Goals

Similar to the hardware improvements for the stretch goals, the software application requires more robust processing of sensor information to support use of this device with more severe forms of visual impairments. The optic subsystem camera would need to recognize the user's hand while the user is attempting to locate the object and provide additional audio cues to guide the user's hand to the object. For user list inputs, the app would also need to process audio input from the user to accurately identify the item being listed.

2.4 System Diagrams

Figure 2.1: Hardware Block Diagram

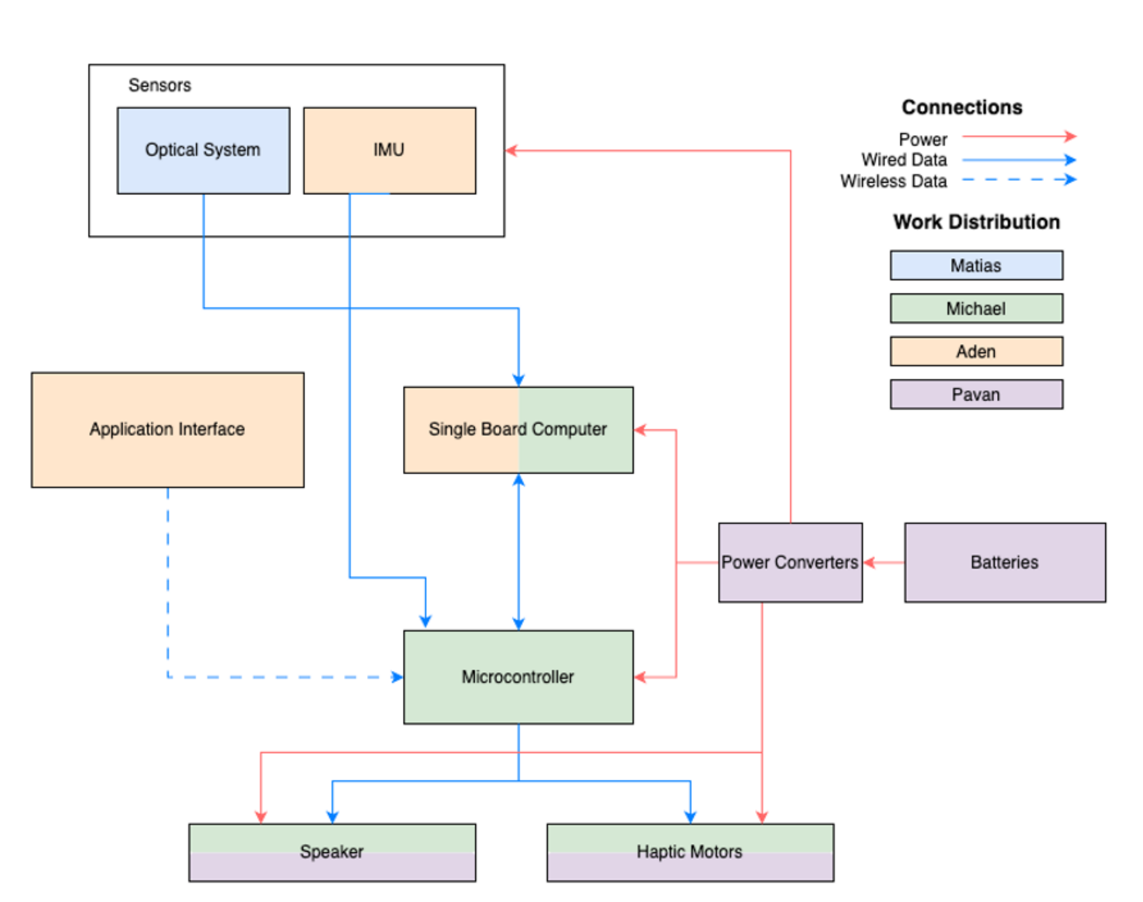

The hardware generally consists of a set of computers connected to various sensors and outside devices for input along with user feedback devices as output. Power will also be an input into the system with the voltages changed as necessary for each system component with the use of boost and buck converts. The sensors used as inputs will consist of an IMU for general location information as well as an IR depth camera system for more localized guidance. A mobile application or similar will be used for the user to input their desired grocery list. On the other hand, haptics and speaker/voice outputs will be used to guide the user throughout the store.

The general placement of the various components and subsystems on the shopping cart is displayed below in Figure 2.2.

Figure 2.2: Hardware Mockup

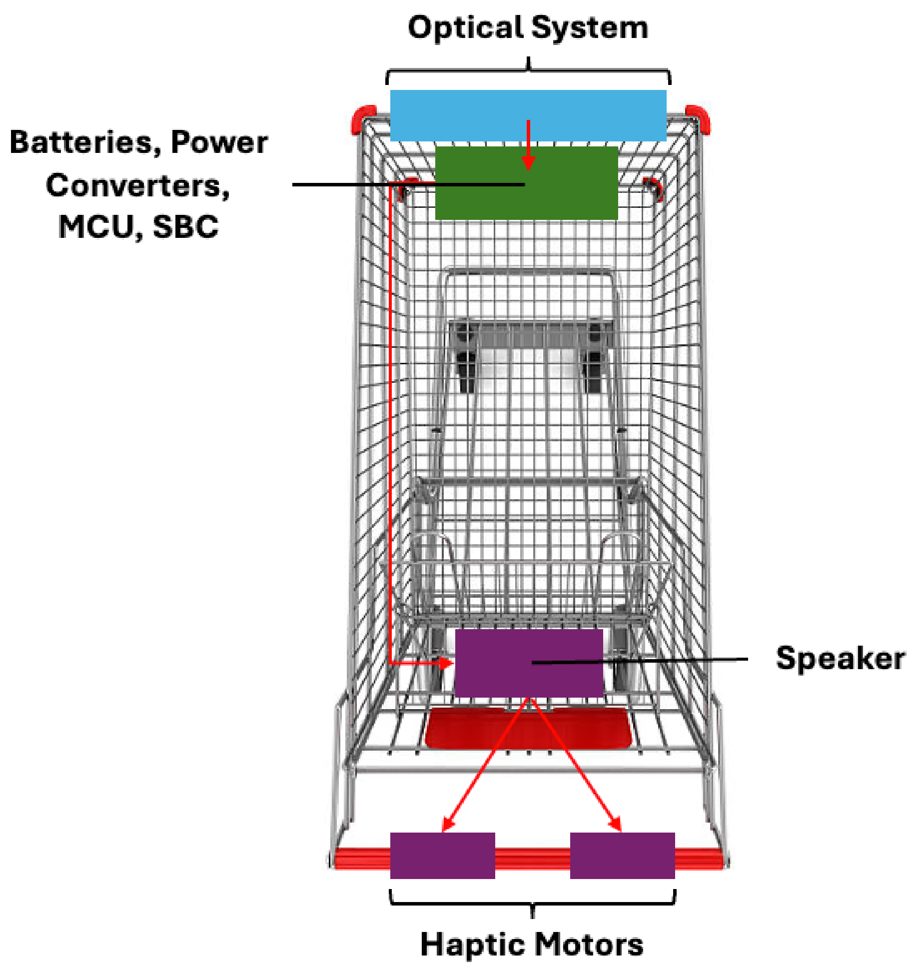

Figure 2.3 below demonstrates the software workflow involving the sensors, logic boards, and output devices.

Figure 2.3: Navigation Software Flowchart

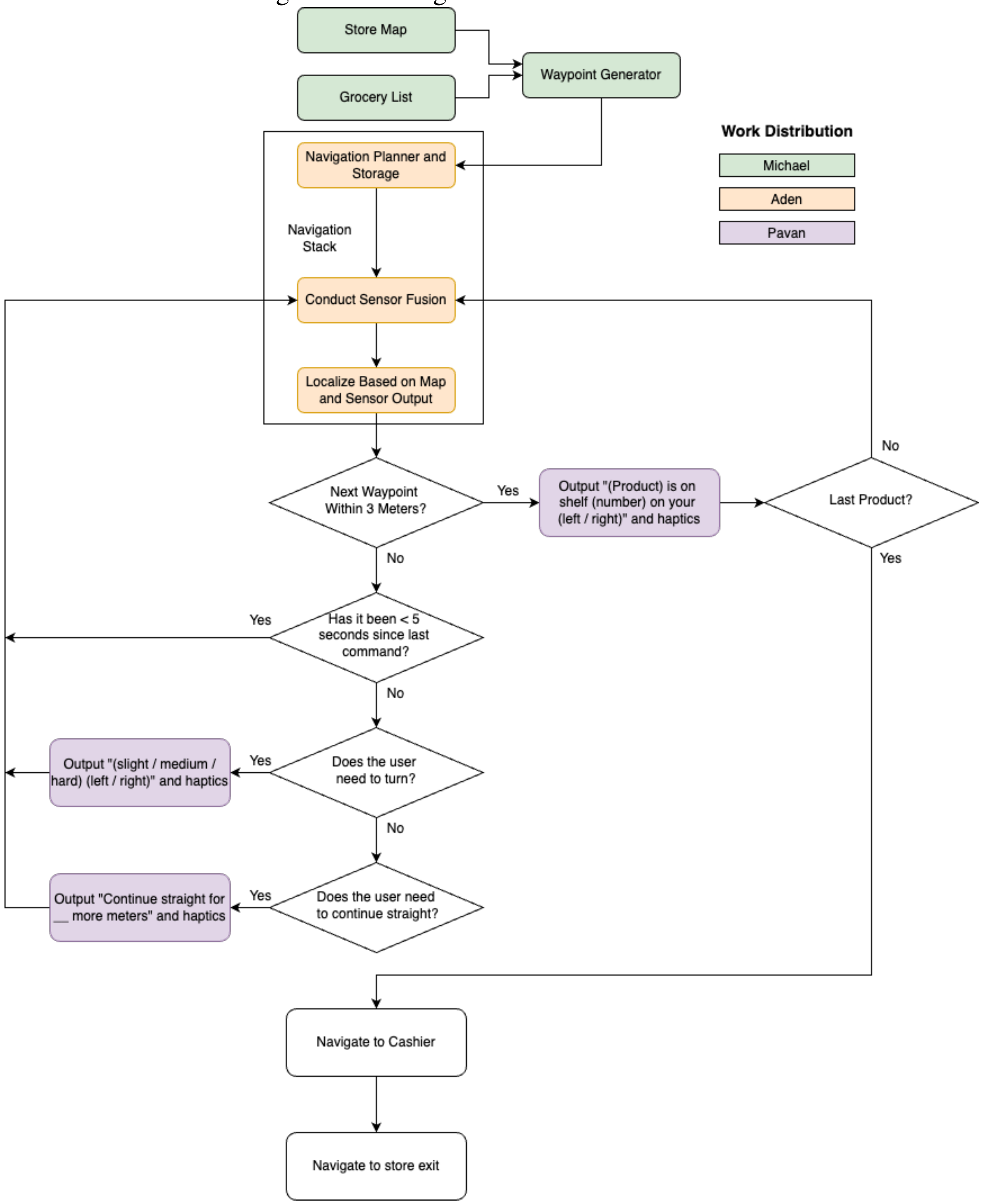

Figure 2.4: Optical Emission Hardware Diagram

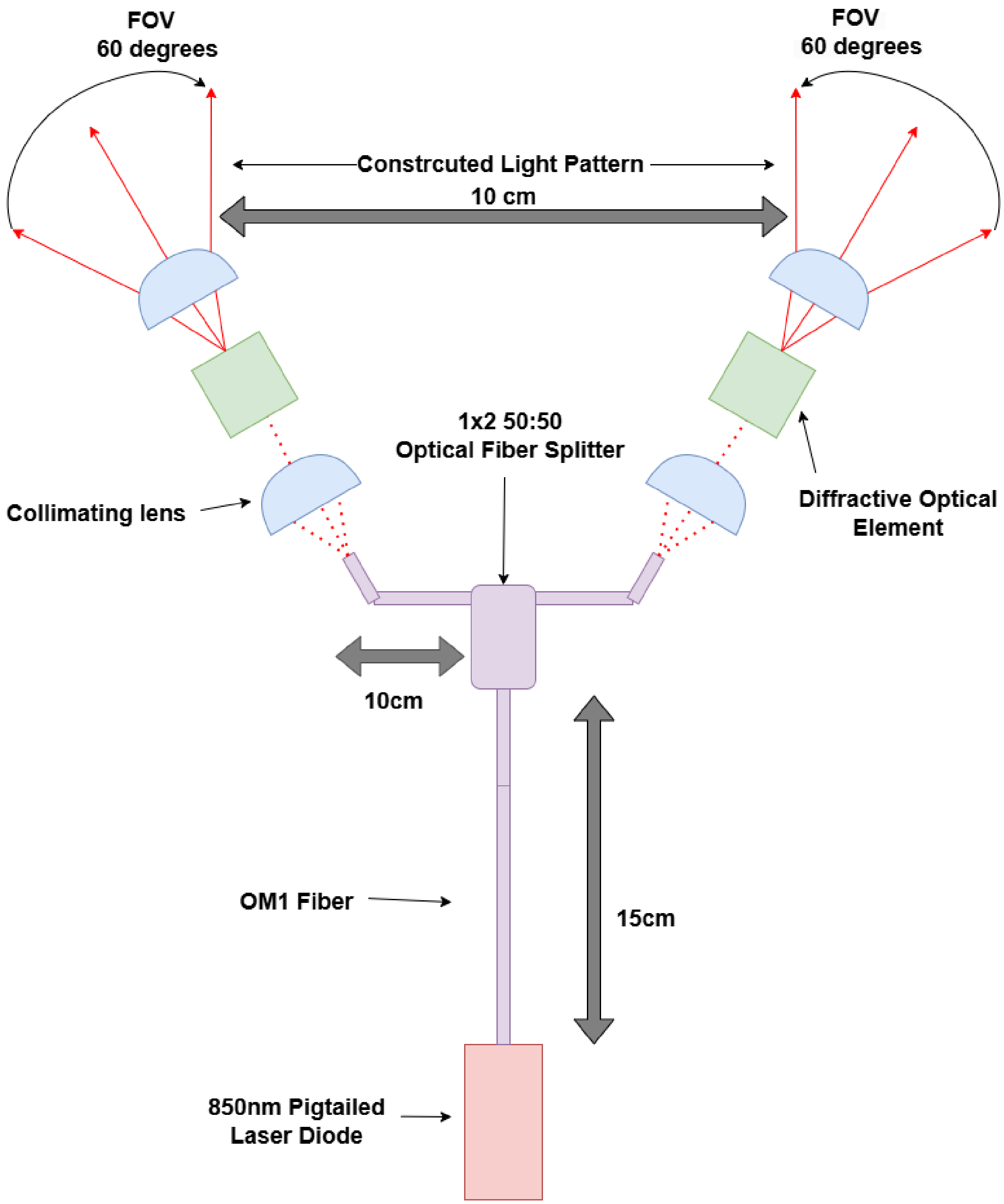

The optical emission hardware flowchart in Figure 2.4 consists of the emission of the constructed IR light (850nm). The light emitted from a pigtailed FP-LD is split into two with an FBT fiber splitter. Afterward, two identical optical systems collimate the light into a diffractive optical element, which shapes the light to create a grid of vertical and horizontal lines of light, and the following lens further diverges the constructed light to increase the FOV.

Figure 2.5: Optical Detection Hardware Diagram

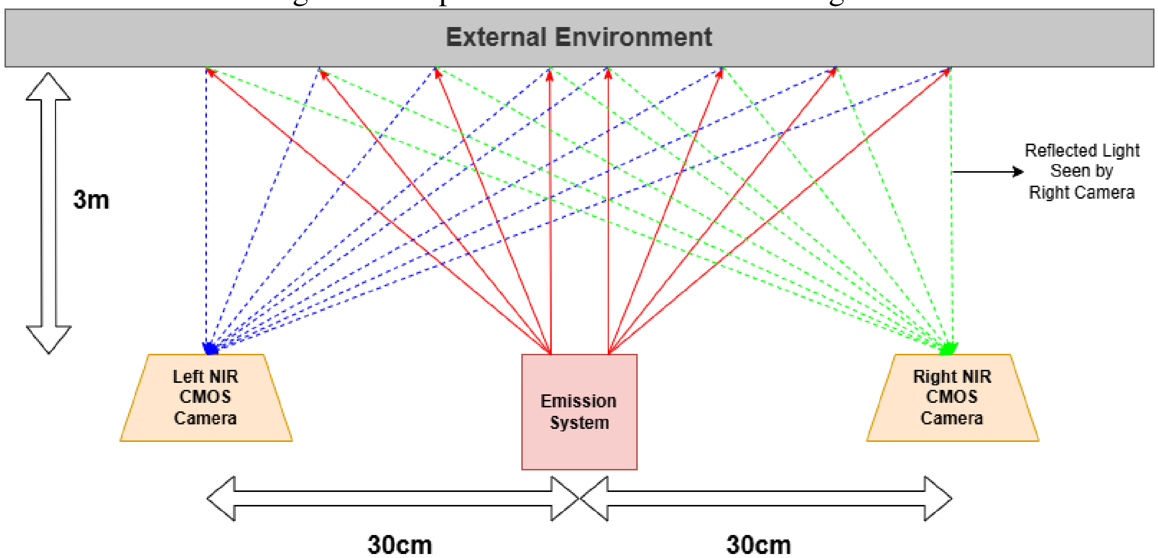

The optical detection hardware flowchart in figure 2.5 consists of two NIR CMOS camera modules at each side of the emission system with a baseline of 30cm. These two cameras capture the reflected structured light that interacts with the environment. This allows us to calculate the disparity between the lines, and transform this into depth calculations.

2.5 Required Specifications

The specifications of the overall system are listed in the below Table 2.1. Specifications for demonstration are highlighted. These specifications include the minimum distance from the requested object the user will be guided to, the success rate of how many of the requested objects the system efficiently navigates to, and the collision avoidance latency.

Table 2.1: Overall Specifications

Specification	Description	Target Value and Unit(s)
Distance User Guided from Product	Users must be brought to an object so that the object is in their conformable visual range, where they can identify and pick it. Audio and haptic cues will indicate to the user when they have successfully reached the target object.	Within 0.5 meter
Success Rate	The device must accurately bring users to the requested object within the specified range.	At least 90%
Collision Avoidance Latency	The object detection and avoidance system must accurately detect objects and obstacles within range and indicate them to the user in a time frame that allows them to react appropriately.	300 ms
Size	The dimensions of the portable device must be able to comfortably fit in a standard shopping cart.	Approx. 50x50x30 cm3
Weight	The device must be reasonable to carry around and not interfere with the ability to maneuver the shopping cart.	2.5 - 5 lbs
Battery Life	Use of the device must last for the duration of the shopping trip, around an hour.	At least 1 hour
Connectivity	The delay between the sensors and the cues to the users must be short enough to provide effective navigational instructions and warn users in time to avoid collisions.	Within 100 ms
Setup/Teardown Time	The portable device must be fairly easy to mount and remove from the shopping cart.	Within 2 minutes

Similarly, the below Table 2.2 includes the required specifications for some of the key components of the system, largely for the optical subsystem responsible for navigation and object detection, and Table 2.3 contains the engineering requirement specifications.

Table 2.2: Optical Subsystem Component Requirements

Component	Parameter	Specification	Unit
Pigtailed Laser Diode	a) Optical Power b) Wavelength c) Operating current d) Operating Voltage f) Fiber type	a) 140 b) 850 c) 286 d) 2.4 e) Multimode	a) mW b) nm c) mA d) V
Optical Fiber	a) V number at 850nm b) Attenuation	a) 36 b) 3.5	b)dB/km
Fiber Splitter	a) Splitting ratio b) Port Configuration c) Fiber Mode Type at 850nm d) Operating wavelength e) Excess Loss f) Splitting Ratio Accuracy	a) 50:50 b) 1x2 or 2x2 c) Multimode d) 850 e) 0.35 f) $\sim\pm7$	d) nm e) dB f) %
Collimating Lens	a) Focal Length b) Diameter c) Coating	a) 5 b) 3 c) AR	a) mm b) mm
DOE	a) FOV (V x H) b) Diffraction Pattern c) Pattern Density	a) >40 x 40 b) Grid c) >50 x 50 lines	a) Degrees
Camera Sensor Module	a) QE at 850nm b) SNR c) Resolution d) Dynamic Range e) FOV (V x H)	a) 50 b) 20 c) 1920 x 1080 d) 70 e) >50 x 50	a) dB b) dB d) dB e) Degrees

Table 2.3: Engineering Requirement Specifications

Component	Parameter	Subsystem and Description	Target Value and Unit(s)
App Display Screen	Output Quality	App - The app display must be at least standard resolution for the user to interact with it and input the item list.	480 pixels - 720 pixels
IR Camera Sensor	Range	Optical - The IR camera sensor must be able to provide object and navigational information in the range beyond the user's comfortable visual range.	1 - 6 meters
IR Cameras	Camera System Field of View	Optical - The IR camera system sensor must be able to gather signal information from a large enough field of view to ensure sufficient object information to the user.	At least 100°
IR Emitter	Field of View	Optical - The IR camera system sensor must be able to gather signal information from a large enough field of view to ensure sufficient object information to the user.	At least 100°
Haptic Motors	Signal Discretion	Electrical - The vibrational motor must be capable of delivering a variety of signals that the user can easily distinguish between.	3+ distinct vibration patterns
Speaker	Output Volume	Electrical - The speaker must deliver audible cues and alerts that can be easily heard in a grocery store environment.	At least 60dB SPL at 0.5m

Figure 2.6: House of Quality

Correlations	
Positive	+
Negative	−
No Correlation	o

Relationships	
Strongly Positive	↑↑
Weakly Positive	↑
No Relation	○
Weakly Negative	↓
Strongly Negative	↓↓

Direction of Improvement	
High	▲
Low	▼

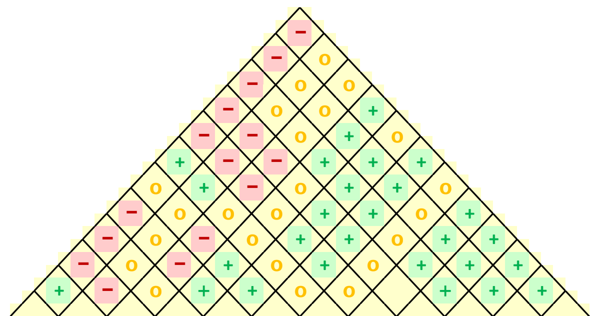

Column #		1	2	3	4	5	6	7	8	9	10	11	12
Functional Requirements / Customer Requirements (Explicit and Implicit)	Direction of Desirability	Size	Weight	Battery Life	Connectivity	Object Avoidance Distance	Distance User Guided from Product	Setup/Teardown Time	Depth Sensing Range	Depth Camera Field of View	Output Quality	Success Rate	Collision Avoidance Success
Direction of Desirability		▼	▼	▲	▲	▲	▼	▼	▲	▲	▲	▲	▲
Affordability	▲	↓	↓	↓↓	↓↓	↓↓	↑↑	↑↑	↓↓	↓↓	↓↓	↓↓	↓↓
Technical Portability	▲	↓↓	↓↓	↓↓	↓	↓↓	↑	↓	↓↓	↓↓	↓↓	↓↓	↓↓
Ease of Use	▲	↓	↓↓	↓	↑↑	↑↑	↓↓	↓	↑↑	↑↑	↑↑	↑↑	↑↑
Reliability	▲	○	○	↓	↑↑	↑↑	↓↓	↓↓	↑↑	↑↑	↑↑	↑↑	↑↑
Store Compatability	▲	○	○	○	↑↑	↑	↑	○	↑	↑	↑	↑	↑↑
Ease of Maintenance	▲	↑	↓	↓	↑	○	○	↑	↓	↓	○	○	○
Multi-Person Use	▲	○	○	↑	↑	↑	↓	↑	○	○	↑	↑	○
Remote Use	▲	○	○	↑	↑↑	↓	○	○	○	○	↑	↑	○
Efficient Routings	▲	↑	○	○	↑	○	○	○	○	○	↑↑	↑↑	↑↑
Avoid Obstacles	▲	○	○	○	↑	↑↑	↓↓	↓	↑↑	↑↑	↑↑	↑↑	↑↑
Target		Approx. 50x50x30 cm3	2.5 lbs - 5 lbs	At least 1 hour	Within 100 ms	Up to 2 meters	Within 1 meter	Within 2 minutes	1 - 6 meters	At least 60 degrees	480 p - 720 p	At least 90%	Within 10 minutes per item

Since the system is mounted directly to the grocery cart, this limits the importance of certain specifications of the overall cart, including those of weight and size, as they do not severely limit the usability of the system. On the other hand, it's incredibly important to achieve the greatest possible success rate, along with a good route planning algorithm and a reasonable object avoidance distance (the latter mostly determined by the IR camera depth system). This is because the reliability of the system is of the upmost importance and comes first before the vast majority of the other goals and objectives for the project as a whole. While we should strive to improve all of the measured specifications to the greatest extent possible but the reliability and performance of the system should come first before the others.

Chapter 3 Research

3.1 Optical Hardware Technologies

3.1.1 Depth Measuring System Technology

Accurate depth measurement is very important for object detection and for navigation. Therefore, various depth-measuring technologies will be compared in order to choose the technology that best fits the use case of this project. The depth sensing technologies discussed will be, passive stereo vision (PSV), active stereo vision (ASV), structured light depth sensing, sonar, and LiDAR. Each technology will be evaluated in its depth resolution (smallest depth difference distinguished between two objects), depth accuracy (absolute error on estimated depth of object), environmental constraints, reliability, feasibility, and cost-effectiveness.

Passive Stereo stereo vision consists of two spatially separated cameras that calculate depth based on the binocular disparity of a point or object in both cameras. The depth resolution of this method is influenced mainly by the camera's pixel density, focal length, baseline distance (the distance that separates the cameras), and the distance to the objects being detected [9]. The depth accuracy of a passive stereo system is mainly affected by calibration errors, noise, and lens distortion, which cause larger disparity errors. Additionally, as the distance to the detected object increases, disparity values become smaller, making the system more sensitive to disparity errors, leading to a larger absolute error in depth estimation. Environmental constraints of PSV include highly reflective surfaces and occlusion of one or both cameras, which affect depth estimation. For our project, the reliability of a passive stereo system would depend on how consistently and accurately it can estimate depth in a supermarket setting. Factors such as featureless surfaces, high reflections or occlusion of a single camera's view would also decrease the reliability of the system. A PSV system is not physically complex to make; it only takes two identical cameras and some calibration to achieve high resolution and depth. But computationally, the device must identify and match different features in both images, to calculate depth through disparity estimation algorithms[10]. This can be computationally intense, especially in a moving and dynamic environment like a supermarket. The cost of this system, apart from the electrical hardware, would only be buying two identical cameras, and the price of these would change depending on their sensor resolution and their lens system, but for this application, average average off-the-shelf camera modules would work.

Active stereo vision system consists of two cameras and a NIR (commonly used but not restricted to to) structured light projector, the depth measurement is similar to the one of a

PSV, but in this case the device doesn't need to find features from where to calculate the disparity, instead the features are given by the projected light in the form of patterns which get shifted by the shape of the object [11]. The depth resolution of this system is dependent on the same variables as the PSV system, but in this case well-defined features from the projected light allow for finer depth differentiation, mainly in featureless objects. However, as distance increases, the density of the projected pattern decreases because the projected pattern expands over distance, reducing the feature density on the objects, which decreases despite precision. In the case of the depth accuracy, having the structure light reduces disparity error, however, the quality of the projected light pattern is propoertional to the error of disparity measurement, therefore a good quality pattern projector must be used to increase depth accuracy while not adding more disparity errors[12] [13]. The environmental constraints of an ASV system include obstruction of one or both cameras, obstruction of the projected light, but most importantly, ambient lighting depending on the wavelength of the projected light and the acceptance spectrum of the cameras. Therefore, NIR light projection and NIR cameras would decrease this environmental constraint, on top of modulating the light to discriminate between the desired NIR light from other NIR sources of light, such as phones or other obstacle detecting sensors[14] [15]. Surface reflectivity and absorption of NIR from different objects is also a concern since it might interfere with the projected lines reducing disparity accuracy. Reliability is increased since variables such as lighting, object's features and color don't take part anymore, rather, the ability to modulate the light, power of structured light and ability to create readable signals from reflection of NIR are the main concerns when it comes to the reliability of this system. The feasibility of a ASV system reduces in the sense that a high quality structured light projector must be added to the system, where more areas of errors and mistakes are introduced, but in the other hand computational power needed is greatly reduced since the system no longer needs to identify features on the objects [16]. The cost of the system is increased with the added projection of light. But the added cost and reduced feasibility do not outweigh the gained depth resolution/accuracy gained and the reduced computational power needed.

Structured light depth sensing is a technology that uses a singular camera and a singular light projector to calculate depth. This is done by shining a known pattern of light onto an object and from a known distance captures the deformation of this pattern with a camera, which is later used to calculate depth [17]. The depth resolution of this method is influenced mainly by the camera's pixel density focal length, the baseline distance (distance between the projector and the camera) and the distance to the objects being detected. All these variables affect the seen disparity between the known projected pattern to the captured shifter pattern. The depth accuracy of this system is based on the focal length, baseline distance, observed shift of the structured light and the disparity error [18]. The environmental constraints are similar to the one of the ASV system, where the projected light has to be in the NIR spectrum and also be modulated to distinguish it from other NIR sources. Obstruction of the camera and/or the projector would also interfere with depth measurements. Surface reflectivity and absorbance of NIR light also play a big role since it hinders the disparity accuracy and signal received at the sensor. The reliability of this system is increased in scenarios such as supermarkets, since it doesn't rely on the quality of ambient light, assuming the projected light is modulated. But on the other hand, the reliability of this system relies heavily on the quality of the projected light, since the design of the light pattern and the quality of the pattern itself play a big role in being able to accurately calculate the disparity with small error [19]. Although the computational power needed is not very high, the alignment and quality of the emission system (assuming a quality off-the-shelf camera is used) has to be very good since most of the systems resolution and accuracy depends on the quality of the projected light. This makes the system more expensive to build since a better light projector is needed to project a very high-quality light pattern, outweighing the fact that only one camera is needed.

Sonar is an acoustic based depth sensing technology that calculates depth based on the time for high frequency sound waves to travel from the emission to the reflecting object and back. The depth resolution of this technology relies on the pulse duration since a shorter pulse allows the system to better distinguish between two objects and different distances, as-well as the sampling rate of the receiver since with a low sampling rate two waves that traveled slightly different distances will seem to have traveled the same distance . The accuracy of a sonar's depth measurement is based on its ability to measure accurately the elapsed time from emission to detection of the sound wave [20]. This measurement can be affected by temperature variations that change the speed of sound waves through the air, as well as the calibration of the electronics, primarily the time-of-flight calculator. The environmental constrains for this system mainly rely on the aspects of the surface from which the sounds waves are reflecting; the sound waves need solid object to properly reflect from, but in a grocery store environment, one of the main things found is other shopping carts which are not solid but rather made of interconnected metal rods which don't have enough surface area to properly reflect sound-waves [21]. The reliability of the system depends on the accuracy of the emitter and receiver and the time-of-flight calculations, but also on the environment which we desire to do depth measurements, which we have acknowledge that is very hard for sound waves to reflect from mesh-like structures (shopping carts) therefore making the system reliable at detecting solid object like people, shelfs, boxes but no other shopping carts. Hardware and software wise, this system is very feasible since only a high frequency speaker and microphones are needed, moreover the clock speed of the receiver isn't high enough that high computing power is needed. Cost-wise, this system is very cost effective since no high-end devices are needed.

LiDAR systems work similarly to sonar; by sending pulses of light and calculating the time it takes for the emitted light to travel from emitter to object and reflect back to the receiver. The depth resolution of a system like this relies on the pulse duration and the clock speed of the receiver. Having shorter pulses provides the system with less overlapping between reflected pulses, making it easier for the detector to distinguish between these pulses. Secondly, the clock speed of the receiver means a higher sampling rate, which decreases timing uncertainty. The depth accuracy plays a big role in LiDAR since factor such as the sampling rate of the detector, signal-to-noise ratio (SNR) and detector response time. Heavily impact the reading of the system [22]. By using time of flight of light, any latency in the calculation of time might give results with a high error rate since light travels 1 meter in 3.33 nanoseconds. LiDAR is not greatly affected by the environment since it works on the IR spectrum. The main concern lies on the object from which the light is being reflected from, these objects might have very high or low reflectiveness, causing false depth readings. The reliability of the system greatly depends on the ability to sample faster than the time taken for the light to travel a distance of 0.5m to be able to detect objects

0.25 meters away from the shopping cart. This system would not be very feasible to make even with the existence of cheap LiDAR systems on the market because this application requires a mechanical LiDAR or Flash Lidar which creates a depth map over a large area [23]. Therefore, creating a LiDAR system of this sort would be very expensive due to the high end optical/electronic materials and devices needed to make a system with high depth resolution and accuracy.

Table 3.1: Depth Measuring System Technology Comparison

Depth Measuring Technology	**Depth Accuracy / Resolution**	**Environmental constrains**	**Reliability**	**Feasibility**	**Cost**
Active Stereo Vision	Medium-High - Depends on light projection / camera quality and baseline	Low-Medium - Sensitive to ambient NIR sources, occlusion and material reflectivity	High - struggles with low pattern density, no need for intense computing	Medium - relies on light projection, requires less computation	Medium-High
Passive Stereo Vision	Medium - depends on camera, baseline, disparity errors	Medium - sensitive to ambient lighting, reflections and occlusion	Medium - struggles with texture-less object, and relies on intensive computation	Medium - relies on intensive computation to find features on objects	Low
Structured light depth sensing	Medium-High - depends on light projection / camera quality and baseline	Medium - Sensitive to ambient NIR sources and material reflectivity	Medium -relies on a single point of view, and projector quality	Medium - requires higher light projection quality	Medium
Sonar	Low-Medium - depends on pulse duration, sampling rate and speed of sounds variations	High - sensitive to non-solid objects	Low - unreliable for not solid objects	High - simple hardware and computation	Low
LiDAR	Very High - dependent on accurate time of flight measurements and pulse width	Low - sensitive to object reflectivity	High - reliable if component quality and sampling rate is high	Low - relies on complex materials and components	Very High

After evaluating the various depth-sensing technologies, we determined that ASV is the most suitable choice for this project. While standard PSV is a more feasible and cost-effective choice, it struggles with demanding computational power to differentiate and match features; ASV mitigates these issues by providing well-defined features through the projected light pattern, improving depth resolution and accuracy by decreasing disparity errors. A structured light system provides equal or better resolution than ASV. However, at the same time, a structured light depth sensing system relies more on the quality of the projected light pattern than ASV because it only has one receiving camera. Although feasible and cost-effective, Sonar does not provide the resolution necessary to differentiate between different objects and, most importantly, not solid objects such as shopping carts. Lastly, although a Flash Lidar system can provide higher resolution and accuracy, the feasibility and cost-effectiveness are extremely low.

ASV provides high enough depth resolution and accuracy for this project's application; with the use of NIR bandpass filters for the cameras and modulated NIR emission of light, the system would be remarkably unaffected by environmental sources of light. All of this outweighs the extra cost of calibration and assembly of the light projector. Therefore, we will explore and build an active stereo system for this project's depth sensing and object detection.

3.1.2 Light Source Wavelength

Quality emission from the light projector and clean, detectable light from the camera is crucial for an ASV system. Therefore, we will compare different wavelengths of light, including 635nm, 850nm, 980nm, and 1550nm. We will evaluate these different wavelengths in the following categories that mainly affect the performance of an ASV system: object reflectivity, environmental constraints, Optical system compatibility and availability, and cost.

635nm wavelength lies in the visible red spectrum, which can bring advantages and disadvantages to an ASV system. At 635nm, common material possesses varying reflectivity but mainly depends on the object's color; if an object is black, blue, or green [24] [25], the reflectivity of 635nm light is significantly decreased due to color subtraction [26]. This would affect the reading from the camera and not have the necessary features where to calculate the disparity. At 635nm, we encounter considerable environmental constraints; it would not be welcome to shine a red light pattern inside a supermarket with other people inside, therefore making it very unwise to use this wavelength for the light projection. Even though we have had problems with object reflectivity and environmental constraints, this wavelength of light is compatible with most off-the-shelf cameras since the most available type of camera sensors work in the visible region. The only drawback would be that the emission would have to be modulated to discriminate between other red light sources like the supermarket lights. This wavelength is extensively used for science experiments and other amateur applications; therefore, products that emit this wavelength would be very available and inexpensive, as well as the cameras.

A wavelength of 850nm lies in the NIR region and is known to be one of the most widely used wavelengths for depth sensing. At this wavelength, reflectivity is slightly better than visible light. However, we no longer have color subtraction [26], making most objects in a supermarket store reflective enough to achieve a readable image on the camera. The only objects that don't reflect more than 20% of NIR are certain types of solid black objects [25], especially some painted with carbon nanotubes and black paint that absorb a high percentage of all visible and NIR spectrum. From an environmental constraints standpoint, 850nm is invisible to the human eye, yet it still focuses on the cornea, making it dangerous at high powers. Considering that the emission system must be eye-safe, this wavelength would disrupt and bother other people at supermarkets, making it suitable for this application. Optically, 850nm is compatible with most common off-the-shelf cameras, although having a lower quantum yield in the imaging sensor since most are designed for visible light, 850nm can still be well detected. In terms of light emitters, this wavelength is very common in LED and Laser Diodes. The main drawback would be alignment since this wavelength is not visible, but alignment should be feasible with a camera. Overall, due to the high compatibility and availability of light sources of this wavelength and components compatible with this wavelength, using it would have a low impact on the cost of the ASV system.

980nm wavelength falls deeper into the NIR spectrum and offers unique advantages for structured light projections as well as disadvantages with sense. Regarding reflectivity, this wavelength has similar characteristics of reflectance to the ones of 850nm, with good reflectivity from most objects due to no color subtraction, but deep black materials still absorb most of this wavelength. Environmental constraints at 980nm are generally low. This wavelength is absent in most artificial lighting systems, reducing background noise. Moreover, the wavelength is still invisible to the human eye, making it suitable for use in a crowded scenario such as a supermarket. Optically, 980nm is still within the responsive range of most off-the-shelf cameras, but the quantum efficiency is lower than 850nm, making it harder to get accurate images on the camera and, therefore, introducing errors in the disparity readings. Regarding cost, most common optical equipment still works with this wavelength, only with some drawbacks, as explained by the quantum efficiency of cameras. Nonetheless, using this wavelength would hinder the cost of making an ASV system.

The 1550nm wavelength still resides in the NIR region, primarily used in LiDAR systems and long-distance optical fiber communication. Regarding reflectivity, many common materials show lower and more variable reflectance at 1550nm. Surfaces such as plastic or dark fabrics have higher absorptions. As a result, light pattern return may be inconsistent, affecting the depth resolution and accuracy. Environmentally, this wavelength has a much higher threshold of when it can harm human eyes. Therefore, more power can be used to get stronger reflections. Optical materials and devices that support 1550 exist in the market but are more specialized. For example, the camera would have to be a NIR specialized camera since most common cameras in the market have a quantum efficiency close to 0% for 1550nm. This would not make the system harder since the technology to support this wavelength is available, but it would make it much more expensive.

Table 3.2: Light Source Wavelength Comparison

Wavelength (nm)	**Object Reflectivity**	**Environmental constraints**	**Optical Compatibility / Availability**	**Cost**
850	High for **most** objects, minimal color dependency	Moderate, invisible but same wavelength found in artificial light sources	Moderate to High, compatible with most visible spectrum **sensors** and available in various light sources	Low
635	Low for dark/green/blue objects due to color subtraction	High, Visible to human, disruptive in public settings	High, compatible with **all** visible spectrum sensors and various light sources available	Low
980	Moderate to high: more absorption by deep black materials	Moderate, invisible but same wavelength found in artificial light sources	Moderate, compatible with most visible spectrum **sensors** and available in various light sources	Moderate
1550	Low and inconsistent, highly material **dependent**	Low, Invisible and eye safe at higher power.	Low, requires **specialized** imaging sensors and emitters	Very High

After comparing the four wavelengths based on object reflectivity, environmental constraints, optical compatibility/availability, and cost, 850nm is the most suitable wavelength for this system. Lower wavelengths can't be used because they are visible and disruptive if used in public, and higher wavelengths struggle with reflection from darker objects, as well as increased cost and lower availability of cameras and emitters. Ultimately, 850nm achieves a strong balance between all the evaluating categories, making it the wavelength selected for the ASV system.

3.1.3 Light Source Technology

The quality of an ASV is dependent on the type of light source used since it plays a significant role in the quality of the projected structured light, which is what our depth calculations rely on. Therefore, we have chosen to compare light-emitting diodes (LED) and Laser Diodes. They'll be compared under the following evaluating characteristics: Beam Quality, Power output and Efficiency, Modulation Capability, Integration capability, and lastly, availability and cost.

A laser diode operates by injecting electrons across a forward-biased p-n junction; the recombination within the narrow active region causes the emission of photons. These photons stimulate further emission of identical photons, resulting in coherent light. Most of these devices include reflective faces on both sides of the p-n junction, allowing for an optical resonator and enabling feedback and amplification [27]. This makes the emission highly monochromatic, directional, and coherent. Laser diodes have high beam quality because the stimulated emission generates directional coherent light, meaning less dispersion, therefore making the light easier to collimate into a smaller beam without the need for big lenses. Laser diodes have a narrow spectral bandwidth, typically in the range of a few nanometers, which ensures minimal chromatic dispersion when the light gets refracted. Laser diodes are capable of delivering high optical power while consuming relatively low electrical power, with an electrical-to-optical efficiency of 30-60% [28]. Moreover, laser diodes come in many different power ratings, making them very useful. In terms of modulation, laser diodes can be modulated at very high frequencies, often in the MHz range. Laser diodes are very compact, and mounts that act as heat sinks are readily available. The only concern with a laser diode would be that a good quality driver that supplies current would be needed since laser diodes are very sensitive to spikes in voltage or current and can be easily destroyed if not operated correctly. Laser diodes are costly, depending on the characteristics, but a normal laser diode would suffice for this application. Moreover, laser diodes of 850nm wavelength can be found in various types and optical powers, making them very available.

LEDs generate light through spontaneous emission when electrons and holes recombine across a forward-biased p-n junction [29]. These devices don't exhibit stimulated emission due to the lack of optical feedback and population inversion. Because of this, the light from a laser diode is incoherent and more omnidirectional, meaning it has a higher divergence. Regarding beam quality, LEDs perform poorly due to the lack of directionality, which causes more considerable divergence [30]. Moreover, the light from an LED has a spectral bandwidth in the range of tens of nanometers, therefore making it susceptible to chromatic aberrations when refracted. Collimation of an LED is indeed possible, but bigger and optically stronger lenses are needed to capture most of the light emitted. All of this can impact the quality of the projected light and, therefore, the features used for depth calculations. LEDs have different power outputs and tend to have a 50-80% energy efficiency [31]. Regarding modulation, LEDs can be modulated but at lower frequencies of around 1 GHz, which is enough for the application of this project. From an Integration feasibility standpoint, LEDs are compact, low-cost, and thermally efficient. They don't require complex drivers, making them very easy to integrate into an ASV system. The big drawback comes with adapting other optical components to compensate for the lousy beam quality of the LED. LEDs are very cheap and available in the market, especially in 850nm wavelength, making them very cost-effective for the project.

Table 3.3: Light Source Technology Comparison

Light Source Technology	Beam Quality	Power Output and Efficiency	Modulation Capability	Integration Feasibility	Availability and Cost
Laser Diode	High, excellent for collimation, and low optical aberrations	Medium-High efficiency, and available in multiple power outputs	High, MHz range	Moderate, requires heat dissipation for high power, and good drivers	High availability, Moderate cost
LED	Very Low, broad spectral output causing aberrations, and poor collimation	High efficiency, Available in multiple power outputs	Moderate, GHz range	Very compact, not heat dissipation needed, and standard drivers	High availability, Low cost

After comparing LEDs and other diode technologies across all important areas, the laser diode is more appropriate for our project since depth calculations depend on the quality of the projected patterns; LEDs would create lower-quality patterns, infusing higher disparity errors in our reading. Moreover, laser diodes hold the advantage of their light being able to be collimated easily and with minimal aberrations, something LEDs lack due to their high dispersion and spectral bandwidth. Although LEDs were found to be cheaper and require more straightforward electronic drivers, they can't outweigh their lack of optical quality. Therefore, we shall explore what type of laser diodes we will use in our next project.

3.1.4 Laser Diode Technology

Now that we've chosen laser diodes as our light source type, we must dive deeper and select which technology within the realm of laser diodes we will use. The laser diode technologies discussed are Fabry-Perot Laser Diode (FP-LD), Distributed Feedback Laser Diode (DFB-LD), and Vertical-Cavity Surface-Emitting Laser (VCSEL). These laser diodes will be evaluated based on the following characteristics that most impact our project: beam quality and collimation, spectrum linewidth and stability, integration feasibility, availability, and cost.

FP-LD is one of the most common laser technologies in the world. These diodes use a simple edge emitting structure where the front and back faces of the semiconductor chip act as mirrors, forming a Fabry-Perot resonator, therefore achieving stimulated emission [32]. This type of laser diode also exists in single-mode or multimode formats. Regarding beam quality and collimation, FP-LDs produce an asymmetric divergence because the laser diode is constructed in an edge-emitting structure, narrowing the divergence horizontally and vertically. This can be a drawback to collimation since extra optical elements and calibration are needed to collimate the light into a circular shape. For spectral linewidth and stability, FP-LDs produce a relatively wide spectrum; for the single mode, the range is 1-3nm, and for the multimode, this range is 5-10nm [33]. These laser diodes are also susceptible to temperature and current delivery changes, where more modes might be activated, and peak wavelength shifts occur. Variations of 0.3-0.5nm per 10C and 0.006nm per mA have been found to normally happen in an FP-LD, making good electronic drivers and heat sinks necessary [34]. Nonetheless, while these conditions are not ideal for ultra-high precision applications, they are acceptable for our light projection system, where tight wavelength control is not critical. In terms of integration and feasibility, FP-LDs are versatile and offered in different types of packages such as TO-can, butterfly, and fiber-pigtailed. Since this type of laser diode is the most used across the world, it will not be hard to find electronic drivers that support it. Regarding availability, since this technology of laser diodes is widely used, it won't be hard to find our desired wavelength with a specific power output. The price of an FP-LD is mostly based on its power, wavelength, and beam characteristics, but they are still a cheap option.

DFB-LDs incorporate an internal diffraction grating inside or adjacent to the active region. This grating acts as a wavelength-selective mirror that suppresses modes apart from the fundamental mode, making it a single-mode laser diode [32]. This type of laser diode, like the FP-LD, is also an edge-emitting device, therefore having the same collimation struggles as an FP-LD, where extra optics and alignment are needed to get a circular collimated beam. Due to the diffraction grating, the beam spectral linewidth and stability of a DFB-LD are excellent and superior to most types of laser diodes. In some cases, spectral linewidth can be as low as 0.024nm, and drift can be as low as 0.01-0.1nm per 10C for temperature and 0.001-0.005nm per mA (with temperature stabilizers) for the delivered current [34]. As mentioned before, the internal characteristics of this technology also allow the laser diode to only output single-mode light. All of this makes DFB-LD ideal for applications where a narrow spectral control is important. Regarding integration feasibility, this type of laser is available in various packages like FP-LDs. However, DFB-LD does require precise thermal control to maintain its narrow linewidth performance, making it vital to have a temperature controller rather than a heat sink. This would make the electronic side of our project more energy-consuming, complicated, and bulkier. Regarding availability, DFB-LD lasers are widely used in telecommunication, spectroscopy, and sensing; therefore, finding a laser diode of this type with our desired wavelength and specific power output wouldn't be very hard. The only drawback is that this type of laser diode tends to be more expensive, not only because of the integrated diffraction grating but also because of the needed temperature control system.

VCSEL differs fundamentally from the other two technologies in both structure and emission characteristics. This laser diode does not hold an edge emitting structure; instead, it consists of a vertical resonator formed by two Distributed Bragg Reflectors (DBRs) placed over and under the active region [35]. This technology can be found in different packaging such as TO-can, butterfly, and fiber-pigtailed. Light from a VCSEL is emitted perpendicular to the wafer surface. Therefore, in terms of divergence, it emits a symmetric circular beam with low divergence, often between 5-10 degrees, depending on the size of the aperture. Due to this, collimation is very easy and efficient, with less alignment and optical elements. In terms of spectral linewidth and stability, VCSELs are generally single-mode laser diodes with narrow line widths around 0.1-0.5nm. The drawback of this technology is its sensitivity to temperature variations, with wavelength drift values usually around 0.07nm per every degree Celsius and 0.005-0.01nm per mA [34]. While not as stable as DFBs, they perform well for systems that do not require very narrow spectral linewidth.

Regarding integration feasibility, VCSELs are very compact and thermally efficient. The vertical emission property allows for more straightforward implementation into an optical system that requires collimating light from the laser diode. Regarding availability, this technology is widely used because of its divergence properties. Therefore, it can be found in multiple packaging types, wavelengths, and power outputs. Nevertheless, from a cost perspective, they are more expensive, and the higher the desired output power, the more it could affect our application since we need strong enough reflected power into the imaging sensor to generate a usable image.

Table 3.4: Laser Diode Technology Comparison

Laser Diode Technology	**Beam Divergence and Collimation**	**Spectral Linewidth and Stability**	**Integration Feasibility**	**Availability**	**Cost**
FP-LD	Asymmetric beam; requires additional optics for collimation or pigtailed packaging	1-3nm(SM) 5-10nm(MM) ∼0.3-0.5nm/10C, ∼0.006nm/mA drift	Versatile packaging, common in general applications	High	Low
DFB-LD	Asymmetric beam; requires additional optics for collimation or pigtailed packaging	0.01-0.1nm; ∼0.01-0.1nm/10C drift ∼0.001-0.005nm/mA drift	Versatile packaging; requires thermal stabilizer	Moderate	High
VCSEL	Symmetric circular beam; low divergence, easy collimation	0.1-0.5nm; ∼0.07/C, ∼0.005-0.01nm/mA drift	Versatile packaging;	High	Moderate; dependent on power output

After evaluating these options, the edge-emitting laser diode (EELD) was selected as the optimal choice for the depth camera system. While VCSELs offer advantages in terms of simpler fiber coupling and reduced speckle noise, their higher cost and lower power output make them less suitable for this application. Distributed feedback lasers, though highly precise, provide features that are unnecessary for the system's requirements and would significantly increase costs. The EELD's high spatial coherence, availability at the required 200 mW power level, and cost-effectiveness make it the most practical and efficient choice. Although coupling into a single-mode fiber requires careful alignment and the use of beam-shaping optics, these challenges are manageable within the project's design constraints and do not outweigh the EELD's performance advantages.

3.1.5 Coupling Technology

After choosing an FP-LD as the light source that will be used for our ASV system, we must find a way to efficiently couple the light into a fiber (to use a fiber splitter to have two outputs from one source). We have chosen to investigate four different solutions; Butt coupling, Cylindrical lenses, Anamorphic prism pairs, and Pigtailed laser diodes. This is a critical step in our research since it can alter the efficiency of our system and introduce difficulties in the construction of our system. Therefore, we will analyze the different options using the following criteria: Coupling efficiency, integration feasibility, availability, and cost.

Butt coupling is one of the most straightforward techniques to insert light from a laser diode into an optical fiber. It involves aligning the end of the fiber directly in front of the emitting facet of the FP-LD without using any optical components. Although this method reduces the need for extra optical components, it can introduce challenges in the alignment and integration [36]. From a coupling efficiency perspective, butt coupling suffers significantly due to the divergence and asymmetry of the laser beam, particularly one from an edge-emitting diode. An FP-LD produces a highly elliptical beam where the fast axis (perpendicular to the junction plane) can have twice as much divergence as the slow axis (parallel to the junction plane). Due to this divergence, most light emitted falls outside the fiber's acceptance cone. Reported coupling efficiencies can be as low as 10-20% for laser diodes with diverging angles around 10x25 for butt coupling techniques [37]. In terms of integration feasibility, although butt coupling avoids the need for extra optical elements, the alignment precision needed for butt coupling is high, where micrometer misalignments can greatly hinder coupling efficiency. This would force our group to use high-precision translating stages to align the fibers accurately. After some research, these devices can be more expensive than buying optical lenses to couple the light into the fiber. Previously, we thought the cost of using this technique would be negligible since there are no extra optical elements; we now realize that mechanical instruments are needed, and even though they are readily available in the market, they can be expensive.

Cylindrical lenses are lenses that only have curvature in one axis, therefore affecting the divergence of a beam on a single axis. This technique is employed constantly to fix the asymmetric nature of an edge-emitting diode beam. This is usually done by using a single cylindrical lens accompanied by a spherical lens, where the cylindrical lens adjusts the fast axis to match the slow axis and the cylindrical lens couples the light into a fiber; another way of using them is by having two cylindrical lenses where each is responsible in coupling the light from one of the beam's axis into the fiber. Regarding Coupling efficiency, the better the cylindrical lenses' numerical aperture matches the acceptance cone of the fiber, the higher the coupling efficiency is. We have found proof that coupling efficiency can vary from 50-90% with correct alignment and the correct cylindrical lenses [38]. Regarding integration feasibility, this technique introduces alignment problems again; the cylindrical lenses must be correctly aligned for the transmitted wave plane to be parallel to the fiber and centered at the center of the fiber core [39]. Therefore, it is essential to use specialized alignment instruments in order to achieve high coupling efficiency. The good thing is that these lenses are readily available in multiple markets and any needed focal length, making this technology very available. The only drawback is that these lenses can be moderately expensive, increasing the overall spending on this project.

Anamorphic prism pairs are just normal prisms and are favorable for our application if used correctly and in a specific configuration. This technology uses the refraction of the prisms, based on the angle of intersection of light, to magnify one of the axes of a beam going through them. This approach is widely used for beam shaping, especially for collimating or coupling light from an edge-emitting diode. Extra optical lenses must accompany this technology to couple the light into the fiber since it only changes their shape. From a coupling efficiency standpoint, this technology has shown to have a throughput of 95% of light when used with antireflection coatings, and later, the coupling efficiency is dictated by the system of lenses used to focus the light into the fiber, which can be as high as 95% [40]. Therefore, a maximum percentage coupling efficiency of 90% is aligned correctly and used with complementing lenses. For integration feasibility, anamorphic prism pairs can be bought already mounted, meaning that no required alignment of the prisms is necessary; the only alignment required would be of the extra lenses. Although these pre-packaged prisms are in their most compact form, they can be larger than the cylindrical lenses used to couple the light, making the setup less compact. The only concern with this technology is that it doesn't directly couple the light into the fiber and only shapes the beam, as stated before; therefore, more alignment is needed for the cylindrical lenses required. The cost of mounted anamorphic prism pairs is usually 4 times as high as buying these unmounted prisms, which might seduce us to quire unmounted prisms, but then we would have to align them, which would be more expensive. The favorable thing is that these prisms are readily available in the market, making them easier to acquire.

Pigtailed laser diodes are pre-packaged units where the laser diode is fixed, permanently aligned, and coupled into an optical fiber. This is done through aspheric lenses, or GRIN lenses, where the selection of optics used inside the pigtailed laser to couple the light is already made by the producer to achieve high coupling efficiency. This approach would eliminate the need for extra optics and simplify our project. From a coupling efficiency standpoint, pigtailed laser diodes often provide high coupling efficiency in the realm of 50-80%, depending on the type of fiber, either SM or MM [41]. This approach is very favorable to our application regarding integration feasibility because it eliminates the need for extra optical components or alignment devices since the manufacturer already does all of that. Pitailed laser diodes are harder to find in specific output powers and types of laser diode, but they are available in the market. The price of these devices is indeed higher than the laser diode itself, making it sometimes up to 3 times more expensive to buy a pigtailed laser diode than the laser diode itself, but this eliminates the extra cost of other lenses or alignment, which, the end, makes it a very viable choice.

Table 3.5: Coupling Technology Comparison

Coupling Technique	**Coupling Efficiency**	**Integration Feasibility**	**Cost and Availability**
Pigtailed Laser Diodes	Moderate-High; 50-80%	Very High; No need for extra alignment or components	Moderate; Cost of the product is substantially less compared to lenses and alignment devices
Butt coupling	Low; $\sim$10-20%	Low; High alignment requirements requiring extra components	High; Increased priced due to the extra required components
Cylindrical Lenses	Moderate-High; 50-90%	Moderate; Requires alignment and mounting of lenses	Moderate-High, Increased priced due to the alignment and mounting devices needed
Anamorphic Prism Pairs	Moderate-High; 50-90%	Moderate; Requires alignment of prisms in bought unmounted and alignment of required lenses to couple the light	High; Increased priced due to the extra required components

After evaluating the different coupling techniques under the same criteria, pigtailed laser diodes emerge as the most suitable for an ASV system. While options such as anamorphic prism pairs and cylindrical lenses offer the same coupling efficiency, their integration feasibility and cost are significantly increased by the components and the complementing components needed for alignment or further beam shaping. Butt coupling, although simple, also needs very high alignment requiring more precision components and making the system more expensive while delivering a very low coupling efficiency. Therefore, we have chosen to buy a Pigtailed FP-LD to make our system more reliable and efficient.

3.1.6 Pigtailed Laser Diode Product

Now that we have decided we need an FP-LD laser diode pigtailed to a fiber, we have selected 4 possible options for our light source in the emission system. The options are as follows: S780 Coaxial pigtail High Power Laser Diode 850nm by Wuhan Shengshi [42], 850nm 50mW/80mW IR Pigtail Laser $5\mu m$ SM Fiber Coupled Laser Diode by Civilasers [43], LASER TREE 850nm 100mW Infrared Fiber Coupled Laser Diode LT-FCLD-M850100 by Laser Tree [44], and High Output Power PF Long Wavelength Pulsed Conditions 850nm Pulsed Laser for OTDR PLD-F85 by Shengshi [45]. In order to effectively choose our light source, we will be comparing the products under the following criteria: Beam power and quality, Electrical requirements, and cost.

The Shengshi S780 delivers 120mW of optical power through an MM fiber. While it is commonly known that multimode fibers attenuate power over large distances, this is of no worry in this application since the length of the fiber will not exceed 1 meter. Another concern with this fiber is the activation of different modes. This can be harmful in systems that require a spatially uniform light. However, this application does not take any play, making it okay to have a multimode fiber as our transport medium. The power level is sufficient to create readable reflections when the power is distributed into the pattern but low enough to be eye-safe. With an operating voltage of 2.4V and an operating current of 240mA, it is compatible with market-ready drivers of low voltage in order to modulate the light properly. At a lower cost than most light sources of these specs, a price of 65 dollars makes it a viable solution for our project to keep it cost-effective.

The Civilaser module delivers 80mW of optical power through an SMF. This type of fiber ensures a clean and stable output while keeping only the fundamental mode of light traveling through the fiber. Due to this, a fiber splitter that uses SMF is required. However, we could still use an MMF splitter; the clean fundamental mode would get shaped and excited into different modes when the light crosses from the SMF to the MMF. With an electrical requirement of 2.4V and 240mA to operate, this system is also compatible with most low-voltage drivers in the market. The price falls into the moderate-high end of the spectrum when it comes to pigtailed LDs with similar characteristics. This is also because of the SMF used since it is harder to couple light into one of these fibers than it is to an MMF.

The LT-FCLD-M850100 pigtailed laser diode by Laser Tree offers 100mW of optical power sent through an MMF. As said before, introducing excitation of different modes won't affect the output from the interaction with the structure light projection technology and the reflections. This laser operates at 2.4V and 240mA, again making it suitable for most drivers available in the market. While at a higher cost due to its reliable source provenience. This could also be an exemplary implementation for our system due to the good documentation and support from Laser Tree, something hard to find by the other Providers.

Finally, the PLD-F85 from Shengshi. This laser delivers 120mW of fiber through an SMF, making it a viable choice due to the combination of high power and fundamental mode creation. This laser operates at significantly higher electrical requirements than the rest. With an operational voltage of 5V and 300mA of operational current, it is harder to find drivers, although they can be available through meticulous research on different online stores. The low threshold current compared to the operational current leads us to believe that this laser is more suitable for precise high-power short pulse uses such as Optical Time Domain Reflectometers (OTDR), where only high energy pulses are used to calculate fiber attenuation and losses. These electrical requirements also mean that this module will experience high temperatures, affecting the output power and degradation of the diode. Cost-wise, this laser is found to be an economically viable solution.

Table 3.6: Pigtailed Laser Diode Product Comparison

Product Manufacturer and Number	Optical Power	Fiber Type	Operating Voltage (V)	Operating Current (mA)	Threshold Current (mA)	Price (USD)
Shengshi S780	120mW	MM	2.4	220	50	65
Civilasers 850nm Pigtailed Laser(SM)	80mW	SM	2.4	240	55	169
Laser Tree LT-FCLD-M850100	100mW	MM	2.4	240	55	180
Shengshi PLD-F85	120mW	SM	2.42.3	300	18	78.66

After a comprehensive evaluation of all the lasers, based on their beam quality, electrical requirements, and cost, the Shengshi S780 is the most suitable for our application. With a standard current requirement of 240mA and voltage of 2.4 volts, finding a driver capable of modulating this laser is very feasible. Although options such as the one from Laser Tree, where reliability on the provider and similar electrical requirements, the price is too high for the budget of this project. On the other hand, the option from Civilasers lacks optical power, which could be beneficial if we encounter high losses in our system. Finally, the electrical integration of the Shengshi PLD-F85 makes it very hard to consider it a possibility. Therefore, the Shengshi S780 pigtailed laser diode will be our light source moving on.

3.1.7 Laser Diode Driver Product

Laser diodes can suffer performance impacts if the supplied current does not match the required specifications. Supplying too much current to a laser diode can cause it to exceed its thermal range, damaging the diode, and any improper current value will affect the resulting light beam quality since it changes the output wavelength and power. Therefore, selecting a proper diode to manage power supply is critical in ensuring the laser diode is able to properly operate and produces the desired output.

There are several types of laser diode drivers, including constant current, pulsing, and low/high power drivers. The selected laser diode, the Shengshi S780, is suited for both constant current and pulsing operation. Constant current drivers supply a steady, unchanging electrical current whereas pulsing supplies spaced bursts of current, similar to a PWM signal.

The FL500 Laser Diode Driver was the first technology explored. It supplies a constant current of up to 500 mA to a single diode, or up to 250 mA each for two diodes. Its input range is between 3-12 V and is specified for low-noise applications. The LDD200P Series Laser Diode Driver was another similar option considered. Supplying a maximum current of 200mA, this constant current driver takes in an input voltage of 5-12 V and is also suited for low-noise applications. The final driver that was considered was the Thorlabs LDC205C Benchtop LD Current Controller, which offers very precise control and fine-tuning of settings to up to 500 mA of constant current or power control. This option was immediately ruled out, however, due to its impracticality for this project. The benchtop driver is more suited for testing purposes rather than integration into a portable product.

Between the FL500 and LDD200P drivers, we had to consider the constant current output we wanted supplied to the diode. The Shengshi S780 laser diode has a forward current of 220 mA, so the drive current to the diode would preferably slightly below this value. The FL500 is capable of a 2-output, 250 mA supply each, which is suited to drive the chosen laser diode. The LDD200P's max supply current is much lower, which may impact the quality of the laser diode's output light beam. A summary of the key features of the three driver options are listed below.

Table 3.7: Comparisons Between Different Laser Diode Drivers

Product	**Mode**	**Input Supply (V)**	**Max Output Current (mA)**	**Price (USD)**
FL500 Laser Diode Driver	Constant current	3-12	500 (or two 250)	$60.00
LDD200P Series 200mA	Constant current	5-12	200	$105.00
Thorlabs LDC205C Benchtop LD Current Controller	Constant current, constant Power	120 (AC)	500	$1210.31

The final chosen driver for the Osram SPL TR85 laser diode was the FL500 Laser Diode Driver operating in dual-driver mode to output a maximum constant current of 250 mA.

3.1.8 Structured Light Projection Technologies

A crucial part of an ASV system is the structured light; as mentioned before, the pattern generated provides the features to make disparity calculations possible. A bad-quality light projection would induce disparity errors and get erroneous depth readings. Therefore, after selecting our pigtailed laser diode, we must choose a technology to transform the single beam light from the diode into a projected pattern. The technologies that we are going to discuss are the following: Diffractive Optical Element (DOE), Digital Micromirror Devices (DMD), Liquid Crystal on Silicon Spatial Light Modulators (LCoS), and finally, Laser Scanning. These four technologies will be reviewed under the following criteria: Pattern

Quality, Environmental Constraints, Integration Feasibility, and finally, Availability and cost.

DOEs are compact, passive components manipulating light through nano- or nano-scale surface relief patterns. This technology introduces controlled phase delays across the wavefront of the incident wave and causes constructive or destructive interference, such as Young's double slit experiment [46]. The small structures allow for further manipulation of the desired pattern, making it possible to have different shapes and thicknesses projected from the DOE. This technology is fabricated using lithographic or direct-write technologies that create microstructures in substrates such as fused silica or polymers. From a pattern quality standpoint, DOEs generate uniform, repeatable patterns with outstanding spatial precision. Unlike other technologies, the pattern produced by a DOE is fixed and cannot be changed, although this might be a problem for a project that requires a change in projected patterns over time. On the other hand, this gives DOEs more excellent stability and precision [47]. However, the pattern is very dependent on the quality and wavelength of the input beam. Aberrations such as pincushion are introduced into the projected light if a different wavelength is used. In terms of environmental constraints, DOEs are very robust. The lack of moving parts and solid-state construction makes the DOE very resistant to vibrations and thermal changes, which is very important for mobile systems like the one for our project. However, their wavelength dependence might be an issue when wavelength drifts occur in a laser diode, which can cause small aberrations in the projected light. Integration feasibility is a strong suit for DOEs. Their ultra-thin form allows for more compact systems. Since this technology is a more complicated and intricate form of a standard diffraction grating, the pattern transmits through the DOE with a certain FOV designed by the manufacturer, limiting the need for extra expansive optics afterward. DOEs are small and thin pieces of plastic or glass; therefore, their mounting can be easily managed, making it very easy to implement into our project. However, misalignment can degrade the pattern and affect the project's overall purpose [48]. Therefore, good alignment and setup of the different optical elements is necessary. In terms of availability, it is increasingly accessible due to improved fabrication technologies. Nevertheless, they are still hard to find for specific wavelengths and patterns. Custom DOEs are available in the market but can be thousands of dollars due to the difficulty of producing a microstructure map to generate a desired pattern, but luckily non-custom DOEs are very cost-effective compared to other technologies

DMDs are a class of micro-electromechanical systems (MEMS) composed of millions of microscopic arrayed mirrors mounted on tiny hinges [49]. Each mirror can move 24 degrees in a single axis, controlled by an underlying CMOS address circuit. Therefore, creating high-contrast structured light and changing the projected pattern might be beneficial for this project. From a pattern quality perspective, DMDs offer exceptional flexibility and resolution; they can generate static or dynamic patterns with precise control over the pattern quality [50]. Although a DMD can create high-quality patterns of light, their quality is directly related to the number of mirrors in the DMD, making the technology more expensive if more mirrors are needed. Lastly, DMDs cannot create high-quality patterns that expand over time; therefore, as in normal movie projectors, lenses must be used to expand the image, which might lessen the quality of the pattern if the lens system is not well-designed and aligned. Environmental constraints are moderate for DMDs. The moving mirrors are susceptible to being contaminated with dust, and they can be damaged after prolonged thermal exposure. Therefore, the DMD system must be contained in a thermally regulated sealed environment to prevent damage. Importantly, DMD systems are invariant to changes in wavelength since the angle of reflection is not affected by it, making this more suitable for a light source that has drifted in this wavelength. Regarding integration feasibility, DMD systems require well-designed illumination paths and high-precision optics, which would increase the cost and complexity of the system overall. Electronically, if a single pattern is used, the DMD does not have to be updated in real-time, making it easier to use but defeating the purpose of having a system that can create different patterns in real-time. Regarding availability, these devices are widely available in different resolutions and applications. The downside is that these devices are more expensive. However, the cost is justified when the application requires real-time control of the projected pattern.

LCoS is a reflective spatial light modulator technology that combines liquid crystals with a silicon backplane. The silicon substrate contains a CMOS circuit that applies voltage to each pixel, manipulating the liquid crystal molecules' orientation. Depending on the design of this device, this modulation alters either the phase or the polarization of incident light, which is reflected by a highly reflective surface behind the liquid crystals [51]. Pattern quality in the LCoS system is very high, as each single pixel can modulate light individually from other pixels, enabling greater spatial resolution control. This makes it a robust option for creating structured light. LCoS does have slower switching speeds due to the liquid crystals, which can be harmful if the project needs ultra-fast pattern changes, but luckily, that is not the case in this project. Lastly, similar to DMD, this technology cannot create patterns that expand at high FOVs; therefore, optical lenses are needed before the device, but not as complex as for DMDs. Regarding environmental constraints, LCoS panels require stable thermal conditions, which require extra components to maintain constant temperature. Due to the liquid crystals, this system is also susceptible to high-power incident light, making it hard to use high-powered laser diodes. Additionally, LCoS relies on polarized light, increasing the complexity of the light emission from the laser diode due to the need for waveplates to alter the polarization of the light. Integration feasibility is moderate, similar to DMDs. While the system is very compact and small, it requires additional components to regulate temperature, optical components to increase the quality of incident light, and optics for the reflected light to increase the FOV of the generated patterns [52]. These systems can be easily found in the market with varying resolutions and applications, and they are usually cheaper than their counterpart DMDs. However, the cost is projected to increase if this technology is implemented due to the need for temperature controllers and specialized optics.

Laser scanning systems do not project structured light, but they can simulate it by rapidly moving the beam of light to trace the desired pattern of light. They do this through motorized mirrors that move at high frequencies or through MEM actuators [53]. These systems are available in one or two axes of movement. This technology can be used regularly for imaging systems and laser projectors such as the ones used at music festivals. From a pattern quality perspective, laser scanning systems can deliver extremely sharp, high-contrast features if the light source is highly collimated and coherent. Environmental constraints such as constant vibrations could produce erroneous pattern projections and affect the depth calculations. Eye safety is also a problem with a device like this because although, over time, the total power is distributed through the projected pattern, some parts of the pattern might have greater power density, which, when using high-power laser diodes, can be harmful to the public. Nonetheless, these systems are robust and can be used in mobile applications. Integration feasibility is moderate to complex since exact control electronics are needed, as well as good synchronization between the camera and the laser scanner because the exposure time of the capturing sensor of an ASV system must be lower than the rate at which the laser scanner completes one or several patter tracings, in order to appreciate the full pattern. A clean optical path from the light source to the laser scanner is needed, but after that, the manufacturer already does the alignment of the mirrors or MEMs actuators. However, these systems tend to be bulky, primarily if they work at high frequencies, therefore increasing the footprint of our pattern emission system. In terms of availability and cost, these systems are widely available due to their use in many systems that require moving or creating shapes with light. Entry-level laser scanners are moderate in price, but higher precision and frequency systems can be costly, especially when the dual axis is needed, such as in this project.

Table 3.8: Structured Light Projection Technology Comparison

Structured Light Projection Technology	**Pattern Quality**	**Environmental Constrints**	**Integration Feasibility**	**Availability and Cost**
DOE	Moderate-High; Fixed pattern and subject to beams quality, wavelength and microstructure precision.	Low; Robust and immune to normal changes in temperature or vibrations.	Very High; No additional components required, and only standard alignment necessary	Moderate availability Low-Moderate cost
DMD	High; Good flexibility and resolution, subject to beam quality	Moderate; Sensitive to dust, thermal stress and can be disrupted by vibrations	Moderate; Requires extra optics and temperature controllers	High availability Moderate-High cost
LCoS	High; High resolution, subject to beam quality	Moderate; Requires thermal stabilizers and can disrupted by vibrations	Low-Moderate; Requires beam polarizers and heat management	High availability Moderate-High cost
Laser Scanning	High; Depending on oscillation frequency of mirrors and precise movements.	Moderate; Can malfunction and produce skewed patterns under vibrations	Low; Requires precise alignment, and quality electronics	High availability Moderate-High cost

After evaluating the four primary light pattern projection technologies, the DOE stands out as the most appropriate solution for the goals of this project. While DMDs and LCoSs can create higher quality patterns and can produce changing patterns, they suffer from difficulty in the implementation due to the necessary optical devices; these technologies also suffer from being susceptible to vibrations, heat, and dust, making it harder to implement on a device that is constantly moved. Laser scanners also introduce necessary electrical systems that make it harder on the electrical engineering side of the project and are susceptible to vibrations. Overall, DOEs are very easy to integrate into our project and very resistant to the environment. Also, being the cheapest option, we will continue with DOEs as our technology to create the light patterns.

By integrating DOEs, the depth camera system ensures high-quality structured light projection, facilitating accurate depth mapping while adhering to design constraints. This decision supports the overall goal of developing an efficient and reliable object avoidance system tailored for indoor environments.

3.1.9 Structured Light Pattern

Before selecting our DOE product, we must select a desired pattern for the DOE to produce. Therefore, we will explore the most commonly used light projection patterns for depth sensing: random dot patterns, Dot arrays, and vertical and horizontal lines. These three patterns will be examined under the following criteria: depth information quality, Environment Robustness, and Processing complexity.

Random dot projection is a typical pattern used in depth-sensing systems, where the goal is to have rich spatial variations in the pattern to enhance the disparity estimation done by the software, such as the face ID in Apple products or the old Xbox Kinect. This method diffuses light into a non-repeating, pseudo-random distribution of small bright spots. In terms of depth information quality, this random pattern offers minimal pattern ambiguity, allowing the stereo-matching algorithm to find unique features with high confidence. This would significantly reduce the risk of false correspondence and, therefore, a more reliable depth estimation through the whole field of view. Regarding environmental robustness, the dot pattern would perform well indoors. The non-repeating pattern is more resilient to partial occlusion and varying surface reflectivities because of the lack of pattern, which, if there were, could confuse the outcome of the depth sensing. One big drawback of this pattern is the fact that shopping carts are not solid objects. Therefore, the lack of an actual pattern would make it extremely hard for the algorithm to find the same dots of light in both capturing sensors. In terms of processing complexity, random dots present a trade-off. On the one hand, the spatial uniqueness of this pattern allows for decreased false matches and improves the correspondence. On the other hand, the lack of a predictable geometrical pattern would mean that the algorithm cannot leverage pattern-based shortcuts, therefore forcing the exhaustive and dense cross-matching across all regions of the images. This would increase processing time and not allow the user of this device to have real-time feedback when something fast is approaching.

A regular dot array pattern consists of evenly spaced dots vertically and horizontally arranged in a grid. This pattern would introduce spatial consistency across the scene, making it easier for the algorithm to match features and calculate disparity [54]. In terms of depth information quality, a dot array would still provide a high spatial coverage depending on the size of the array. However, it suffers from ambiguity due to the repetitive pattern. For example, identical local neighboring dots may be confused with one another, introducing errors in the disparity and, therefore, errors in the depth calculations.

Regarding environmental robustness, a dot array is more sensitive to occlusion and reflection issues from objects in the environment, especially featureless objects. The biggest drawback, similar to the random dot pattern, is that this pattern would suffer trying to detect non-solid objects like shopping carts. In terms of processing complexity, a dot array offers moderate efficiency. The algorithm can benefit by using geometric assumptions due to the known spacing between the dots and different distances. However, this would decrease ambiguity, making it easier for the algorithm to confuse neighboring dots.

A pattern holding a series of vertical and horizontal lines is also widely used for depth sensing due to its strong edge and contour features, which help extract geometrical information from objects [17]. Regarding depth information quality, line patterns provide sparse but reliable structural data. This pattern enables high precision in detecting edges from objects. Finally, the depth information also depends on the number of horizontal and vertical lines, which can cause lower reflected power. Regarding environmental robustness, line patterns like this one work on a wide range of surfaces due to the pattern being continuous. Like all the other patterns, it would suffer when encountering non-solid objects like shopping carts, but in this case, since we have continuous lines, the algorithm can interpolate or reconstruct missing segments more effectively, making this pattern the best pattern to visualize non-solid objects. In terms of processing complexity, line patterns are relatively simple to handle. The feature-detecting algorithm can leverage the geometrical nature of the pattern as well as Hough transform techniques. This pattern would also decrease the search time during stereo matching. This results in a lower computational demand, which is crucial for this project and other projects that need real-time data.

Table 3.9: Structured Light Pattern Comparison

Pattern Type	**Depth Information Quality**	**Environmental Robustness**	**Processing Complexity**
Horizontal and Vertical Lines	Moderate; Suffers from ambiguity, Dependent on number of lines	Moderate-High; Effective with non-solid objects	Low; edge detection is computationally efficient
Random Dots	High; Unique local features, low ambiguity	Moderate; Ineffective with non-solid objects, resilient against occlusion	High; Exhaustive feature matching required
Dot Array	Moderate-high; Suffers from pattern ambiguity, dependent on number of dots	Low-Moderate; Ineffective with non-solid objects	Moderate; Geometric assumptions would help,

After evaluating the three most commonly used patterns for structured light projections based on depth sensing, the most suitable choice is the horizontal and vertical line pattern. It offers fewer total depth points than the other two patterns because a high number of lines would cause a significant decrease in the reflected power because of power density across the whole pattern. It provides a strong balance between feature reliability and the computational power needed. Unlike a dot pattern, the continuous structure offers good, reliable features when encountering non-solid objects such as shopping carts, making this one of the main deciding factors when choosing the light pattern for the ASV system.

80

3.1.10 DOE Product

Now that we have selected DOE as the technology for creating the light pattern, we have selected four products: HOLOEY DE-R256 [55], Laserland QYG-004 [56], Digigram DTC-25 [57], and Lasermate DOE-SG60 [58]. These four products will be analyzed based on their Grid size, FOV, Material, and cost. In order to achieve the best results for this project, we need a resistant DOE that can create the most significant number of features for the ASV system to use for depth calculations. We also need a high FOV to minimize the need for extra expansive optics after the DOE.

The product DE-R256 features a grid size of 51 vertical lines, 51 expanding at a FOV of 30 degrees. This provides a high density of lines at a distance of 3 meters. The high density of lines is important for an ASV system because the more lines in an area, the more features our system can calculate disparity from, decreasing the error in depth calculation. The calculated density of lines over a 100cm$\hat{2}$ square placed 3 m away from the emission is 3.1 lines on the vertical axis and 3.1 lines on the horizontal axis. Suppose we used every intersection from these lines and every space in the lines between the intersections, and then we could claim them as features. Mathematically, we would have 22.63 features in a 10x10cm$\hat{2}$ box 3 meters away, more than enough data points to get accurate disparity information. From the material standpoint, Polycarbonate (PC) presents very good mechanical properties and a very high Glass Transition temperature of 145C. This temperature describes when materials transition from a glassy and rigid state into a flexible and rubbery state, where damage to the etched structures can start to happen. This material also possesses a very low absorption to 850nm wavelength, which means most of the incident light will be transmitted, and very low electromagnetic energy will be absorbed by the material as thermal energy. This could be a good addition to our project at a reasonable cost of 72 dollars.

The product QYG-004 features a grid size of 51 vertical lines by 51 expanding at a FOV of 30 degrees, similar to the product before. This provides a high density of lines at a distance of 3 meters. The high density of lines is important for an ASV system because the more lines in an area, the more features our system can calculate disparity from, decreasing the error in depth calculation. The calculated density of lines and number of features in a 10x10cm$\hat{2}$ object 3m away is the same as the product before. In terms of material, this product is made of polymethyl methacrylate (PMMA). It presents good mechanical properties and average thermal properties. PMMA has a Glass Transition Temperature of 110C, meaning it takes less thermal energy. The good thing is that this material is highly unabsorbable in the VIS and NIR region; there is no overheating and damage to the etched microstructures. At first, the source of this product was not very reliable, but after contact with the seller, we opted to try this product because it is incredibly cheap.

The product DTC-25 projects a 60 x 60 grid pattern at a FOV of 40 degrees. While this might look more impressive because of the higher count of lines and the higher FOV, the calculated line density at an object 3m away with a 100cm2̂ area is only 2.7 lines, almost half a line less than the other two products. However, this would still mathematically mean a possible number of 16.47 features from where to calculate disparity in an object 10cm wide and 10cm tall. In terms of material, this product can be made out of Polymethyl Methacrylate (PMMA) or Polyethylene Terephthalate (PET). Both materials present similar mechanical properties and somewhat similar thermal properties. PMMA has a Glass Transition Temperature of 110C and 70C for PET. The good thing is that these two materials are highly unabsorbable in the VIS and NIR region; there is no overheating and damage to the etched microstructures. This product costs 80 dollars, which is very similar to the first and fourth options, making it also a good option for our project, mainly because of the exemplary optical qualities of PMMA.

The product DOE-SG60 projects a 60 x 60 grid pattern at a FOV of 40 degrees. These are the same characteristics as the last product. Therefore, we would only be able to achieve a number of 16.47 features from where to calculate disparity in an object 10cm wide and 10cm tall. In terms of material, this product can be made out of Polymethyl Methacrylate (PMMA) or Polyethylene Terephthalate (PET). These materials were also discussed on the product before. PMMA has a higher Glass Transition Temperature of 110C while PET is only 70C, and both of these materials are exceptionally transmissive and unabsorbative in the VIS and NIR. This product costs 100 dollars, making it the most expensive from our roster and the least attractive choice, but it is still a good contender.

Table 3.10: DOE Product Comparison

Product Manufacturer and Part Number	**Grid Size (V x H)**	**Field of View (V x H)**	**Material**	**Line Density in a 100cmˆ2 area 3m away / Possible features**	**Cost (USD)**
Digigram DTC-25	60 x 60	40 x 40	PET or PMMA	5.4 16.47	80
Laserland QYG-004	51 x 51	30 x 30	PMMA	6.2 22.63	1.5
HOLOEYE DE-R256	51 x 51	30 x 30	PC	6.2 22.63	72
Lasermate DOE-SG60	60 x 60	40 x 40	PET or PMMA	5.4 16.47	100

In conclusion, the product chosen for this project is DIgigram DTC-25. Although this was not initially the most obvious option, we must consider expanding optics after the DOE to achieve more than 50 degrees of FOV, instantly making both DTC-25 and DOE-SG60 the best contenders. Laserland QYG-004 will still be purchased mostly for roughness testing and temperature testing, but this product wasn't a viable contender because there is no guarantee of these specs being real since it's being bought on a very well-known webpage. Furthermore, the product from HOLOEYE, which has excellent thermal resistance and mechanical strength, still falls short due to its lower line grid number. Finally, the Digigram product wasn't a viable solution mainly because of its cost. In conclusion, we will use the Digigram DTC-25 as our DOE to create structured light.

3.1.11 NIR Sensor Technology

Even if an ASV system has a very sharp and strong structured light projection, the possibility of accurately measuring disparities between features relies on the imaging sensor used. If a sensor with poor resolution cannot difirentiate between features, we will not be able to accurately calculate depth and defeat the whole purpose of this system. Therefore, we have chosen to investigate the following sensor technologies: Complementary Metal-Oxide-Semiconductor (CMOS), Scientific Complementary Metal-Oxide-Semiconductor (sCMOS), Charged-Coupled Device (CCD), and Electron-Multiplying Charged-Coupled Device (CCD). These four sensor technologies will be examined under the following criteria: Spectral Compatibility and Sensitivity, Image Quality, System Integration, Cost, and availability.

CMOS sensors are the most commonly used imaging sensors in the world. These sensors have a photodiode in each pixel to convert incoming photons into electrical charge; each pixel has an amplifier that converts this charge into a readable voltage, meaning that each pixel has its readout circuitry [59]. Under spectral compatibility and sensitivity criteria, CMOS sensors exhibit a quantum efficiency of 50% at 850nm, while it can change with different CMOS sensors, typically around 50% [60]. In terms of image quality, CMOS has increased its number of pixels, hence its resolution over the last two decades. However, off-the-shelf CMOS cameras usually present more read noise than other specialized sensor technologies [61]. They also possess a good dynamic range, meaning that the sensor will not get oversaturated when struck by a high-intensity light, but not as good as specialized sensors. As for system integration, CMOS sensors can be found in many modules, which makes it easy to integrate into our project. They are also power efficient. Since this type of sensor is widely used, many resources are available online for the use and implementation of image processing. Finally, in terms of cost and availability, CMOS is by far one of the most accessible and cost-effective choices for camera sensors in the market. They can be found in many resolutions and form factors, making this technology suitable for our project.

The more optimized CMOS sensor is an advanced class of CMOS technology specifically designed to have high performance in scientific imaging. Compared to its counterpart CMOS sensor, this technology offers higher performance in accurately capturing low signals. From a spectral compatibility and sensitivity perspective, the sCMOS sensors offer higher efficiency at certain levels and night ranges, depending on the application and model. These sensors are known for having a much higher sensitivity to NIR due to their back-illuminated sensors, which increase low-light performance [59]. Under image quality, sCMOS sensors deliver high resolution, low read noise, minimal dark current, and a wide dynamic range. They are also designed to reduce fixed pattern noise and pixel non-uniformity, making them ideal for precision imaging where detection and differentiation of features are important. These qualities would improve disparity estimation if implemented into our project. Regarding system integration, CMOS can be more energy-consuming and require more computational power to handle sophisticated data. Nonetheless, these sensors are readily available in the market with many applications and modules, especially in the NIR imaging region. Regarding cost and availability, as said before, it can be easily found in the market but at a significantly higher price than its counterpart, CMOS. This would increase the price of this project significantly but offer much better depth imaging.

CCD sensors are one of the earliest and most established imaging technologies. These sensors transport charge across the chip sequentially through a network of potential wells, using clocked voltages to shift the charge packet from one pixel to the neighboring one until it reaches a readout register. The final charge is converted into a voltage, which minimizes variation across pixels. Because the same amplifier reads out all the pixels, CCDs produce high uniform responses and low fixed pattern noise [59]. Regarding spectral compatibility and sensitivity, CCDs typically show a good quantum efficiency in the visible spectrum but worse in the NIR range, depending on the sensor design. Back-illuminated CCD sensors do offer higher quantum efficiency at our desired wavelength but make them more expensive. Regarding image quality, this technology has low readout noise, good uniformity, and high dynamic range. However, they are subject to slower readout speed, making it harder to work on real-time applications. In terms of system integration, CCDs are more challenging to integrate than other sensor technologies due to the need for external analog circuitry and timing control. However, they can be bought as modules where this has already been implemented. When considering cost and availability, CCDs tend to be more expensive, especially those with back-illumination technology; moreover, they are not as used nowadays, making it harder to find many options in the market.

EMCCD sensors are specialized CCD sensors designed to capture extremely low light signals. They operate similarly to a CCD but introduce an electron multiplication register before the readout amplifier. This register amplifies the signal through impact ionization, enabling the detection of a few photons [59]. In terms of Spectral compatibility and sensitivity, EMCCD sensors are highly effective. Most of these are back-illuminated and can achieve quantum efficiencies as high as 90% in the visible spectrum and 80% in the NIR spectrum. This makes it ideal for situations where illumination is scarce. Under Image quality, EMCCD is exceptional, the signal amplifier allows an almost noiseless readout, and the sensor maintains a high dynamic range and good spatial uniformity.

System integration can pose challenges due to the need for complex high-voltage clocking electronics and thermal management to manage dark current. These demands make it very difficult to implement a technology like this into our system. EMCCD sensors are costly and complicated to find from different providers. While this sensor provides excellent imaging, it would increase our system's complexity and the cost of the whole project.

Table 3.11: NIR Sensor Technology Comparison

Sensor Technology	Spectral Compatibility and Sensitivity	Image Quality	System Integration	Cost and Availability
CMOS	Moderate; QE of 50% at 850nm, higher in back-side illumination sensors	Good resolution; moderate noise; decent dynamic range	High; Low power and easy integration	Low cost High availability
sCMOS	High; QE of >60% at 850nm; Good for low light	Exceptional resolution; Low noise; Wide dynamic range	Moderate; Higher power consumption, higher computational power	Moderate-High cost Moderate-High availability
CCD	Moderate; QE of 50% with back-side illumination	Low noise; Excellent uniformity; Slower readout	Moderate; Higher power consumption, larger size, outdated	Moderate cost Moderate availability
EMCCD	Very High; QE of >90% at 850; Good for low light	Ultra low noise; High uniformity; few photon detection	Very low; Complex electronics, cooling requirements	High cost Low-Moderate availability

After evaluating the four imaging sensor users with the same criteria, CMOS emerges as the most suitable for our ASV system. Although sCMOS and EMCCD sensors provide much superior performance in the NIR region and at low light levels, they are found to be very expensive and complex to integrate into our system. While offering good image quality, CCD technology has slower readout speeds and integration challenges, as well as being outdated and bulky. Therefore, we are choosing CMOS sensors because of their moderate to good image quality in the 850nm region, easy integration, and cost-effectiveness.

3.1.12 NIR CMOS Camera Module Product

After selecting CMOS as our desired sensor, we must choose a camera and CMOS sensor product that best fits our purpose. For this, the sensor must behave very well in low light conditions because of the bandpass filter and perform well in the NIR region. For this, we have selected the Quantum Efficiency (QE) at 850 nm, which determines how effectively the sensor can convert NIR photons into an electrical signal, with higher values translating to better sensitivity. Signal-to-Noise Ratio (SNR) provides image clarity, quantifying how distinguishable the signal is from background noise, which is very important when detecting NIR. Dynamic range, on the other hand, refers to the range of light intensities the sensor can capture without loss of detail in features; this is very important due to higher reflections of constructed light if an object is found near the emission output. Finally, the resolution provides the spatial detail of the captured image. Finally, the price allows us to balance cost and performance.

The 2,2MP Mira220 sensor [62] is a well-rounded imaging solution with decent NIR performance. With a QE of 54% at 850nm, it delivers relatively strong sensitivity compared to other popular sensors in the market. Its SNR of 40dB and dynamic range of 62dB contribute to reliable signal integrity, especially when distinguishing objects reflecting more or less light. With a resolution of 1600x1400 (2.2MP), the sensors support a moderate spatial resolution, which is key for differentiating features of projected light and avoiding disparity errors. The balance between resolution and SNR makes this sensor a good option for our application, the only drawback being the QE, meaning half the incident light from reflected NIR light will not be converted into an image. Despite this moderate performance in our use case scenario, this camera module is listed for 110 dollars, nearly 3 times as much as other camera modules that behave similarly.

The 1MP OV 9281 sensor [63] offers a compact, cost-effective imaging solution tailored to NIR applications. With a quantum efficiency of 30% at 850nm, which is adequate for short-range sensing but still notably lower than other sensors, it makes up for it in dynamic range and affordability. This camera module, listed with an SNR of 36dB and a dynamic range of 68dB, could still be used for mid-distance imaging, compensating for its QE. This sensor would be more appropriate if a nonrestricted amount of power were used as emission to compensate for the QE but still be able to handle the low and high reflection with its dynamic range. However, in this project, as it's intended for public setting use, the amount of optical power allowed to be used is capped, making this a less attractive solution. The standout benefit is the low price of 25 dollars, making it a good testing camera if the budget allows for one.

The Thorlabs CS165MU [64] is a more scientific-oriented monochrome camera designed for precision optical applications. This means that it comes with some enhancements but also some drawbacks. The QE at 850nm is a mere 20%, making it the lowest NIR-sensitive camera in our selection. However, Thorlabs combats this with its spectacular SNR of 69dB, the highest of the group, which indicates precise and extremely clear imaging, a characteristic well-suited for static environments. Its dynamic range is average at 66.4dB, which allows for visualizing small changes in brightness thanks to the SNR. The resolution is 1440x1080 (1.6MP), which offers a relatively moderate spatial resolution. The biggest drawback of this product is the price of 850 dollars. While the cost might justify its performance, this camera is better suited for laboratory experiments.

And finally, the IMX462 sensor [65]. This sensor stands with an incredible QE of 90%, possibly due to its capability of allowing NIR light to seamlessly go through its Bayern filters at each pixel. This allows this camera to have a spectacular conversion of incident NIR light into readable images. However, this also has to be accompanied by a high dynamic range, which this sensor offers at a staggering 72 dB. These two characteristics of the sensor complement each other by allowing more NIR to be transformed into signals and by being able to detect those high-low signal points across the sensor. Regarding image quality, IMX462 offers an SNR of 42dB, higher than its economic counterparts. This allows for precise image data, which is crucial for feature detection and distinction. Its resolution of 1920x1080 (2MP) also provides a more significant spatial resolution to complement the lack of noise by accurately measuring in which pixel we can find different features of constructed light. Finally, all of this imaging power only costs 40 dollars, making it a very, if not the most attractive, solution for our imaging.

Table 3.12: NIR CMOS Camera Module Product Comparison

Camera / Sensor Name	**QE at 850nm (%)**	**SNR (dB)**	**Resolution**	**Dynamic Range (dB)**	**Price (USD)**
Arducam 2MP IMX462	90	42	1920 x 1080 (2MP)	72	40
Arducam Pivariety 2.2MP Mira220	54	40	1600 x 1400 (2.2 MP)	62dB	110
Arducam 1MP OV9281	$\sim$30	38	1280 x 800 (1MP)	68	25
Thorlabs CS165MU	20	69	1440 x 1080 (1.6MP)	66.4	850

After a comprehensive evaluation of the four best solutions for our imaging, the IMX462 camera module stands out as the best sensor for our ASSV system. This sensor offers a strong SNR of 42dB, but mainly, the QE of 90% at 850nm, accompanied by a dynamic range of 72dB, makes the difference compared to all the other options. The Thorlabs camera module would be a great fit for different high-quality imaging in controlled environments and also for a group that can afford it. The other two sensors offer suitable parameters, and OV9281 is very cheap compared to the market. However, the technology from SONY makes the IMX462 a clear winner, and the camera module will be implemented in this project.

3.1.13 850nm Bandpass Filter Technology

Our CMOS camera is able to detect images in the NIR region. However, we must be able to block out all other lights in order to avoid getting unnecessary data and have a better view of our structured light. In order to do that, we would need a bandpass filter, which only allows a small range of wavelengths to be transmitted through the filter. Therefore, we will examine the following technologies of filters available: Dielectric Interferance, Absoprive, and Hybrid, which mix the first two technologies. In order to choose one, we will analyze each one using the following criteria: transmission at 850nm, blocking efficiency, integration feasibility, and availability and cost.

Dielectric interference filters are among the most commonly used technologies to block out unwanted wavelengths of light. These filters are fabricated using alternating layers of dielectric materials with different refractive indices. By designing the thickness of each layer, these filters cause constructive and destructive interference to transmit or block specific ranges of light [66]. In terms of transmission at 850nm, dielectric interference filters offer excellent performance. Some variants of this technology can exceed 90% transmission in the desired wavelength [26]. They can also be designed to have a Full Width Half Max (FWHM) as narrow as 10-20nm; in our case, we do not need that, but other FWHMs are available in the market. These filters have a high Optical Density (OD) on the unwanted wavelengths, with some having OD values of 4-6. This would provide strong support for the unwanted visible light in our system. Regarding integration feasibility, these filters can be millimeters thick. They can be bought mounted or unmounted in protective housings, making it very easy to install them inside the CMOS camera's modular lens system. However, the filter must be well aligned since the light must have an incident angle normal to the face of the filter; otherwise, it will not be effective, and other wavelengths of light might get blocked or not blocked. Regarding availability and cost, dielectric interference filters are widely available in the market, with different FWHMs and transmission wavelengths. They can be expensive in the American market. However, if outsourcing from Asian countries with more significant production, this technology would be very viable for our project.

Absorptive filters are one of the oldest technologies used to block certain wavelengths of light. This technology uses colored glass or polymers injected with specific dyes or compounds to block out unwanted ranges of wavelengths [67]. In terms of transmission at 850, these filters do not perform very well, having 40-70% transmission in NIR applications. This would limit the signal strength incident on the CMOS sensor, affecting the depth estimations. We find the same problem with the blocking efficiency of this filter; with OD values of 2 or 3 common in this technology, we would get 99-99.9% of the unwanted light blocked, allowing for 1-0.1% of this light to hit the sensor. One main factor when considering the feasibility of integrating this type of filter into our system is that most absorption-based filters are commonly long pass or short pass. Therefore, two filters would require only a short range of wavelengths. This would ultimately make it harder to insert them inside the lens module. The good thing about these filters is that they are not affected by alignment; therefore, they do not need to be placed inside the lens module but are probably in front. In terms of availability and cost, this type of filter is widely available and very cheap, making it an attractive solution to block visible light from entering our CMOS camera.

Hybrid filters combine the principles of the last two technologies, which capitalize on the strengths of each type. Typically, a thin-film interference coating is applied to an absorptive glass substrate. This allows for precise spectral selection by the thin film and suppression of secondary transmission peaks by the absorption filter. Regarding transmission, hybrid filters perform similarly to a dielectric filter, ranging from 80-90% transmission [68]. Therefore, this level would be enough for our application and a viable option. The same is seen in the blocking efficiency, where, thanks to the thin film, we can get a blocking OD of 4 or higher, meaning we would block more than 99.99% of the unwanted light incident on the filter. Although this technology has two stacked filters, the thickness of a hybrid filter is still within a few m limiters, making it suitable for integration inside the camera lens module. Nevertheless, we still have to properly align the filter since the incident light is not close to having a normal angle to the face of the filter, which would cause problems with which bands are cooked or not. This technology is far less standard and more complex to find in specific wavelength transmissions. Therefore, their cost tends to be higher since they are used for specialized systems, making our system more expensive

Table 3.13: 850nm Bandpass Filter Technology Comparison

Filter Technology	Transmission at 850nm	Blocking Efficiency (OD)	Integration Feasibility	Availability and Cost
Dielectric Interference	High; >90%, narrow or wide FWHM	Very High; OD4-OD6	Moderate-High; Sensitive to angle of incidence, very thin	High availability Moderate cost
Absorptive	Moderate; 40-70%,	Moderate; OD2-OD3	Moderate; Need of two filters stacked, not sensitive to angle of incidence	High availability Low cost
Hybrid	High; 80-90%	High OD4	Moderate; Sensitive to angle of ' incidence	Low availability High cost

After evaluating the three filter technology options, we determined that dielectric interference is the most suitable for our application. The high peak of transmission and High OD in the blocking areas make it a good choice to give the CMOS camera the best opportunity to visualize the reflected light pattern and have fewer disparity errors. Although very available and cheap, absorption-based filters encounter problems with implementation, where we would need two to allow only a bandpass through. Additionally, hybrid filters are costly and not available. Therefore, with good alignment and integration, Dielectric interference filters will work best without an ASV system.

3.1.14 850nm Bandpass Dielectric Filter Product

Now that we have found a CMOS camera module and optical filter technology, we must find an appropriate filter that allows for wavelength drift while also having good blocking and transmission properties and being easy to integrate due to size. The filters we have chosen to analyze are the following: Nano Macro 850nm BPF [69], Shenyang Ebetter 850nm BPF [70], Everix Ultra-Thin 850nm BPF [71], and Thorlabs FBH850-40 [72]. We will evaluate these on their spectral performance, mechanical properties, and cost.

The filter from Nano Macro offers a Full Width Half Max (FWHM) of 20±3nm, a peak transmission of ¿90% with a blocking OD of 2-6. The FWHM of this filter does not allow for much wiggle room in terms of the lacing wavelength of the diode. Therefore, a stable current and temperature must be maintained to lace in between this range of wavelengths. Moreover, the transmission is perfect for our application. The OD range is very broad, but blocking 99% of unwanted light is more than enough for our case. Mechanically, the optical glass provides rigidity and sound transmission. However, the filter size is an issue since it will not fit inside the camera lens module. However, with proper communication with the provider, the sizes of these filters could be cut down to fit our applications. In terms of cost, this filter is very cheap and could be a viable option if the issue with the size is resolved.

The filter from Shenyang offers a much better wiggle room of FWHM from 10-50nm, fitting our cause ideally to avoid problems with detection if our laser module drifts in wavelength. Moreover, the filter has an OD of 3-6, which fits our use perfectly while still maintaining a peak transmission of greater than 90% at 850nm. Mechanically, the vast size range of 0.5-600x0.3-50mm gives us an incredible opportunity to perfectly fit the filter inside the camera module with no trouble while maintaining the good properties of optical glass. At just 5 dollars, this option is not very easy to integrate into our device but also to our budget.

The Everix Ultra-Thin filter has a normal FWHM of 33.5nm. However, by having a transmission average of greater than 65%, the integration into our system becomes questionable since this would cause significant problems with reflected light getting through the filter. While the filter is OD 2, it does not show the flexibility and power of the other filters when blocking unwanted light. However, this filter is 0.4mm thick and 12.45mm in diameter, made from a polymer, which means it's flexible and very easy to integrate inside the camera module because of its thinness. We would also avoid problems with damage caused by mechanical stress. However, if the filter is bent, incident light won't be normal to the surface of the filter, causing bad blockage of unwanted light due to incident angle dependency. The cost does not represent the moderate performance it provides for a price of 70 dollars. Therefore, it is no opponent to the previously discussed filters.

The Thorlabs filter has the best performance out of all of them. With a peak transmission of 90%, 40nm FHWM, and an OD greater than 5, this filter tops all the other filters in terms of performance. Showing that this filter is more well-suited for precision optics. Mechanically, the filter comes in a compact, protective casing with 25mmx3.5mm dimensions. This size is good for our integration and would be an excellent contender, except for the price. This filter, priced at 165 dollars, makes it economically unviable to use in our ASV system.

Table 3.14: 850nm Bandpass Filter Product Comparison

Product Name	**CW (nm)**	**FWHM**	**T%**	**OD**	**Size (mm)**	**Material**	**Cost (USD)**
Nano Macro 850nm BPF	850	20+-3nm	>90	2-6	80x1.1	Optical glass	10
Shenyang Ebetter 850nm BPF	850	10-50nm	>90	3-6	0.5-600 x0.3-50	Optical glass	5
Everix Ultra-Thin 850nm BPF	850	33.5nm	>65% Avg	∼2	12.45x0.4	Polymer	70
Thorlabs FBH850-40	850	40nm	>90	>5	25x3.5	UV Grade Fused Silica	165

After a thorough evaluation of all the filters, the Shenyang Ebetter 850nm BPF emerged as the most suitable choice for our system because of its good optical performance and size, which makes it easy to integrate into the camera module, as well as its unbeatable price of only 5 dollars. Other filters, like the one from Nano Macro, offer similar optical strengths, but physically, the integration into the system would be complex. Finally, the option from Thorlabs exceeded this project's performance and cost requirements.

3.1.15 Fiber Optic Splitter Technology

In order to get two outputs from one pigtailed laser diode, we must find a way to split that fiber into two fibers that share the power equally. For this, fiber splitters are spliced into the existing fiber from the pigtail, and the splitter divides the power into multiple outputs equally or in different percentages. For our case, we will explore the two most common technologies of fiber splitters: Fused Biconic Tapered (FBT) splitters and Planar Lightwave Circuit (PLC) splitters. These two technologies will be analyzed using the following criteria: Insertion and excess loss, Wavelength uniformity, and Availability and cost. We won't be analyzing their integration feasibility since both of these technologies come in similar-sized sealed modules, and both require splicing of the input fiber.

FBT splitters are one of the earliest and most established technologies for splitting light from fibers. The splitter is created by fusing two or more fibers together under rapidly high temperatures while being tensioned apart to create a perfect taper in the fused region, similar to the splicing process. An almost perfect taper region allows for the light from the input fiber to be split into multiple outputs [73]. From the insertion and excess loss perspective, FBT splitters show slightly higher losses than newer technologies. For a standard 1x2 50:50 FBT splitter, the typical insertion loss ranges from 3.2dB to 4dB, meaning an excess loss of 0.19dB to 0.99 dB [74]. For clarity, insertion loss is the ratio of input power to the output power of a single output. Therefore, a perfect split from one input to two outputs would equal an insertion loss of 3.01 dB. This might be a problem for low-power systems. However, when we can select our input power by selecting a different pigtailed laser diode, this does not become a problem except for being more energy-consuming. When evaluating wavelength uniformity, FBT splitters are moderately wavelength-dependent due to the physical nature of the fused region. They are often optimized for telecom bands such as 1310nm or 1550nm. Regarding availability, a FBT splitter for 850nm can be found, but it's not very available in the market; that being said, this is a very cost-effective option for splitting fibers.

PLC splitters are made using photolithography techniques, which etch optical waveguides into a silica-based substrate. These waveguides can be etched to split into two, and so on, making it possible to get many outputs from one input [73]. This process allows for a more controlled splitting of light. Therefore, in terms of the insertion and excess loss, it's not uncommon to find PLC splitters with excess losses of 0.1dB to 0.2dB in a 1x2 50:50 configuration, meaning an insertion loss of 3.11dB to 3.21 dB [74]. This is due to the waveguides' high precision, making it a very attractive option for telecommunications systems. PLC splitters demonstrate excellent uniformity across more significant ranges of wavelengths, often 1260nm - 1650nm. Concerning availability, many producers make PLC splitters dedicated to lower regions of NIR, such as 850nm, making it possible to find a PLC splitter for our cause. However, they can be found to be more expensive compared to FBT splitters, especially in high output counts.

Table 3.15: Fiber Optic Splitter Technology Comparison

Splitter Technology	**Insertion and Excess Loss (dB)**	**Wavelength Uniformity**	**Availability and Cost**
FBT	Moderate; Insertion loss: 3.2-3.5 Excess loss: 0.19-0.99	Moderate; Sensitive to wavelength changes of more than 100nm	High availability Low cost
PLC	Low; Insertion loss: 3.11-3.21 Excess loss: 0.1-0.2	High; Sensitive to wavelength changes of more than 200nm	High availability Moderate cost

After comparing both splitter technologies, FBT emerged as the most suitable choice for this application. Although PLC splitters offer better losses and wavelength uniformity, they are subject to mostly being available in a high number of outputs and not in 1x2 configurations. The higher losses of the FBT can be controlled with a higher-power laser diode, defeating the advantage of PLC splitters. Therefore, without significantly increasing the cost of this ASV system, we will use an FBT splitter.

3.1.16 Fiber Optic 2x1 50:50 FBT Splitter Product

The selection of an FBT 1x2 50:50 fiber optic splitter is critical for power efficiency and distribution. We have chosen to analyze the following three products: Thorlabs TG625R5F1A [75], eBay (item #315291630925), and Go4Fiber Part# MST-1X2-85-50/50-R-3-1 [76]. The main characteristics we are analyzing in these splitters are the following: Insertion and Excess loss, Splitting ratio accuracy, Operating wavelength range, and their cost. The insertion and Excess loss will tell us how much power is lost in the fused region where one fiber becomes two. The splitting ratio accuracy will tell us how much the power from one output can vary from the other output. The operating wavelength range will tell us how much range we have for our laser diode wavelength to drift. Finally, the cost will tell us how economically practical it would be to use that product.

The Thorlabs TG625R5F1A splitter is advertised as a ”1x2 MM Dual-Window Fiber Coupler, 62.5 micrometer Core, 0.275 NA, 50:50 Split, FC/PC”. In the datasheet, we could find that this splitter has an insertion loss of $\leq 4.2dB$ and an excess loss of $\leq 0.6dB$; this would mean that if a 100mW is input into the splitter, each end would have a minimum output of 38mW. While this is optically acceptable, we are wasting a lot of electrical energy, which could be a problem in terms of battery life. The splitting ratio accuracy is +-5%, which aligns with the acceptable tolerances of most FBT splitters. In terms of operating wavelength range, the fiber used in this splitter (Ø62.5 µm core, 0.275 NA OM1 graded-index (GRIN)) means it works best for 850nm and 1300nm light, with a ±40nm range. Although this might be concerning if we reach wavelength drifts of over 40nm, this fiber still works at bigger or smaller wavelengths, just at a higher attenuation cost, which, for our short distance, this attenuation is negligible. Cost: This product is very expensive at 249.90 dollars, which makes it challenging to use in our project due to our tight budget.

The product, with item number #315291630925 from eBay, claims to be an ”850nm MM 50/50 Coupling Ratio ST/PC 1x2 FBT Coupler FBT Fiber Optic Splitter”. We can find that this product has an insertion loss of $\geq 3.8dB$ and an excess loss of $\leq 0.3dB$, which is an excellent tolerance for FBT splitters. This means that a 100mW input would turn into two 41.7mW outputs. This would make our system more energy efficient. This splitter has a uniformity of 0.6dB, which translates to a splitting ratio accuracy of approximately +-6.5%, which is also acceptable for our system. In terms of operating wavelength range, this splitter uses the same Ø62.5 µm core, 0.275 NA OM1 graded-index fiber (GRIN) as the Thorlabs product, making it again suitable for our application. Cost-wise, this product is 28.49 dollars. This is an excellent price, considering no minimum order quantity is required.

The third product, ”Go4Fiber Part# MST-1X2-85-50/50-R-3-1,” is said to be a ”Multimode 1X2 coupler/tap, OM1 62.5/125um fiber, 850nm, 50/50 split ratio”. From the spec sheet, we know this product has an insertion loss of $\leq 3.9dB$ and an excess loss of $\leq 0.8dB$, making it also a perfect contender between the three products. These losses would mean that the two outputs of a 100mW input would be 40.7mW, which is also acceptable for our system. This splitter has a uniformity of 0.6dB, translating to an accuracy of approximately +-6.5% splitting ratio. In terms of operating wavelength range, this splitter uses the same Ø62.5 µm core, 0.275 NA OM1 graded-index (GRIN) fiber as the last two products, making it again suitable for our application. This splitter costs 40 dollars, making it very attractive for our budget.

Table 3.16: Fiber Optic 2x1 50:50 FBT Splitter Product Comparison

Product Distributor and Number	**Insertion and Excess Loss (dB)**	**Splitting Ratio Accuracy**	**Operating Wavelength Range**	**Cost (USD)**
eBay #315291630925	Insertion: $\leq 3.8dB$, Excess: $\leq 0.3dB$	50:50 +-6.5%	850nm ±40nm, With the possibility of handling other wavelengths at higher attenuation	28.49
Thorlabs #TG625R5F1A	Insertion: $\leq 4.2dB$, Excess: $\leq 0.6dB$	50:50 +-6.5%	850nm ±40nm, With the possibility of handling other wavelengths at higher attenuation	249.90
Go4Fiber # MST-1X2-85-50/50-R-3-1	Insertion: $\leq 3.9dB$, Excess: $\leq 0.8dB$	50:50 +-6.5%	850nm ±40nm, With the possibility of handling other wavelengths at higher attenuation	$40

In conclusion, we chose the eBay #315291630925 product due to its low price and excellent loss. Although Thorlabs is a reputable source of optical equipment, the price for their splitter is economically impossible for this project, and they have higher losses than the other two products. Although the splitter from Go4Fiber is also relatively cheap, eBay offers a money-back guarantee if the product doesn't fit our system and has to be returned. Therefore, moving on, we will use the eBay product in our system.

3.2 Electrical Hardware Technologies

3.2.1 Localization

General location information is needed to be gathered so that the system can determine what aisle or section of the store the user is in, cornerstones of both the navigation and route planning algorithms. There are several methods that can be used for this purpose including Inertial Measurement Units (IMUs), GPS tracking, and simple estimates based on the last known product gathered.

IMUs contain both a gyroscope and an accelerometer, which combined allow a software system to estimate where the object is moving, which is used to provide a relative location.

Along with this information, a known location at which the data starts is used to give an estimate of the absolute location of the object that the IMU is attached to. One downside of this technique is that most inexpensive IMUs tend to "drift" over time as their sensors are not completely accurate and therefore, they tell the software they are moving at a different pace than they actually are. Although this is a problem for all IMUs, including those used in high-stakes commercial and military applications [77], the problem is much more pronounced with the inexpensive IMUs that will be used for this prototype. While the IMU used should be well calibrated, this limitation should be taken into account when determining what method to use for localization. Although this is a major limitation, a major benefit that using an IMU has over other solutions, assuming that you have a good known starting location, is that since the calculations are relatively primitive from sensors which are physically on the unit, location changes are able to be determined very quickly.

On the other hand, GPS calculates location information based on information sent by some of 32 orbiting satellites deployed by the US Government. These satellites have a known location and trajectory around the world and each repeatedly send radio signals with timestamps which are kept in close sync with one another. The GPS receiver then uses these timestamps from as many satellites as it can gather to triangulate the location using some math [78]. Because the receiver is a different distance from each satellite, it can use the difference in time for the radio signals to reach it to determine its location, Using linear algebra, a system of equations, such as the one shown below, using the spherical coordinate system can be comprised to find the receiver's location. The more satellites that can be used for this task, the better accuracy the receiver will have. This type of GPS has a 50% accuracy at 16 meters from the true location [Page 10 of that paper]. Because this project has localization in a very confined vicinity for which a 16 meter diameter would cause the system to believe it is in a completely different position than it is, GPS is therefore eliminated from use for this reason alone.

$$\begin{Bmatrix} (x_0 - X_1)^2 + (y_0 - Y_1)^2 + (z_0 + Z_1)^2 = d(\Delta t_1, e)^2 \\ (x_0 - X_2)^2 + (y_0 - Y_2)^2 + (z_0 + Z_2)^2 = d(\Delta t_2, e)^2 \\ (x_0 - X_3)^2 + (y_0 - Y_3)^2 + (z_0 + Z_3)^2 = d(\Delta t_3, e)^2 \\ (x_0 - X_4)^2 + (y_0 - Y_4)^2 + (z_0 + Z_4)^2 = d(\Delta t_4, e)^2 \end{Bmatrix}$$

Each of these have their own advantages, with the main ones being the simplicity of each solution, along with pre-made drivers with support in popular algorithms for most commercial off-the-shelf (COTS) IMUs. On the other hand, their drawbacks are quite unique, with the IMU drifting quite substantially over time since the last known given location, GPS not being very accurate - especially if the location of the store doesn't happen to have many satellites for the module to utilize at that time - although it does provide some movement information similar to the IMU, and simple estimates based on the camera movement being even less accurate even though it wouldn't require additional hardware.

Since each item gathered is a known point for the IMU and it's not expected to take an exceptionally long amount of time between which items are gathered, this limitation, unlike those inherit in the other possible solutions is able to be overcome. In addition, slight drifting is not something that would be likely to impact the results from the navigation algorithm in a significant way. Because of these reasons, we have decided to use an IMU for general location information, leaving object detection to the IR depth camera system sensor and associated algorithms.

Table 3.17: Comparison of Localization Systems

Localization System	Advantages	Disadvantages
IMU	Native ROS Support Widely used, easy to implement Accurate with relative precision.	Accuracy drifts with time
GPS	Hard to implement Good for broad location information (starting location)	Accurate within 50-100 ft (not fine enough for this project) Less accurate indoors
Approximations	Very simple to use and implement	Least accurate.

The following are a comparison between several popular IMUs that can be used for this purpose:

Table 3.18: High Level IMU Comparison

IMU Name	Advantages	Disadvantages
Bosch BMI270	Has ROS2 drivers Robust on-chip noise filtering Contains Titan Core for on-chip configuration.	More complex, needs software loading on startup More development time because of complexity.
Bosch BMI323	Has ROS2 drivers Robust on-chip noise filtering. Newest solution from this list, best community and manufacturer support.	Does not allow on-chip configuration with Titan Core.
TDK MPU6000	Has ROS2 drivers Older solution means large back catalog of prior support. Lower default frame times, easier to filter noise in post-processing	Older, therefore falling out of favor since some drivers must be backported Little to no noise filtering on chip.

Table 3.19: IMU Components Comparison

Part Number	DoF	Voltage Input	Digital Interfaces	Magnetic Compass?
Bosch BMI270	6	1.71-3.6V	SPI, I2C	No
Bosch BMI323	6	1.71-3.63V	SPI, I2C	No
TDK MPU6000	6	2.375-3.46V	SPI, I2C	No

Because of these reasons and the specifications of each of the individual IMU solutions, we will be using the Bosch BMI323 sensor as the IMU for this project primarily because of the best cost per performance of the compared solutions, along with robust hardware and community support due to its popularity and simplicity in configuration since we do not require the complexity that comes with the configuration of the Titan Core microcontroller on the BMI270 IMU that it is compared to in the above chart.

3.2.2 Audio Output

The audio system for the device is responsible for delivering cues to the user to indicate how and when they should maneuver the cart. This includes commands such as ‘turn right,’ ‘turn left,’ ‘stop,’ etc. Therefore, the audio system must be able to output discrete sounds that the user can interpret as the different commands and be easily heard within a noisy grocery store environment. The audio output system must also be small and lightweight to ensure the device remains portable.

Options considered for the audio output include piezoelectric buzzers and on-board mini speakers. Piezoelectric buzzers are typically smaller and more energy-efficient than speakers; however, they are only capable of producing various tones rather than coherent words or phrases. To avoid the user needing to correlate different tones to the different commands, a mini speaker that can output clear verbal commands is the better choice.

For the mini speaker, we browsed options suited for 'voice range' and had to select one with an appropriate nominal impedance for our purposes. Three products that were considered include a 2.5 Inch Full Range Speaker, 1.1 Inch 8 Ohm Voice Range Speaker, and 1.5 Inch 8 Ohm Voice Range Speaker. The three products along with their relevant parameters are listed in a table below for comparison.

Table 3.20: Comparisons between Three Different Speaker Models

Product	Part #	Nominal Impedance (Ohms)	Rated Power (W)	Sensitivity (dB SPL)	Frequency Range (Hz)
2.5 Inch Full Range Speaker	93144	4	3	88.5	200-20000
1.1 Inch (28 mm) 8 Ohm Voice Range Speaker	28RN08M-1	8	8	86	650-6000
1.5 Inch (40 mm), 8 Ohm Voice Range Speaker	40RN08M-1	8	1	81	350-6000

One of the important parameters under consideration for speakers is their nominal impedance. Speakers with lower impedance are generally more efficient at converting the same input power into higher volumes with less distortion. However, due to their lower resistance, which permits more current to pass through them, speakers with lower impedance can generate more heat. For the purposes of a small speaker that a user can hear within close range, an overly efficient audio system is not required. Higher impedance speakers are generally more commonly used and compatible with a wider range of drivers.

Comparing the two 8 Ohm speakers, we see that the main difference is in their rated power. Speakers with higher rated power are capable of producing more volume, but in this case the speaker rated for 1W should be sufficient. The sensitivity parameter indicates the volume produced by the speaker at a distance of 1 meter when 1W is applied. A sensitivity of 81dB SPL for product 40RN08M-1 should be more than sufficient given that the user will mostly be within 1 meter of the speaker at all times. 80dB SPL can be associated with traffic noises or a noisy restaurant. Any higher rated power will likely be extraneous and impose additional unnecessary demands on the power source. Therefore, lower rated power is preferrable for a portable system where energy usage needs to be optimized across components.

By comparing the three speaker models, product 40RN08M-1, the 1.5 Inch 8 Ohm Voice Ranger Speaker, appears to be the best choice for this product's audio system for its appropriate nominal impedance, low rated power, and sufficient volume and frequency capacity to produce audible sound cues.

A speaker will require using an amplifier since the microcontroller's pins will not be able to deliver sufficient voltage and current. There are several classes of amplifiers available, with a table for comparison below. Out of the available options, the class D amplifier was selected for its high efficiency.

Table 3.21: Comparisons of Different Amplifier Classes[79]

Amplifier Class	Typical Efficiency	Pros	Cons
A	∼15-35%	No possibility of crossover distortion.	Inefficiency = heat Single ended designs prone to hum and higher levels of distortion.
B	∼70%	Relatively high efficiency.	Potential for significant amounts of crossover distortion and compromised fidelity
A/B	∼50-70%	More efficient than Class A. Relatively Inexpensive. Crossover distortion can be rendered moot.	Efficiency is good, but not great.
G & H	∼50-70%	Improved efficiency over Class A/B.	Costlier than Class A/B but higher power levels are achievable in a smaller form factor.
D	>90%	Best possible efficiency Light weight.	Pulse width modulators operating at relatively low frequencies can compromise high frequency audio reproduction. Some designs produce varying sound quality depending on speaker load.

Exploring available Class D amplifier ICs, we shortlisted to ensure that the output was higher than 1W and the amplifier could handle the 8 Ohm load. A widely used model that met our design specifications was the PAM8302AASCR amplifier. This amplifier has a 1-channel output, maximum power of 2.5W, and minimum load of 4 Ohms, which meets the requirements of our speaker.

3.2.3 Haptic Output

Haptic motors are used in this device to supplement the directional audio cues that the user receives. The motors will interface with the shopping cart's handlebars so that the user can perceive the tactic feedback while pushing the cart. The motors need to small enough to where the user can easily connect them to the handlebar and powerful enough for the user to perceive the vibrations through the handlebar. Varying intensity of the haptic motors will be used to communicate proximity to an obstacle, and delivering vibrations on one side of the handlebar will indicate the user to turn in that direction.

When considering types of haptic motors, we compared eccentric rotation mass (ERM) motors, linear resonant actuators (LRAs), and piezoelectric haptic actuators. ERM motors, which use DC voltage, produce vibrations by rotating an off-center weight. LRAs, which use AC voltage, rely on a linear oscillator to vibrate and typically offer more precise vibration control compared to ERMs. Piezoelectric motors offer the most precise haptic control and are more expensive than both ERM motors and LRAs.

However, ERM motors also have a larger startup and response time compared to LRAs and especially piezoelectric motors. This response time is generally within 100ms, which is acceptable for this device's use case. A table comparing the three different motor types is displayed below. Since this application does not require high precision in the different haptic outputs or response time, ERM motors appeared to be the best choice due to their ease of integration and lower cost.

Table 3.22: Comparison between ERM Motors, LRAs, and Piezoelectric Haptic Actuators

Motor Type	**Mechanism**	**Drive Signal**	**Power Consumption**	**Haptic Feedback**	**Size**	**Cost**
ERM	Rotation of an unbalanced mass	DC Voltage	Moderate	Strong but imprecise	Larger than LRA and Piezo	Low
LRA	Linear oscillation of a mass on a spring	AC Voltage at resonant frequency	Low	Moderately strong, more precise than ERM	Compact	Moderate
Piezo	Deformation of piezoelectric material	AC Voltage at high frequencies	Low to moderate	Very high precision	Ultra-compact	High

The selected ERM motor was a 10mm by 3mm flat coin type vibrational motor. This motor is rated up to 12000 RPM, with a DC input voltage range between 1.5V to 3.7V. Its small size makes it ideal for interfacing multiple motors with a shopping cart handle, and its RPM is sufficient for the user to perceive cues and feedback.

ERM motors may be controlled either through a transistor or a dedicated driver. Using a transistor requires PWM to vary the motor's vibrational intensity, which offers less control when compared to using a driver. Greater differentiation between the unique motor output levels is preferred for this project to facilitate users being able to identify and distinguish between them. To control the haptic motors, the DRV2605L haptic motor driver was chosen. This is a widely used low-voltage motor driver for both ERM and LRA applications, and it simplifies ERM motor control via I2C to provide a range of smooth haptic effects without complex PWM tuning. The different levels of haptic vibrational intensity will indicate to various directional and warning cues to the user. It outputs up to 5.2V, which is sufficient to supply the required voltage for the chosen ERM motors [80, 81].

3.2.4 Low-Level Logic

There are two main compute classes used for low-level and low-power compute for most systems: micro-controllers and custom logic. Custom logic can be implemented through either an Application-Specific Integrated Circuit (ASIC), which comes with a singular configuration from the factory, or a Field-Programmable Gate Array (FPGA), which has gates that can be reprogrammed at will using software.

This software normally is provided by the FPGA manufacturer such as Xilinx's Vivado or Intel's Quartus Prime but can also be done with general solutions such as those from commercial operators including Siemens, Cadence, and Synopsys, or with open source toolchains such as Yosys. Each of these tools utilize files written in a Hardware Description Language (HDL) such as Verilog, SystemVerilog, or VHDL, and then performs the processes of synthesis, implementation, and bitstream generation to finally get a file which defines the configuration for each gate within the given FPGA. The design, synthesis, and implementation steps are where each solution differentiates itself, with different levels of netlist optimization and reduction, along with tools to assist development. UCF has access to the free versions of the Xilinx and Intel tools as well as educational licenses to the Cadence and Synopsis toolchains. Since each FPGA chip type is unique, a BHDL file, normally supplied by the manufacturer, is used to define the configuration and pinmap for each FPGA. These are then used as part of the toolchain to generate the final bitstream generation top map the given netlists onto the FPGA. Each of these toolchains additionally includes software to then program the FPGA and potentially debug it if the bitstream includes a debugger.

ASIC development goes through much of the same process as in FPGA development, up until the FPGA is programmed. With an ASIC, after a few more operations are performed, the relevant files are provided to the fabrication facility which then produces the wafers with your ASIC. Because the logic isn't configurable, the size of the ASIC is able to be much smaller than a comparable FPGA, while also being significantly cheaper, by several orders of magnitude normally, on a per unit basis. While this is the case, ASIC development has very high fixed start-up costs for the parts the fabrication facility needs to develop unique for the submitted design. Additionally, partly because of this, a high minimum order quantity exists. Combined, these problems, along with losing the flexibility to change the design if any bugs are found late in the process and the amount of lead time needed to finally get the ASICs, mean that they do not nearly offer good competition to FPGAs for the purposes of prototyping or even small-scale production runs. This means the use of custom ASICs must be eliminated from consideration.

On the other hand, most of these drawbacks are not present with FPGA development as described above as they can be easily reprogrammed at will and normally do not have any significant minimum order quantities because they are standard designs that can and are shipped to many different customers to then place their own designs on. While this is the case, the main drawback of FPGAs is the high per-unit cost as compared to a comparable ASIC. This doesn't affect the viability of this project much as only a small number of FPGAs will be purchased and only a single FPGA will likely be used in the final design. This means that FPGAs remain a viable choice for which to implement the low-level logic for this project.

Microcontrollers, such as the MSP430, are off the shelf components that can be used for this purpose as well. Although they lack the ability to perform quite as much specialized compute without overhead such as the way that FPGAs and ASICs are capable of, they also have many advantages over these other solutions. Some of these advantages include, but are not limited to, standardization, both in programming and use, library availability, and ease of use. While FPGAs and ASICs are designed with HDLs, as described above, microcontrollers are generally programmed with standard programming languages, with additional custom libraries, such as C. This means that microcontrollers are therefore easier to program for those who have more experience with these programming languages, including the members of this group, as it allows the skills learned from previous Computer Science and Embedded Programming classes to be used directly. In addition, because these specific configurations are widely used, their standardizations means that many libraries and other software already exist which support some of the lower-level logic that would otherwise need to be programmed manually if using an FPGA or ASIC. Further, since these chips are simpler in design and produced at a much larger scale than either FPGAs or ASICs, they are again significantly cheaper per unit than either other solution in the amounts that would be ordered for this project, as well as normally lacking a minimum order quantity.

Table 3.23: Comparison of Low-Level Compute Systems

Type	Advantages	Disadvantages
Microcontroller	Easy to program, Existing libraries, Existing familiarity through previous classes (Embedded Programming)	May be slower and consume more power for a given task than other solutions.
FPGA	Limited existing familiarity through existing classes (Digital Systems, etc) Faster, more power efficient than microcontrollers Can order single FPGA	More expensive than microcontroller Harder to program correctly, not many IP libraries available for our use.
ASIC	Fastest	Must tape out many ASICs More expensive (overall) than other solutions Not easy to use or design Long lead time No existing familiarity

Therefore, due to the ease of programming, wide use, and cheap cost, among other reasons, a microcontroller will be used as the low level and low power logic for this project. This microcontroller will interact directly with most of the peripherals and control them while the high-level single board computer, as discussed in the next section, will perform more complex tasks such as the route planning and mapping algorithms along with hosting the web server for the user to interact with on their mobile device.

Some potential microcontrollers that could be used for this purpose include those from the STM32, ESP32, and MSP430 microcontroller families. Each of these are a family of similar microcontrollers of which we can choose from for the best mix of performance, power consumption, on-board storage size, and available peripherals. These families are compared in the below table:

Table 3.24: Comparison between Low-Level Compute Technologies

Family Name	Benefits	Drawbacks
STM-32	Wide use in industry - easy to source individual chips	Harder to source development boards with fast turnaround
ESP-32	Familiarity with Use - Existing Embedded Systems Class Easy C Libraries Wide use in industry Easy to source individual chips and development boards	Can be slightly more expensive than competing solutions.
MSP430	Tends to be a cheaper solution Easy to source individual chips and development boards	Lesser Capabilities, Simple Nature.

Because of the reasons presented in the chart above, because each of the options are quite similar, the features that finalized the decision to use the ESP-32 included the wide software and hardware support from the wider community, along with each of our prior experience in using the family in the previous classes and projects. Our familiarity with the processor will allow us to design and implement its functionality much faster than the other microcontroller families, even if most of the features are quite similar.

Out of these choices, the ESP32-WROOM-DA [82] decided to be used for this project primarily due to the wide use in commodity development boards that can be very quickly delivered and have the chip de-soldered from. In addition, some other reasons for choosing this specific variant include it having slightly higher needs than we currently have, such that we are not greatly concerned about running into hardware limitations, while also having low power draw and a sufficient amount of memory. We decided on these amounts as ideal because of the requirements from the following devices that will be connected to it, along with the processing required for their input and output: speaker, IMU, and haptic feedback motors. In addition, some other small tasks will be ran on the microcontroller, and the slight oversizing helps ensure that we have enough power in order to perform these tasks as well in addition to that required for the input and output for the peripheral hardware components that will be connected to it. In the end, even though the processor has been declared end of life by the manufacturer, it continues to be the most widely available variant of the ESP32 on development boards that can be cheaply obtained from online retailers such as Amazon. The key specifications for the ESP32-WROOM-DA can be found in the below table, and power usage information found in the relevant section found later in this chapter.

Table 3.25: Specifications of ESP32-WROOM-DA Microcontroller

Core Count	Max Core Clock	ROM	Flash Memory	Crystal Oscillator Frequency
2	240 MHz	448 KB	8 MB (SPI)	40 MHz

3.2.5 Single Board Computer

There are many options available on the market for higher-performance computing devices which will run an operating system and the more complicated algorithms used for navigation and route planning throughout the grocery store. These solutions range from single board computers to complete desktop computers and servers, each with their own benefits and drawbacks. For example, a very large server or desktop computer would not be ideal in this scenario because of the increased power consumption - therefore requiring a more robust power distribution system - along with a large size, a likely need for active cooling, and a higher price.

A laptop or mini PC could also be embedded in the product, which would alleviate the concerns with the large size and some of those regarding the power consumption of the final system, but still is much more powerful and expensive than is needed for this project, and therefore uses more power than other embedded solutions.

Another popular embedded solution is a single board computer. Popularized by the Raspberry Pi, first released in 2012 and now ubiquitous in the space, there are plenty of similar devices, some of which provide a very similar feature set and others providing something different for a different use case. These devices normally do not have a built in display or battery, neither of which are needed in this project, but contain many peripherals including USB and General Purpose Input/Output (GPIO) pins that can be used for many different purposes. Some additional examples of single board computers include, but are not limited to, the following:

- NVidia Jetson Nano
- Rock Pi
- Latte Panda

While the Raspberry Pi utilizes an ARM64 Cortex processor, with the latest Raspberry Pi 5 version having a quad-core processor at 2.4 GHz and up to 16 GB of RAM, several competitors - including NVidia and the LattePanda - utilize a processor with an AMD64 instruction set. [83] While the Arm processor in the Raspberry Pi and similar solutions uses less power than its AMD64 counterparts due to the use of a Reduced Instruction Set (RISC) - as compared to the Complex Instruction Set (CISC) that is implemented in Instruction Set Architectures (ISAs) such as AMD64 and x86 - it also does have some disadvantages.

The main disadvantage of using an ARM processor is the lack of software support due to it being less popular overall. However, due to the popularity in the embedded computing market, especially with the Raspberry Pi, this is not much of an issue for the software that will likely be used on this system for the navigation and route planning algorithms.

While a comparable single board computer (SBC) could be used to power this portion of the system with slightly more functionality or power than the Raspberry Pi, the latest Raspberry Pi 5 with 8 GB of RAM will be used for this project due to the good software and hardware support due to the popularity of the Raspberry Pi series of SBCs along with a greater likelihood than some smaller competitors of being in stock at any given moment when the board needs to be purchased for the next steps in this project. Although there was a substantial period of time throughout the past few years during which Raspberry Pis were almost constantly out of stock - one big reason that clones started appearing - this issue appears to be mostly solved at this point in time and there should not be worry about being able to procure the Raspberry Pi 5 or a highly similar model which will also perform the same function nearly identically to that of the Raspberry Pi 5.

Table 3.26: Comparison of Single Board Computers

Product	**Advantages**	**Disadvantages**
Raspberry Pi 5	Dual core ARM processor, enough for our uses Several SKUs for different amounts of RAM Official support for ROS2	Modern, less backtested support.
NVidia Jetson Nano	Standard and known formats	Relatively old Not used by many products.
Latte Panda	High compute power, more than enough for our uses.	High power requirements High heat generation High cost

3.3 Power Supply Unit

This section covers the choices made in power supply and distribution for our system, including the electrical requirements of each component, the chosen power source, and regulators to allocate the appropriate voltage and current to every component used throughout the overall system.

3.3.1 Power Requirements

To determine the total power requirements of the system, a list of all components that would intake power from the battery sources was generated. To estimate the average power consumption, a 90% efficiency with DC-DC converters was assumed to ensure that the chosen battery would be sufficient. Components such as the laser diode, speaker, and ERM haptic motors are excluded from this list as they will indirectly receive power from the battery through their drivers and amplifiers, which account for their specific voltage and current requirements. The CMOS Camera modules are also excluded as they are powered by the Raspberry Pi 5.

Table 3.27: List of Components with Voltage and Current Electrical Specifications

Component	Supply Voltage	Maximum Current Draw	Maximum Power Consumption	Average Power Consumption (90% Efficiency)
FL500 Laser Diode Driver	3-12V (5V)	250 mA	1.25W	1.39W
Bosch BMI323 IMU	1.71-3.63V (3.3V)	790 uA	0.0026W	0.003W
PAM8303AASCR Class D Amplifier	2-5.5V (3.3V)	450 mA	1.485W	1.65W
4x DRV2605L Haptic Motor Driver	2-5.2V (3.3V)	80 mA x 4 = 320 mA	1.056W	1.17W
ESP-32 Microcontroller	3.0-3.6 V (3.3V)	40 mA	0.132W	0.15W
Raspberry Pi 5	5V	5A	25W	27.77W
Total	-	6.06A	28.93W	32.14W

The total estimated power consumption for all of the components directly connected to the main power supply is 32.14W.

3.3.2 Power Source

There are several potential methods for powering the system components, including rechargeable batteries, disposable batteries, external power sources (e.g., wall outlets), and solar power.

Using wall power can be immediately ruled out, as it would significantly compromise the portability of the system. Relying on a wall outlet would either require an excessively long extension cord, which would be both inconvenient and a potential tripping hazard for the user and other shoppers or severely limit the mobility of the device.

Similarly, solar power is impractical in this context. The lighting conditions in most grocery stores are insufficient to generate the necessary energy for reliable system operation. This could result in inconsistent power delivery, leading to brownouts that would reduce the system's usability and risk damaging certain components.

With these options eliminated, the choice comes down to disposable versus rechargeable batteries. While disposable batteries may have a lower upfront cost and are easy to replace, they have a significantly higher long-term cost compared to rechargeable batteries paired with a charger. Additionally, the convenience of disposable batteries can be replicated by using multiple rechargeable battery packs, allowing quick swaps if needed.

However, for this application, the ability to swap batteries is likely unnecessary. The system will not be in continuous use for extended periods, and any downtime between uses can be utilized to recharge the batteries. Given these factors, rechargeable batteries are the most suitable power source for this project, balancing cost-efficiency, portability, and system reliability.

3.3.3 Battery Technology

When selecting the appropriate battery technology for this project, key factors to consider include energy density, cost, rechargeable cycle life, safety, and potential risks. The options evaluated are Lithium-ion (Li-ion), Lithium Polymer (LiPo), and Nickel-Metal Hydride (NiMH) batteries. Each of these technologies offers distinct advantages and drawbacks, which are summarized in the table below.

Li-ion and LiPo batteries provide the highest energy densities, making them well-suited for portable systems requiring extended runtimes in a compact form factor. LiPo batteries are typically preferred in applications that require high current draw, while Li-ion batteries are more efficient for delivering longer runtimes at lower discharge rates. In contrast, NiMH batteries, though safer and more affordable, are generally bulkier and heavier, making them less favorable for portable applications where form factor is critical.

Cost also plays an important role. NiMH batteries are usually the least expensive but may not deliver the necessary energy density for this application. LiPo and Li-ion batteries fall within a similar price range, although high-discharge-rate Li-ion cells that rival LiPo performance can be more costly.

Rechargeable cycle life varies across the technologies. NiMH batteries can last up to 1,000 cycles, but since the power demands of this project are unlikely to involve frequent full charge-discharge cycles, the slightly shorter cycle life of Li-ion and LiPo batteries remains acceptable. However, newer models of Li-ion batteries, known as Lithium Iron Phosphate (LiFePO4) batteries, can support much longer life cycles, matching and even exceeding those of NiMH batteries.

Safety, is a primary concern—especially given that the system will be operated by users with low vision, which necessitates minimizing risk during handling. LiPo batteries, while capable of delivering high current, are particularly sensitive to swelling, punctures, and thermal runaway, even when paired with protection circuitry. NiMH batteries are the safest option, but at the expense of portability. LiFePo4 batteries are generally considered safe, with many battery products including protection circuitry and battery management systems. The comparisons between the three battery technologies are summarized in the following table [84, 85, 86, 87, 88].

Table 3.28: Comparison Between Battery Technologies

Battery Technology	Energy Density	Output Capacity	Cost	Rechargeable Cycle Life	Safety	Potential Risks
Li-ion	High	Moderate	Moderate	500-5000 cycles	Moderately safe with protection circuits	Overheating, thermal runaway without protection
LiPo	Very high	High	Moderate	300-500 cycles	Less safe, prone to swelling and puncture	Thermal runaway, risk of swelling without protection circuitry
NiMH	Moderate to low	Low	Low	Up to 1000 cycles	Very safe	Bulky and heavy

After evaluating these factors, the decision was made to use LiFePo4 batteries, a safer subset of Li-ion chemistry, for this project. LiFePO4 batteries maintain the rechargeability and compact size advantages of Li-ion cells, while offering enhanced thermal and chemical stability, making them much less prone to overheating or combustion. They also offer a longer cycle life than standard Li-ion and remain within a manageable cost range.

3.3.4 Battery Charger

The battery charger may be either built into the overall system or it could be located externally. A built-in charger would be more convenient for the user as wall power could be provided directly to the unit, with or without a simple external AC to DC adapter, and also simplify the design of the overall unit as the batteries wouldn't need to be easily replaceable from the outside of the unit. A built-in charger may also significantly increase the weight of the overall unit and consequently require a more complex design to dissipate the heat generated from charging the batteries, potentially requiring active cooling. This is the case even though the convenience benefits are relatively minor.

On the other hand, using an external battery charger would require the user to be able to remove the battery pack - requiring additional packaging around the battery pack for safety - and a small additional unit. These drawbacks are relatively minor compared to the alternative of requiring active cooling for additional components of the unit, being able to utilize additional COTS products such as a balanced charger, and having the unit be lighter overall - therefore leading to easier maneuverability and usage. Because of these reasons, it will be more advantageous for the goals of this project to use an external battery charger.

3.3.5 Battery Capacity

A requirement of the system is that it has sufficient power to operate for at least one hour. To ensure the battery can support the full system during this time, the rated Watt-hour

(Wh) of the battery must meet or exceed the total average power consumption of the components. Additionally, the battery must be capable of supplying enough current to support the system's maximum current demands.

For this application, a 12V, 10Ah LiFePO4 battery was selected as the primary power source. This chemistry, a subset of lithium-ion technology, is known for its enhanced safety, thermal stability, and long cycle life—exceeding 2,000 charge cycles under standard use. The battery provides a total energy capacity of 120 Wh, which is well above the system's estimated requirement of 32.14 Wh, offering a comfortable margin for safe and sustained operation.

The 10Ah capacity indicates that the battery can deliver 10 amps for one hour or, conversely, 5 amps for two hours. The system's maximum current draw is approximately 6A, placing it well within the battery's recommended continuous discharge rating of less than 30A. This ensures that the battery can safely power all components without approaching thermal or electrical limits.

In terms of runtime, the battery's 10Ah capacity exceeds the system's 6A maximum draw, indicating that the system can theoretically run for more than 1.5 hours under worst-case power conditions. This aligns with the design goal of achieving at least one hour of operational runtime. Additional testing will be conducted to validate the battery's actual discharge performance under load and ensure that it consistently delivers the required current to all components.

This LiFePO4 battery provides a strong balance of safety, energy capacity, and current delivery, making it well-suited for this system's portable power requirements.

3.3.6 Voltage Regulators

To ensure that each component receives the correct voltage, a series of step-down or buck voltage regulators are required. The two main types of voltage regulators are linear regulators and switching regulators.

Linear regulators operate by dissipating excess voltage as heat, making them step-down converters with relatively simpler designs that produce less noise and are more cost effective compared to switching regulators. However, they are significantly less efficient, especially when stepping down from high to low voltages where the excess can contribute to a lot of heat generated within the system.

Switching regulators on the other hand use high frequency switching elements and energy storage components to efficiently convert voltage levels, reaching efficiencies of over 90%. This allows them to handle higher electrical and thermal requirements, but they can be more design and cost intensive due to requiring additional components. They are more suited for applications with higher voltage and current demands where system performance is critical, whereas linear regulators are preferred for simpler, low cost and low noise applications. The main features of the two regulator types are compared below.

Table 3.29: Regulator Types[89]

Regulator Type	Efficiency	Heat Dissipation	Noise	Cost	Applications
Switching	High (∼90%)	Low	Higher	Higher	High-power, high-efficiency
Linear	Low (∼30-50%)	High (excess power dissipated as heat)	Very low (ideal for sensitive circuits)	Lower	Low-power, low-noise

The chosen Li-ion battery outputs a maximum of 11.1V, but several of the components operate at voltages much lower than that. The components are categorized by the voltages they require in Table 3.30 with a suitable voltage regulator product. Since the step-down conversions are relatively large, switching regulators were chosen as the ideal regulator type for this project to avoid excessive heat generation due to the linear regulator's lower efficiency.

Table 3.30: Voltage Regulator Technologies for Listed Components

Operating Voltage	**Components**	**Voltage Regulator Technology**
5V	Raspberry Pi 5 Laser Diode Driver	TI LM2679-5.0 Step-Down DC/DC Switching Regulator
3.3V	ESP32 4 x Haptic Motor Driver IMU Class D Amplifier	TI LM2679-5.0 Step-Down DC/DC Switching Regulator

The TI LM2679 Step-Down Voltage Regulator was chosen for its robustness. It handles an input voltage range between 8-40V and outputs 3.3V, 5V, or 12V at up to 5A. The chosen battery technology is suitable as a supply for these regulators, and the output current is sufficient to account for the maximum draw for the listed components. For the components requiring 5V, the regulator was designed in WEBENCH to convert an input of 9-12V into 5V at 5A to ensure proper voltage and sufficient current for the Raspberry Pi. Since a single regulator cannot output more than 5A, a second 5V regulator was included to supply power to the laser diode driver. This regulator was set to output a maximum of 2A in the event that a different laser diode was required. Similarly, another regulator was designed to output 3.3V at 2A for the MCU, haptic motor drivers, class D amplifier, and IMU. The 5V regulators have an estimated efficiency of 87.9%, and the 3.3V regulator has an estimated efficiency of 90.6%.

3.4 Communication Protocols

3.4.1 Wired vs Wireless

There are many advantages and disadvantages to each communication method, some of which are more important than others for our specific use cases. One major advantage wired communication methods have over wireless methods is in resilience to interference. Today, there is a lot of RF and wireless signals on just a few common bands which can easily interfere with each other and introduce the need to handle both this excess data along with any that may not be received, the rate of which is likely higher than in similar wired communications. This means that the reliability of data transfer suffers when using wireless instead of wired. In addition, wired signals are able to potentially be transmitted faster than those with similar wireless methods. This is true in terms of both latency and total throughput, partially because of the overhead introduced because of the reliability qualms discussed just prior, along with other encoding and decoding overhead.

On the other hand, wireless communications are much more flexible in that the devices don't need to be physically connected to communicate with each other. Although there are some problems introduced with wireless communication methods which may not be ideal for every scenario, there are some where the convenience and flexibility of a wireless network can overcome the drawbacks.

Taking this all into consideration, we will use wired communication methods for all communications except for with the device that will be loading the item list before the navigation phase, which will use existing wireless standards such that we don't have to directly implement the interference mitigations. One of the main reasons most everything will be connected physically is because they will already need to be for power distribution, which eliminates the flexibility introduced by using a wireless standard. On the other hand, the device that will be loading the item list will be standalone and have its own power source.

3.4.2 Wired Communication Protocols - Series vs Parallel

There do not exist too many differences between the functionality provided by series and parallel protocols in the modern era since series communication has achieved speeds that are more than fast enough for most uses while having many usage advantages over parallel protocols. Some of the reasons that parallel communications would want to be used in this case would be if a lot of different data would be required for processing at the same time, not just in close vicinity to each other. This is because of the nature of the two different ways of transferring data, with series communication sending a single bit per lane back-to-back with a limited number of lanes. Some modern standards that implement series communication include USB, Thunderbolt, and most other modern standards. On the other hand, parallel communications send multiple bits at the same time across many different lanes. This causes the need for an increased number of physical wires to connect the devices for data transfer, which makes most everything between the connected devices more expensive for implementation, including the controllers, connectors, and cables. Because it has been possible to further increase the transmission rates of serial communication standards such as USB (20 Gbps with USB 3.2 Gen 2x2) and Thunderbolt 4 (40 Gbps), the need for parallel standards has dwindled. This causes the serial standards to become even more mature, further increasing our reasoning for choosing to use a series communication standard for most of the connections throughout this project. Many other series protocols are available to be used without much overhead and will be discussed in an upcoming section.

While this is the case for most of the data throughout the systems, there is a data stream present within this project that is best suited for parallel data transfer: the information from the Depth sensor system. This is the case because the sensor streams a near constant and consistent amount of data to the processor for the software to interpret for object detection and avoidance. This use case is best matches for a parallel data stream over one that is serial because of this constant information flow without the explicit need for bit-accurate information being received due to the refresh rate of the information being received from the sensor. In addition, since the sensor is being built from scratch as a sub-system of this project, we are more able to easily influence the data technologies used throughout it than for COTS components. Due to these unique requirements for the LiDAR sensor, parallel data is more likely to fit the needs for this specific component than a serial connection as will be used for the remainder of the communications.

3.4.3 Wireless Communication Protocols

Two of the main consumer wireless protocols available for use in common microcontrollers and commercial off the shelf devices such as smartphones are WiFi (IEEE 802.11) and Bluetooth. Both of these protocols use the same base 2.4 GHz frequency but there are some major differences between them. Two of the main differences between the two protocols are speed and use in direct connections. WiFi is much faster than Bluetooth, at 300 Mbps for even the old 802.11b/g/n standard vs 2 Mbps for the relatively new Bluetooth 5.0 standard. Although this is the case, because constant data streaming isn't needed for this application and it isn't very time sensitive with high amounts of data being transmitted from the device to the compute on the shopping cart attachment, this limitation of Bluetooth isn't of greatest concern. In addition, Bluetooth supports many more Low Energy states than does WiFi, which means that it can draw less power from the batteries, either allowing us to have less capacity or longer battery life for the system as a whole.

On the other hand, Bluetooth is designed for point-to-point connections, and the devices don't even need to be paired under certain scenarios, while WiFi was designed first for broader network traffic with an access point and many other devices. Because of this designed usecase, Bluetooth also has much less of a usable range than does WiFi, especially when both are used on the 2.4 GHz band, which will be used in this project. While this has been somewhat remedied by the introduction of the WiFi Direct standard, the implementation of WiFi for point-to-point use is still not as mature or widely used as is Bluetooth for this purpose.

One additional concern with the use of WiFi is congestion that may occur with many access points in a small area. This is especially a concern in the 2.4 GHz spectrum, which has many fewer channels than are present in either the 5 GHz or 6 GHz spectrum allocations. This is much less of a concern with Bluetooth as the range and transmit power tend to be less than with WiFi. Since some grocery stores are small and may have many networks themselves as well as those from their neighbors, this is something that must be considered. Although this is the case, because the use of WiFi throughout the main use of the system is not critical, this can be mitigated by other means, such as physically moving to a different location within the store to load the items into the user's shopping list if this becomes a problem.

Mainly because of these limitations of Bluetooth, WiFi is much more widely used in industry for HTTP traffic since the vast majority of use cases would require more than a single device on an Access Point, something that can be easily accommodated securely over WiFi using a modern security standard such as WPA3, which Bluetooth does not support.

While this is the case, even with this limitation, WiFi is much more robust in supporting TCP and HTTP traffic which will be used for the web server hosting the grocery list input application. With all this information taken into account, the WiFi communication standard will be used between the single board computer, containing a wireless chipset, and the mobile application which will input the required data for route planning.

Table 3.31: Wireless Communication Technology Comparison

Name	Advantages	Disadvantages
WiFi (IEEE 802.11)	Greater bandwidth More established use for HTTP Designed for use between many systems	May be overkill May conflict with nearby networks
Bluetooth	Meant for use between two systems.	Lesser bandwidth Lesser range

3.4.4 Abstracted Wired Communications Protocols

Robotics in itself has historically posed a major problem in parallelization for embedded systems. With the need to constantly be reading sensors, running sensor processing and fusion algorithms, and making intelligent decisions based on that data poses a problem for the typically low compute microcontrollers or single board computers found on robots. That said, an acceptable level of concurrency has been achieved, and it is through the collective contributions of thousands of software developers that this infrastructure exists.

With that said, the most common approach to handling these concurrency problems is the implementation of high-level inter-process communication protocols. For instance, a robot would be debilitated if it had to pause its control algorithm for an extended period of time, but it still needs to receive localization and planning data consistently. At a high-level, this is usually solved through the implementation of a publisher-subscriber system, that allows processes to speak to each other during run time. This can be done through a custom implementation in a low-level language such as C++ or Rust, the integration of a middleware DDS (like the one in ROS2), or the use of something in between, such as MQTT.

The main tradeoffs when comparing these three approaches contrasts development time and overall performance. For instance, while it is much easier to develop with the extremely extensive toolset that a DDS provides, not all of the functionality is needed, and thus may cause memory or compute bloat that can significantly harm a robot's performance utilizing a single board computer such as a Raspberry Pi or Jetson Nano. On the other hand, it can take full-time robotic software developers months to fully design and implement an effective pub/sub model in Rust or C++. Given these demonstrated tradeoffs, and the previous development experience of the developers on our team, we have decided to utilize a DDS due to its marginally worse performance when compared to its toolset and support that has been developed for over a decade.

Table 3.32: Abstracted Wireless Technology Comparison

DDS Implementation	Latency	Scalability	Ease of Implementation
DDS	Moderate	High	Moderate
MQTT	High	Moderate	Moderate
Custom Rust/C++	Low	Low	Difficult

3.5 Software Technologies

3.5.1 Input and Output Control

3.5.1.1 Grocery List Input

The decision on how to configure the Single Board Computer (SBC) to receive grocery lists is hierarchal in nature, but with the highest-level decision being made of whether to establish a mobile application or a website. That said, the easiest configuration to work with would be to set up a web server on the SBC.

A web server is more practical, at least for the proof of concept being designed here, compared to other solutions such as a mobile application for several reasons. Some of these reasons include mobile apps needing to be developed for each application separately with most approaches, and even with platform-agnostic solutions such as Google's Flutter framework, still requires tailoring of the application to each platform. This would likely lead to the limiting of the application to a single platform which is much less flexible to the end user. In addition, mobile applications must meet strict standards and be approved by Apple if it is wanted to be used on Apple devices as there is no easy way to sideload on an iOS device unlike on Android, where the process is trivial.

In addition to avoiding these pitfalls, a web server has some additional advantages, including using standard HTTP and TCP protocols for all data transfer, instead of potentially needing to develop our own standard or API endpoint solution which would likely need to be the case with a mobile application.

There are many web frameworks that can be used for the website. Some of these frameworks include Google's Flutter, AngularJS, and Django, each of which provide their own advantages. Each of these platforms uses a common language, with Dart, JavaScript, and Python being used respectively. While Django and AngularJS are solely used for web applications, Flutter provides the additional flexibility of allowing the build of native applications for Android, iOS, Windows, Mac, and Linux if there was a want for adding such functionality in the future. While it's not without configuration to perform such builds, there is minimal configuration needed. In addition, while each of the listed frameworks are open source projects with a plenty of usage along with community support and development, Flutter is maintained by Google which has provided extensive documentation and has dedicated a lot of resources to developing the platform as something that will be able to be used on many different platforms far into the future. Because of these advantages that Flutter has over other Web Application Frameworks, Flutter will be used to host the website that will be used to collect the grocery list to be used for navigation purposes.

3.5.1.2 Map Generation and Storage

Before any navigation can be conducted, there are two maps that the shopping cart needs in order to, one, properly plan routes, and two, effectively localize in the store. The first map can simply be referred to as a ‘product map’, which is more technically described as a grid-based representation of the store, the aisles, and a description of which products are contained in each cell of the grid.

A product map, as stated, will be utilized to provide a low-fidelity representation of the store that our chosen routing algorithm can work on. Once we have the complete list of groceries from the web-based input, a routing algorithm can effectively derive the optimal order of waypoints to navigate to. These waypoints can represent specific product locations, but can also represent the pharmacy, the deli, or the restrooms, for example.

While these maps sound simple on the surface-level, the actual generation or acquisition of this kind of map can prove to be quite difficult. For one, while a floor plan of the store in terms of physical layout might be kept by each store, it is highly unlikely that each store knows where each product is placed on an aisle distance-wise. It is extremely unlikely that we will be able to know that, for instance, carrots are exactly 3.3 meters down aisle 12, which could be 5 meters from the border wall of a store. To address this, we will be generating these maps through the manual collection and marking of product locations in the store, along with the manual measuring of the stores layout, i.e. aisle lengths.

The opposition to this manual approach is the store’s automation and systemization of product shelf organization. This would require intense collaboration with how stores operate to accommodate our product, and we would likely have to demonstrate an intensely large userbase before we could convince a store to do this just for our product. Additionally, we can attempt to utilize the store’s aisle system to make a general estimation of a products position. While this attempt would result in a more scalable approach that utilizes predefined information, the main downside is that an estimation for a products position is extremely worrisome when attempting to integrate into a planner. Because of this uncertainty, it would be best now to build the prototype utilizing a manually generated product map for now, and address the problem of scalability if need be in the future.

3.5.1.3 Control Output

In most vehicles with autonomous navigation capabilities, autonomous control is essential to the smooth traversal of any route. Reducing stray from a route, oscillatory behaviors, and all the other control-theoretic behavioral characteristics of a closed-loop controller is usually the job of a control engineer tuning a PID, MPC, or other controller.

In our case, because the control is actually conducted by the customer themselves, our control will be accomplished through a simple indication scheme to communicate with the customer when to turn or move forward. For abstract instructions such as telling the customer when to turn around or when they arrived at a waypoint, an audio system will be used due to the infrequency of those events. But for the constant control of turn intensity and reaffirmations of going straight, it is undesirable to constantly have a voice indicator.

With that we have a few options to approach choosing a control output, with the most obvious being: a vibration mechanism, audio outputs, and semi-autonomy. Audio outputs, as stated, can be extremely useful for directions. It is easy to be extremely verbose and diverse in the instructions being relayed, but, constant audio input can be overwhelming both to the customer we are aiding and to the surrounding store customers. While this seems like a trivial point, it is important to also make note that despite not having audio communication for every direction (ie straight, left, right), we do plan on having audio output for abstract instructions and indications such as “navigating to the next task”, “please turn around”, and “aisle blocked, rerouting”, as examples.

Another option would be to have some level of autonomy for the cart to aid the human. This would include implementing rudimentary control abilities onto the cart. This implementation would consist of custom motor mounts and wheels, an addon to the power system to support these motors, and software development to calculate the control signals sent to these motors. While this is possible in the sense that there are tools to aid in this development, it not only provides additional, unneeded, engineering work, but also provides an unintutive interface for the customer to figure out. Instead of having them push the cart themselves, they would essentially be guided by a cart, which defeats the point of the project attempting to grant these visually impaired people more autonomy than the previously had.

As a better alternative to both of these options, we have to target another sense for communication, and because audio and visual are both ruled out, the most natural sense to target is touch. The control scheme we have come up with will be the variation of intensity that a vibration mechanism outputs to the grocery cart handle. As the cart needs to turn more left, for example, the vibrations’ frequency and amplitude will increase proportionally on the left side of the cart. Ideally, when going straight there will be no noticeable intensity.

3.5.2 Navigation

3.5.2.1 Simultaneous Localization and Mapping Implementation

Simultaneous Localization and Mapping (SLAM) is a revolutionary tool in robotics that has been iteratively developed over the past two decades. There are two main components to SLAM, mapping and localization. Mapping is the generation of a 2D or 3D cost-map based off sensor (normally LIDAR or active stereo vision system’s), that gives a route-planning algorithm an idea of the obstacles that lie in between the initial and final states attempting to be navigated. Localization, on the other hand, is the online computation and estimation of a robots current position in a map.

Due to our reliance on an active stereo vision system, this severely limits the amount of software tools available to us, as the majority of development, especially for tools compatible with the Nav2 framework, has been for the support of LIDAR-based SLAM. That said there are still several services available for our case.

RTAB-Map is a versatile SLAM library that supports 2D and 3D mapping. It is particularly effective for active stereo vision systems and is well-suited for applications requiring a developed infrastructure and real-time updates. It has a well documented use case for both mapping and localization, and has been shown to work well with Nav2 planning algorithms. Importantly, it interfaces well with Nav2, is available on the most recent ROS2 distributions, and has an active community for tuning support.

Alternatively, the slam_toolbox package for ROS2 provides an efficient and user-friendly SLAM implementation. Its comprehensive documentation and ease of integration make it an excellent choice for projects with tight development timelines. This tool is ideal for generating 2D costmaps, enabling subsequent localization and planning processes. That said, slam_toolbox is typically geared towards the use of LIDAR, and despite some support for active stereo vision systems, it is still weak on point-cloud-based SLAM.

ORB-SLAM3 is a feature-based SLAM algorithm renowned for its accuracy in visual localization. It supports monocular, stereo, and active stereo vision inputs, making it a versatile option. However, its complexity and resource requirements may not align with all prototype use cases. The main downside to this tool is its incompatibility with recent ROS2 releases, such as Humble or Jazzy, which are essential to the interface between it and the rest of the system.

For our shopping cart prototype, we have chosen RTAB-Map as the primary localization tool. This decision is driven by its mature infrastructure and compatibility with active stereo vision, which align well with our hardware and development needs. RTAB-Map's robust performance in real-time environments ensures reliable localization while maintaining development efficiency.

Table 3.33: SLAM Implementation Comparison

SLAM Implementation	Available Infrastructure	ASV Interface Quality	NAV2 Interface Quality	Available Documentation
RTAB-Map	High	High	Moderate	High
Slam-toolbox	High	Low	High	High
ORB3_SLAM	Moderate	High	Low	Low

3.5.2.2 Route Planning Algorithm

Given a product map and a list of groceries that the customer is searching for, a routing algorithm is subsequently needed to order the waypoints to navigate to. Once this order of waypoints is generated, a standard planning algorithm, such as A*, RRT*, etc., can generate smooth, continuous paths to these waypoints in succession.

With that said, the routing algorithm is essential for the seamless navigation of the grocery store. Specifically, it needs to be able to create an optimal route that navigates to all relevant waypoints, starting from the store's entrance and ending at the checkout and exit. By optimal, this implies the shortest absolute distance traveled throughout the route. Luckily, there is has been planning of research conducted for this exact problem, but usually in the context of warehouse navigation.

There are four main strategies that address this problem: S-Shape, Largest Gap, Combined, and Optimal. Each strategy has pros and cons, which are usually direct trade-offs between complexity and optimality. The S-Shape strategy, for example, is quite simple. It simply requires that all aisles with waypoints that need to be visited are fully traversed, thus leading the navigator to make S-shapes as they traverse. While the implementation of this algorithm would be extremely simple to develop, the total distance covered is quite large compared to the optimal strategy, especially in increasingly complex floor layouts.

An opposition to this is the optimal routing strategy, which provably calculates a shortest route. This optimal routing strategy can be extended to layouts with cross aisles as well, and thus lends itself to fully autonomous robots that don't have human implications, such as the annoyance of having to do a U-Turn in a busy aisle.

While this optimal routing strategy performs the best quantifiably, it is not the prevalent strategy in most implementations. Most times, a warehouse implements a heuristic-based strategy, such as S-shaping or Longest Gap, due to the ease of understanding for the operators. But even these heuristic based algorithms can prove to be poor when interfacing with people. Our team is looking for an algorithm that is significantly easy to use and minimizes navigation confusion for the customer.

Thus, it would be best for our team to use the simple, and elegant S-Shape routing algorithm.

Table 3.34: Route Planning Algorithm Comparison

Routing Algorithm	Ease of Use	Distance Optimality
S-Shape	High	Moderate
Optimal Routing	Low	High
Heuristic-Based	Moderate	Moderate

3.5.2.3 Object Avoidance

One of the extremely convenient parts about utilizing the ROS2, and specifically NAV2, infrastructure to implement the necessary autonomous navigation functionalities, is that a lot of implementations of common tools exist already. For object avoidance specifically, the problem is not commonly segmented from the continuous-domain route planning problem, due to the fact that our sensors can effectively detect and map potential objects, and the common planning algorithms can adjust dynamically.

The main argument to be made in our object avoidance implementation, then, is which planning algorithm to select in order to navigate the user from waypoint to waypoint. There are a few considerations for this decision, but none significantly impact performance success. Rather, the decision should be made in order to optimize some performance characteristic. Due to the nature of the project, it is natural to attempt to optimize general safety of the path, and that includes chooses a planning algorithm, that prioritizes that as well. To this extent, we shall compare three commonly used planning plugins in Nav2: the NavFn Planner, Smac Planner 2D, and Smac Hybrid-A* planner.

The three planners, fortunately, have well documented use-cases and pro/con lists available for comparison use. Firstly, both the NavFn planner plugin and the Smac 2D Planner plugin are described as being utilized for typically Circular Differential, and Circular Omnidirectional robots. In layman terms, this signifies that these algorithms are typically used for robots steered by two differential drives, as opposed to the common Ackerman steering mechanism most are used too. While the grocery cart is technically steered by Ackerman wheels, this is not of top significance due to the control being conducted by a human operator. Alternatively, it is beneficial that the algorithms are utilized for circular situations, as this signifies that the planner will keep the cart as far away from objects as is the largest radius of the cart. Alternatively, the Smac Hybrid-A* Planner is utilized specifically for circular Ackerman robot types, and due to that distinction, it would be best to go with this plugin.

This decision signifies a priority on safety for the operator, as it will purposefully prioritize maximum distance from potential collisions.

Table 3.35: Object Avoidance Algorithm Comparison

Planning Plugin	Drive Train Compatibility	Safety	Available Documentation
SMAC Hybrid-A*	High	High	Moderate
NavFn	Moderate	Moderate	High
SMAC Planner 2D	Moderate	Moderate	Moderate

3.5.3 Integrated Development Environment

Given the extremely interdisciplinary nature of the project, a versatile development environment that can be used for development of all different components of the system is extremely important. Because of this requirement, tools that are focused around a single language or protocol such as the Jetbrains suite of projects, will be avoided.

This leaves us with a large range of potential development environments with various levels of support and complexity, with everything from a simple text editor, such as Notepad, to a versatile IDE such as Microsoft's Visual Studio Code. Due to the lack of basic syntax highlighting and other related functionality of simple plain text editors, these are therefore removed from consideration. On the other hand, there is another level of text editors with such functionality and are exceptionally lightweight such as Notepad++. While these tools offer some advantages over plain text editors, they still don't offer many of the ease-of-use features prevalent in mainstream IDEs such as code completion. Because of this, we will make use of one of these code editors, which include the aforementioned Visual Studio Code as well as Atom, also developed by Microsoft, and Sublime Text.

Visual Studio Code will be the main choice for the development throughout this project primarily due to the extensive support for the program as generated by individuals through an extremely robust list of extensions which provide functionality such as syntax highlighting, formatting, hints, and more. These extensions exist because of the popular nature of the development environment and have implemented the features listed above and many more such as language support for most every programming language.

Table 3.36: Summary of Development Environment Options

Type	Examples	Benefits	Drawbacks
Generalist Full IDE	Microsoft Visual Studio Code	Supports most all languages, Most functionality present via plugins	More resource-intensive than simpler solutions
Plain Text Editor	Nano Notepad	Easy to use Lightweight	No formatting, No syntax highlighting or code completion
Enhanced Text Editor	Notepad++ Notepadqq Microsoft Atom	Lightweight Have some development extensions	Lack of extensive plugin support and special features
Specialist Full IDE	Jetbrains Microsoft Visual Studio	Powerful functionality	Resource-intensive, only supports handful of languages.

3.5.4 Single Board Computing Software

3.5.4.1 Operating Syste Kernel

There are several methods that can be utilized to run the previously-described map planning, navigation, and other algorithms on the single board computer. The decision first must be made which operating system to run on the SBC, with the main options with major differences being:

- Windows IoT (Internet of Things)
- Linux
- FreeBSD

FreeBSD is much less popular than either the Linux or Windows NT kernels and therefore less software is compiled to run on it. Additionally, for similar reasons, there are less hardware drivers available, meaning that the SBC or some peripherals may not even be able to function on it without a custom driver implementation, which is beyond the scope of this project, especially considering that there are other options with those drivers included. On the other hand, there are some benefits of using FreeBSD such as stability because of long-term support (LTS) kernels, but the other kernel options also provide this functionality without the drawbacks associated with the use of FreeBSD. Therefore, the use of the FreeBSD kernel is eliminated from this decision process.

On the other hand, Microsoft's Windows IoT uses the extremely widely-supported Windows NT kernel, like their flagship desktop operating systems, except with less system processes to make the system more lightweight than the desktop operating system as less functionality is needed for an embedded system such as will be used throughout this project. Due to this, there is wide hardware support for peripherals and other devices unlike the

FreeBSD kernel. In addition, a lot of software is already designed to be ran under a Windows environment and therefore there is a moderately robust software support environment available. On the other hand, the Windows NT kernel was made first for a desktop environment with a graphical user interface (GUI) through video display outputs and many other features that will not be necessary for such embedded applications, the system will have a higher overhead than other solutions such as FreeBSD or Linux. In addition, because of this, while there is robust software support for programs that are normally run on the desktop, there is less support for purely embedded applications, meaning that there may exist the eventual requirement to eventually run some software under a virtualized Linux kernel which would only further increase the overhead of the system. Like FreeBSD, there does exist a long term support branch (LTSC) version of the Windows IoT operating system which is designed to be more stable than the bleeding edge. Although this is the case, while many SBCs today have more than enough power to run a Windows environment, this has not always been the case, and furthermore, it is widely seen as unnecessary by many because of the additional power requirements and overhead needed to run Windows. While this option isn't eliminated for discussion, there is likely a better option, the Linux kernel.

The Linux kernel is the heart of many different operating systems (called distributions), including Ubuntu, Debian, Fedora, Red Hat Enterprise Linux (RHEL), and more. It is a UNIX-based operating system similar to FreeBSD and is incredibly modular, with the vast majority of functionality being built on top of the kernel instead of into it. This therefore makes the kernel very lightweight, which allows "server" variants of most major distributions, including Ubuntu Server, Debian base, and more. These variants can be extremely well customized due to the open source nature of the kernel which allows for a wide range of different distributions made specifically for each different task.

While many different distributions exist, the ones previously stated are used the most widely and therefore have the most support from the community and package maintainers which make them easier to use for most applications. Similar to the previous options, both LTS and Stable, as well as testing versions of the kernel are available to be used - the latter of which are not considered for a finished product that does not require the use of bleeding edge hardware but may be severely impacted by bugs that may appear in these versions.

Most distributions offer variants with both the bleeding edge Stable kernels as well as those utilizing the LTS versions, which normally also take the same approach to their software repositories with LTS variants having older software and mainly updating for bug fixes compared to those of more updated released. For example, Canonical, the company behind Ubuntu, releases LTS versions every two years - supported for 5 years, which can be further extended with a paid support plan - as well as interim versions every six months without a LTS release - which are only supported for nine months. These versions are intended to be released in April and October of each year, with the LTS releasing on even years. As we do not require bleeding edge software support but value stability with this project, an LTS version of the distribution of choice would be used.

Because of these advantages that the Linux kernel has over the other options discussed, including unparalleled software support from both the community and SBC vendor, along with the lightweight nature of the kernel, the Linux kernel will be used as the base for the operating system that will be ran on the SBC.

Table 3.37: Summary of SBC Kernel Options

Name	Advantages	Disadvantages
Linux	Natively supports ROS Widely used	May not be as easy to use for those unfamiliar.
Windows IoT	Ease of Use	Heavier, more dependencies Doesn't natively support ROS
FreeBSD	Very stable, especially compared to Windows NT	Doesn't natively support ROS

3.5.4.2 Linux Distribution

There are many Linux distributions with good support for ARM64 CPUs such as the one that exists on the Raspberry Pi single board computer chosen earlier in this section, with minor differences existing between them, mainly due to software support, age of the software that exists, and the amount of community adoption that exists for the specific distribution.

Because of this, three main distributions will be compared for this use case:

- Debian 12
- Ubuntu 24.04 LTS
- Raspberry Pi OS (formerly Raspbian)

For each, the server version will be used to reduce overhead and potential security vulnerabilities present with a desktop environment as a GUI is not needed for this project. The system will mostly be interacted with over SSH so that the system can be mounted in a spot where it may be inaccessible while inside the cart attachment but still have near-complete external access to the software installed on the system.

Raspberry Pi OS exists with versions for both 32-bit and 64-bit architectures and is designed specifically for use with the Raspberry Pi by the system manufacturer. Because of this, the most direct support from the vendor exists when making use of this distribution. Raspberry Pi OS is a very lightly modified version of the latest stable version of Debian, with some additional packages designed to make it easier to develop for the Raspberry Pi in particular. While this is the case, this additional software will not be needed for the development of this project and only adds additional points of conflict for the software that will be installed on the system. In addition, if the software for navigation is decided to be ran directly on the host operating system, Raspberry Pi OS is not on the list of officially supported distributions at this time. Debian, the parent distribution of both Raspberry Pi OS and Ubuntu, is widely supported in many use cases, especially in server environments. One major flaw that exists with making use of a Debian image is that the latest long term support version has software that is more outdated than other similar distributions, including Ubuntu, since although they use the same package format and package manager (apt), they have different package lists as maintained by different people. As Debian is designed to be ultra-stable, the older packages are maintained for longer than the other distributions. While this is good for stability, it causes some problems when it comes to using modern bleeding-edge packages such as those that will be used for the navigation algorithms throughout the design. If the software for navigation is decided to be run directly on the host operating system, Raspberry Pi OS is an officially supported distribution, being listed as having "Tier 3" support.

Ubuntu has an even greater following than its parent distribution, has a long-term support edition with updated packages, and has official images for the Raspberry Pi. This means that Ubuntu 24.04 LTS has most all of the advantages from the previous choices that were analyzed while also not having the drawbacks present in Debian. While there exist some additional packages on Ubuntu as compared to Debian, these can either be disabled or left alone, as they do not utilize much of the system performance. In addition, being an LTS version, the stable version of the Linux kernel is used along with mostly-static versions of most software in the repositories which are newer than those from the latest stable version of Debian. This version pinning, mainly excluding security updates, allows for more consistency between installations and greater community support for any potential problems that may arise. Finally, Ubuntu 24.04 LTS is the "Tier 1" supported distribution by the navigation software used throughout this project, which means that it is tested to work very well and is the most likely to work the best of any other distribution if the software is run directly on the host operating system. Because of this, Ubuntu 24.04 LTS Server will be the distribution and version of Linux that will be installed on the Raspberry Pi single board computer.

Table 3.38: Summary of SBC Operating System Options

Name	Advantages	Disadvantages
Ubuntu	Very stable Tier 1 ROS support	Snap packages have more overhead - can be uninstalled
Debian	Stable	Older software Tier 3 ROS support
Raspberry Pi OS	More modern software	Tier 3 ROS support

3.5.4.3 Software Runtime Environment

There are several methods for running software inside the Linux environment on the single board computer, each presenting their own advantages and drawbacks. The methods that will be considered include "bare metal" - installing the software onto the system directly - as well as virtualization and containerization. While a bare metal software install is the most lightweight of the presented solutions because it doesn't need to run additional software on top of the system kernel in order for the program to run, the overhead introduced by modern virtualization and containerization solutions such as KVM and Docker, respectively, are very lightweight and have several advantages that are appealing in this case.

The biggest advantage of both virtualization and containerization over bare metal installations is portability - each of these solutions can be packaged into easily replicable formats from the distributer to then be installed on a system such as our single board computer. Among other things, this would reduce system-specific problems that might occur due to the unique hardware and software environment that will be deployed. Although it doesn't happen too often, sometimes software, especially common libraries with differing versions, conflict with each other and cause hard-to-debug issues to arise with an otherwise working configuration.

Containerization methods such as Docker, Kubernetes, and LXC use virtualization under the hood to take an even more modular approach to setting up services, with each individual component normally having its own container within a "stack." These components can then interact with each other over an internal network as if they were each separate computers. These containers normally have completely immutable filesystems and data is stored in external mount-points elsewhere on the disk. Because of the way that the containerization paradigm is designed, there is far less overhead than exists within full virtual machines. A sample visualization of this can be seen directly below:

Figure 3.1: Containerization Methods Visualization

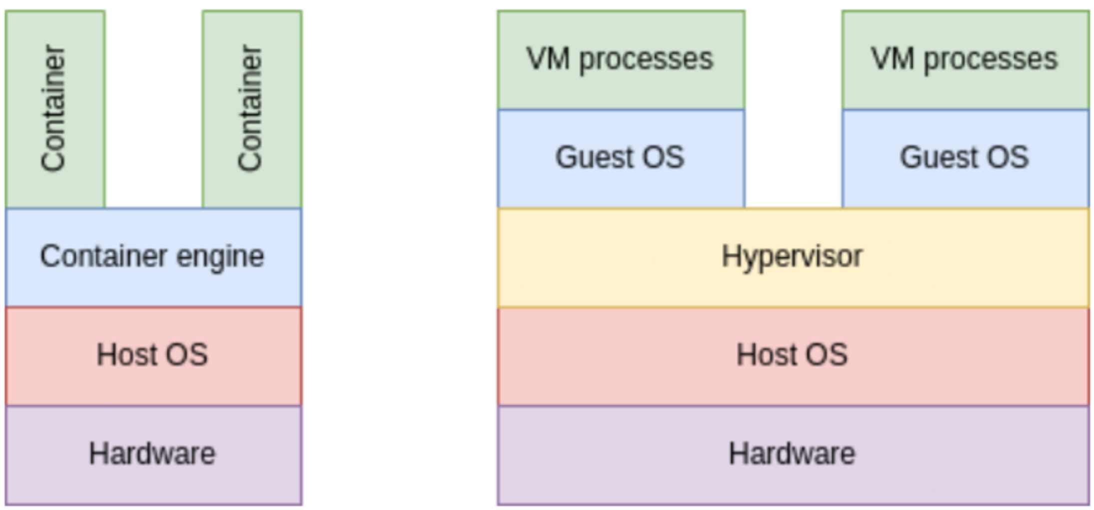

While virtual machines have to each have their own kernel and operating system, containers use the containerization environment's engine to use some resources from the main system, which additionally allows the container images to be much smaller than those equivalent images that may be used for a virtual machine. Due to the popularity of virtualization solutions such as Docker, many services have pre-configured images, either from the original publisher or trusted sources such as LinuxServer.io, hosted in common repositories online (such as DockerHub) which can be easily pulled and then used by anyone wanting to use the image.

Because the data for the containers is stored outside of the container itself, to update the container, one simply pulls the newest version and discards the old, instead of updating the services separately like would be done in a virtual machine or directly on the system. This leads to less room for potential errors to arise because of a bad update, bugs which are incredibly hard to diagnose.

Due to this, there are some disadvantages, mostly security-related, of using containers over more standard virtualization solutions. The main disadvantage is a greater risk of potential attacks escaping containers onto the host machine as compared to virtual machines where, although it is theoretically possible for some attacks to escape a virtual machine, the task is much harder because the kernels and operating systems are completely isolated from the host machine. Because only trusted software will be used on the single board computer in addition to regular backups as the prototype progresses, this is not a major factor in this decision.

While there are many advantages to using virtualization or containerization technology such as described above, the main disadvantages of limited and indirect hardware access along with the higher overhead inherit in these types of solutions, the software will be installed directly on the single board computer's host operating system for this project. To alleviate some of the drawbacks of doing this, there will be regular backups and snapshots taken of any progress made to the system along with only installing completely trusted software onto the machine.

Table 3.39: Summary of SBC Runtime Environment Options

Type	Advantages	Disadvantages
Bare Metal	Least overhead Native ROS support	Harder to create backups.
Virtualization	Regular backups / snapshots	Not supported for ROS Most overhead
Containerization	Native ROS support (Docker) Regular backups / snapshots	Some overhead - less than full virtualization.

3.5.4.4 Data Storage Methods

There exist many different data formats for which the product information can be stored such that it can be easily looked up by the system when the user enters it as their choice. The average number of items (known as Stock Keeping Units or SKUs) in a grocery store in 2018 was about 33,000. Assuming this figure has held somewhat steady and slightly overestimating the number of items that will be needed to be searched for, we should expect at most 40,000 items in the database. Associated with each item will be its approximate location - aisle, shelf, and position within the aisle. Therefore, with this known quantity of information, we can determine the most appropriate storage format for this data.

A table breaking down the main differences between the main options that are being considered can be found directly below.

Table 3.40: Summary of Data Storage Format Options

Name	Storage Size	Advantages	Disadvantages
JSON	Medium	Standardized, easily machine-readable Widely used in many applications Records can have unique properties.	Cannot be directly edited in a user-friendly way
Relational Databases	Very large	Easy to use common language for storing large quantities of data and the relations between them.	Creates additional software overhead, needs SQL queries
MongoDB	Very Large	Easy to interact with.	Creates web dependency - cannot be run locally.
XML	Medium	Standardized, easily machine-readable Records can have unique properties.	Cannot be directly edited in a user-friendly way
CSV	Small	Standardized, easily machine-readable Easy to use and human-friendly Can be directly edited in common programs such as Microsoft Excel	Every record (row) must have the same properties (columns)
Custom test format	Varies	Can be customized to fit our needs exactly.	No standardization, drivers, or libraries. Completely unnecessary with existing robust solutions

Because it's a widely used standard which can be easily implemented in most software stacks including Python and other common applications without much additional processing overhead unlike is the case with relational databases, JSON will be the format used to store the data for the product information. This will allow each product to have different fields as necessary in the different parts of the store, unlike in CSVs. Since we are storing a relatively small amount of information, a relational database is not needed for this application. If more stores are supported in future implementations, we may consider a relational database as there will be a much greater quantity of data that will justify this added complexity and overhead.

Chapter 4 Related Standards and Design Constraints

4.1 Industrial Standards

4.1.1 PCB Design Standards

PCB design standards ensure that a PCB is manufacturable, safe, and reliable. Much of the design standards are outlined by the Institute of Printed Circuits (IPC). The most common standard is IPC-2221, which contains detailed information for designers on best practices to facilitate performance and manufacturing quality and reduce errors.

General design considerations outlined by IPC-2221 include material selection based on electrical, thermal, and mechanical properties, guidelines on defining the number of layers and thickness, and layout optimization for minimizing costs and potential defects. The shape and aspect ratio of the PCB is also an important detail highlighted by this standard, as it takes into account manufacturing capacities and tolerances. This involves guidance on proper component placement, streamlined trace routing, and overall board orientation. These considerations ensure compatibility with the PCB manufacturing process.

Current management specifications include minimum trace width guidelines to prevent short circuits between traces, which is especially important for designs with higher current loads. Via size, spacing, placement, and types are additional considerations that must be compatible with the electrical and mechanical requirements of the design. Proper inclusion of vias allows for the board to handle the specified current loads and avoid interference with other components.

Thermal management specifications include additional material selection choices with the appropriate thermal conductivity for effective heat dissipation. Additional thermal relief methods covered by IPC-2221 include the inclusion of heat sinks and thermal vias for designs with heat-generating components. These considerations support PCB reliability, especially over prolonged use.

Following some of the IPC-2221 guidelines along with those outlined by manufacturers, the following considerations will be made to simplify design and repair. Precautions will be taken to avoid parts smaller than 0805, with proper justification for any implemented parts that are smaller and necessary. IC components will be selected to have pins on the side rather than underneath to simplify soldering. This enables ease of soldering and testing PCB design. Daughter boards will be developed to breakout dense assemblies and ICs to create backups that can be easily replaced. Bypass capacitors will be implemented in power supply lines to stabilize voltage spikes. A minimum trace width of 0.033” will be used, with appropriate scaling depending on current demands. Ground planes will be included, with proper connections using vias if multiple ground planes are required.

4.1.2 Wired Communication Standard - I2C

Inter-Integrated Circuit (I2C) is a widely used protocol for serial communication, which in this case will be between the microcontroller and peripheral target devices. One of the main advantages of I2C is minimal wiring, as it only requires two communication lines. Multiple devices, either controllers or targets, can be connected through the two-line bus, and target devices are distinguished by unique I2C addresses. The two lines are the Serial Data Line (SDA) and Serial Clock Line (SCL), and communication is bidirectional through a half-duplex system. Data to and from the targets are transmitted through SDA, and clock data is synchronized through SCL. Both lines are connected to a common voltage supply through a pull-up resistor and are ‘open-drain’ or ‘idle-high.’

I2C communication begins with a START condition, where SDA drops from high to low while SCL remains high. After claiming the bus, the controller transmits the address of the target and the intention to either read or write data. The target acknowledges the connection, upon with the controller transmits the data and receives an acknowledgment from the target that the data was received. Communication is terminated with a STOP condition where SDA transitions from low to high while SCL is high. Data transmission is always done when SCL is low to distinguish it from the START and STOP conditions.

There are several I2C modes, each supporting different data rates. These include Standard-mode (100kbps), Fast-mode (400kbps), Fast-mode Plus (1Mbps), High-speed mode (3.4Mbps), and Ultra-Fast mode (5Mbps).

4.1.3 C++ MISRA Standards

The MISRA C++ standards (Motor Industry Software Reliability Association) are a set of coding guidelines developed to ensure the safety, reliability, and maintainability of C++ software, particularly in safety-critical and embedded systems. Originally created for the automotive industry, these standards have since been adopted across various fields, including robotics, aerospace, and industrial automation. MISRA C++ provides rules that focus on preventing undefined behaviors, ensuring memory safety, avoiding concurrency issues, and improving code readability. By enforcing a strict coding discipline, the standards help developers avoid common pitfalls in C++ programming, making the software more predictable, secure, and less prone to errors in high-stakes applications where system failure could lead to significant consequences.

The MISRA C++ standards are crucial in the development of mobile robotics, especially in safety-critical systems where reliability and error-free operation are paramount. In mobile robotics, such as in our NAVIS project, where autonomous decision-making, sensor integration, and motor control are integral, MISRA ensures that the software adheres to strict rules designed to avoid undefined behaviors, data races, and memory issues. By following these standards, robotic systems, such as our grocery cart, can achieve higher levels of safety and robustness. This is particularly important in unpredictable environments where any software malfunction could lead to catastrophic failures. MISRA's emphasis on predictable execution, low-level control, and memory safety significantly reduces the risk of bugs and helps engineers develop more resilient, dependable robotic systems.

In embedded systems, which we are planning to use to enable serial communication between our sensors and our SBC, following MISRA C++ standards can have substantial benefits. This system needs to run on hardware with limited memory, processing power, and real-time responsiveness, making efficient code crucial. The strict guidelines for memory management and performance optimization in MISRA ensure that our embedded application will remain predictable, avoid memory leaks, and operate within its resource constraints. In the context of ROS2 MISRA-compliant C++ code helps ensure that ROS2 nodes behave deterministically and that message exchanges between nodes do not lead to deadlocks or undefined behavior. The focus on avoiding dynamic memory allocation, excessive use of global variables, and undefined exceptions aligns well with the real-time, performance-sensitive nature of both embedded systems and ROS2 applications, providing a reliable framework for critical robotic operations.

4.1.4 ROS2 Robotics Standards

ROS2 is a crucial component to many robotic prototypes these days, with applications for robotic arms, rovers, and much more. But over the past few years, ROS2 has taken an even more important role in the robotics industry, and has begun making its way into performance-critical applications and products. With this shift, and also to maintain the general integrity of the ROS2 ecosystem, a system was derived to regulate and standardized the ecosystem. These standards, title ROS Enhancement Proposals (REPs), give consistency on how to achieve the most common problems that ROS2 is used for, including for concurrent logging, package management and scale, real-time use best practices, and even Python and C++ style formats.

The REP system includes a proposal, reviewal, and acceptance stage, and once a REP is accepted, it is logged and accepted as a standard. For our application specifically, we have to take a deep dive into the REP list to highlight REPs that affect system design and development for autonomous systems, and for mobile robotics specifically. This includes implications for the integration of the NAV2 stack, real-time sensor and computation performance, and general package and programming development style.

The most relevant REPs have been listed below, with summaries of their implications and regulations following them.

1. **Style Guide for Python Code (REP 8):** This REP specifically limits the style guide for all Python code in an effort to standardize all custom and official ROS2 development.

2. **Coordinate Frames for Mobile Platforms (REP 105):** This REP specifies naming conventions and semantic meaning for coordinate frames of mobile platforms used with ROS.

3. **ROS 2 Releases and Target Platforms (REP 2000):** This REP defines the timeline of release for new ROS2 distributions, but more importantly, what the target plat-

forms are for those distributions. This limits are availability to use different hardware architectures, ISAs, and operating systems.

4. **Package Quality Categories (REP 2004):** This REP defines categories that indicate the quality and maturity of packages within the ROS ecosystem. A package's classification into a specific category, or quality level, depends on the policies it follows. These categories cover policies related to versioning, change control, documentation, testing, dependencies, platform support, and security.

5. **ROS 2 Common Packages (REP 2005):** This REP describes the common packages of ROS 2, allowing for us to utilize the pre-built tools and infrastructure more effectively.

4.1.5 802.11 Wireless Communication

The 802.11 protocol is a set of standards developed by the Institute of Electrical and Electronics Engineers (IEEE) to define wireless local area network (WLAN) communication, more commonly known as Wi-Fi. The larger 802.11 family consists of one-way, over-the-air modulation techniques that all utilize the same communication protocol. Originally formed in 1997, the 802.11 protocol has evolved significantly since its inception in terms of maximum link rate, and available radio frequencies.

The 802.11 protocol has faced many limitations throughout the years, that have been incrementally solved through the complex versioning employed by the Wi-Fi alliance and standards updaters. Generally speaking, however, the employment of 802.11, the use of WiFi, not only has implications in technical innovation, but also for the growth of small-businesses and consumers alike. This includes true flexibility and mobility due to the robustness of the wireless system, cost-effectiveness, scalability, and overall increased productivity because many devices could easily connect to the internet and to a local network with minimal technical knowledge needed.

The ESP32 microcontroller fully supports the 802.11b/g/n Wi-Fi standards, allowing it to establish wireless communication without additional hardware. Technically speaking, it can operate at a data rate up to 150 Mbps, has multiple antennas to minimize channel fading, and applies the Wi-Fi MAC protocols automatically. The ESP32 can connect to other networks, create its own network, or do both at the same time. It is also easily implementable on the ESP32, with plenty of infrastructure already existing in the WiFi.h library.

By leveraging 802.11, the ESP32 can host an HTTP server that receives and processes requests over Wi-Fi. The advantage of using 802.11 Wi-Fi over traditional wired connections is the ability to deploy devices without the need of a wired connection, which is an unreasonable assumption for parts in highly dynamic physcial environments.

Overall, the 802.11 protocol is crucial for enabling efficient, high-speed, and flexible wireless communication, making it the ideal choice for receiving wireless information when the physical distance between the MCU and the packet sender can be great distances. Specifically, the ESP32 is an ideal tool to utilize the protocol, due to its on board WiFi chip and extensive software tooling to enable its use.

Table 4.1: ANSI Z136.1

Laser Class	**Power Range**	**Hazard Level**
Class 1	$\leq 0.39\mu W$ (Visible), $\leq 1mW(IR)$	No hazard under normal use
Class 1M	Varies (depending on Beam divergence)	Safe for unaided viewing but hazardous with optical instruments
Class 2	$\leq 1mW$ (Visible Light, 400-700 nm)	Safe due to blink reflex prolonged exposure hazardous
Class 2M	$\leq 1mW$ (Visible Light, 400-700 nm)	Safe for unaided viewing but hazardous with optical instruments
Class 3R	$1 - 5mW$	Direct exposure hazardous reflections generally safe
Class 3B	$5 - 500mW$	Direct exposure hazardous; diffuse reflections usually safe
Class 4	$500mW$	Severe hazard can cause eye and skin burns, ignite materials

4.1.6 Laser Classifications

The classification of lasers is an essential aspect of safety compliance, particularly in systems employing high-power sources. Laser safety is regulated under ANSI Z136.1 and IEC 60825-1, which categorize lasers based on their potential hazards to the human eye and skin. These classifications, summarized in Table 4.1, define permissible power levels and viewing conditions under which laser exposure remains within safe limits.

The laser diode used in this system operates at 850 nm with an output power of 200 mW, placing it in Class 3B when in its raw, collimated state. Direct exposure to the beam at this level is hazardous and may cause irreversible retinal damage. However, the final classification of the system is influenced by additional optical elements, including a Diffractive Optical Element (DOE). The DOE expands the emission into a structured light pattern across a 50° × 50° field of view, redistributing the optical power across multiple beamlets. This redistribution significantly reduces the intensity per unit area, thereby altering the effective classification of the system. The calculations used to determine the power distribution and resulting MPE values, including the methodology for determining the fraction of emitted power entering the eye, are detailed in Appendix D.

The classification of the full system is determined by assessing its exposure levels relative to the Maximum Permissible Exposure (MPE), which specifies the threshold at which laser radiation becomes hazardous. For 850 nm radiation at 0.1s exposure, the MPE is 10.1 W/m². Measurements of the system's power distribution indicate that at distances less than 10 cm, the exposure exceeds this threshold, maintaining a Class 3B hazard level in close proximity. However, as a result of the DOE-induced divergence, the power density falls below the MPE threshold at distances greater than 10 cm. Beyond this point, exposure remains within safe limits, classifying the system as Class 1, where it presents no hazard under normal viewing conditions.

4.2 Main Contraints

4.2.1 Time

The main constraint that we must deal with during this project is time. This project spans two semesters, of which the summer semester is three weeks shorter than the main fall or spring semesters during which most senior design projects are completed. Because of this condensed time to complete the entire engineering design process and end up with a functioning prototype product meeting all of the requirements, the scope of the project is somewhat limited, among other decisions that are made to ensure that we are able to complete the planning and initial fabrication stages throughout the Spring and the remainer of the fabrication throughout the 12-week Summer semester.

In addition, unlike in most industry products, this is a hard deadline that is set for a functional product which we must make in order to be successful in this class and the degree programs. To somewhat mitigate this, we were able to work with our advisors prior to the official start of the Senior Design classes, as seen in the timelines in Chapter 10, to get a head start on planning the project and writing this report. This allows us to have a substantial portion of the project planning process complete and the project approved before the start of the semester when having to complete the process along with other classes.

It is certain that we will face many problems that will have to be debugged and solved throughout the course of this project. Having a hard headline means that we have a condensed time period in which we can complete this process without rushing and introducing more errors. Because of this, we may have to prioritize breaking bugs over those which may cause an inconvenience as there may not be adequate time to solve all the possible problems that arise.

Certain manufacturers, especially those in the process of PCB fabrication, are located overseas and may take a substantial amount of time to make and ship the completed products. While this may not be a large issue initially, it is something that should not be ignored throughout the process. Additionally, due to this time constraint, as well as the financial cost of ordering more revisions of the PCB, revisions to the PCB could prove to be a large problem.

Beyond that, certain software components are bottlenecked by having completed the hardware inputs, especially the optical hardware. Because of this, the extensive time that it will take to complete and fine tune the software will have to be delayed until these hardware components are almost complete. Other than this, most of the systems can be fabricated in parallel by the team members so that the project can be completed in the allotted time.

There are several ways that we have and can do to mitigate this major constraint. Starting the design process early allows us to have some more time in fabrication, assuming that we stick to the stated schedule. On a related note, having a tight but do-able schedule agreed upon by all members, which can be accomplished by tools such as a GANTT chart, are imperative to being able to complete this project on time. Finally, having a good culture where the team meets often with updates, asks for help as needed, and completes their tasks as agreed upon, will significantly aid in the process of completing the project within the given constraints.

4.2.2 Funding

As this project is not receiving external funding, there is technically no limit to the price that can be spent. That being said, we will attempt to limit the total price to the greatest extent possible that does not highly impact the functionality of the project so that we can each have the lowest out of pocket cost for this project. An attempt to secure funding from several external sources were attempted and failed, therefore we will have to fall back on using our own funding throughout this project.

This tight constraint means that many tradeoffs will have to be made which impact both the cost of the project as well as its abilities. For example, the single board computer was chosen as one with a limited amount of RAM although additional memory would likely help with certain software components due to the price increase of the more capable variant. Although this change would not be needed, having the additional capacity afforded by more RAM would have been appreciated. This constraint realistically also limits the amount of hardware testing that is able to be completed, as it would be ideal to spend the least amount possible on revisions that will not end up in the final project. For example, additional PCB revisions will increase total cost of the project and therefore it may be more advantageous to fix some potential problems on the board by hand instead of having additional fabrication cost, time, along with additional testing time that is required of the new board to ensure it works as intended.

One major system that may be restrained by the budget is the optical system. As certain components can quickly get expensive, a conscious effort must be made to select the best value components for the laser diode, fiber, cameras, and other components of the optical system. While this system will be a major focus of cost reduction, we must ensure that the products that are chosen are reliable and that is not a sacrifice that is made. This is crucial because the optical system is a main bottleneck for the functioning of this project in totality - as without a vision system the software will be severely hamstrung in being able to navigate the grocery store as compared to having a well functioning system as intended.

Other tradeoffs and potential problems with limiting the cost of the project can be seen in the House of Quality in Chapter 2. In addition, the cost breakdown for this project by sub-system can be seen in Chapter 10.

4.2.3 Testing Locations

The final major constraint that must be considered is a location to test the system. Since the product is designed to be used at a grocery store, this would be ideal. However, there are several challenges that could make finding a store to allow us to test in hard or impossible. These challenges include liability concerns that may come with using the product while other customers are using the store or the additional expenses incurred by the store by employees if the product is to be tested outside of standard working hours.

In addition, even a small potential problem that could be caused by testing our system will likely be a cause for grocery stores to not allow us to test on their premises as they have no bearing on the product being a success and therefore it will not help them monetarily. Some of these issues were listed just above, with several more that could additionally be given.

Given this reality, although we will attempt to find a grocery store to allow us to test the product, we must make contingency plans in case we are unable to do so. This would mean that we should find a location that is close enough in design to a grocery store while also having a very high likelihood of allowing us to utilize the space for testing the system during Senior Design 2. Some potential locations that could be suitable for this operation include the UCF library, as the aisles of books would make a good analog for the aisles of grocery items, or a manufactured space designed to mimic the layout of a grocery store. Since each of these would likely be performed on campus, we would need to obtain permission from the University prior to testing, which should be easier than doing so for a grocery store. Although a library isn't a perfect analog for a grocery store, namely as the aisles tend to be more narrow and the books are much less distinguishable from each other than are food items, it would be a good selection for this case if we are unable to use a grocery store as a testing location.

If a different location is selected, an effort must be made to ensure that it aligns as close as possible with the expected layout of a grocery store along with providing evidence in our report and to the review committee that this is in case the fact.

Therefore, while this is a major constraint of the project, there are several suitable alternatives that could be deployed in a situation in which we don't have access to the use of a grocery store for testing purposes.

4.3 Other Constraints

4.3.1 Component Availability

Certain components of the project may have seasonal availability or otherwise be out of stock for long periods of time. One major example of long-term disruptions to product availability is the Raspberry Pi, a variant of which is being used in this project. Throughout much of 2020-2023, the Raspberry Pi was almost constantly out of stock. The manufacturer claimed that this was due to the supply chain shortages which started in April 2020 along with an associated increase in demand for the popular hobbyist board while many people were isolated indoors for an extended period of time. Due to this, all variants of the Raspberry Pi were generally unavailable during this time period from official retailers or for the MSRP, but instead were being sold for much more by "scalpers" who attempted to take advantage of the shortage.

During this time, many alternatives launched to compete with the Raspberry Pi while promising wider availability for those who wanted to do projects. While some were practically clones of the Raspberry Pi, others brought new features to the table. Many of these alternatives were compared in the "High Performance Compute" section of Chapter 3.

While this was the most widespread shortage that would have had a great impact on this project, it is but a demonstration that any of the materials with a single source could be subject to the same problems as the Raspberry Pi. To mitigate these problems, we intend to purchase critical components, as well as backups as needed, as early as possible to ensure that we are able to obtain them within a reasonable amount of time. In addition, whenever possible, components with several sources will be used so that we can be almost certain to be able to purchase them from a supplier even if there are issues affecting the others. Some components we are able to do this for include simple electronic components such as capacitors and resistors, along with some more specialized components such as batteries, mirrors, and fiber optics.

4.3.2 Data Availability

To adequately perform the project, data about the location of the items within the grocery store must be available. Since this information is normally not made publicly available as it is not needed for the vast majority of customer use cases, we will have to make a special request to the grocery store in which we are testing the project to obtain this data.

Although we do not expect to meet resistance when asking for this information for the uses of this project if it is available, we do believe that this information may not be readily available for many stores. In addition, if the information is available in their system, it may not be in a format that can be easily understood by the software for this system. If this is the case, we will have to make a software program to convert between the formats such that it can be used within the project.

If the complete information is completely unavailable or if we are unable to test the prototype in a grocery store and have to resort to a different location, for the purposes of this project, a sample inventory will be used to represent the inventory that would exist within a grocery store.

4.3.3 Feasibility

There exist several components within this project which are single sources of failure, a component in which the rest of the overall system will not adequately function without it working correctly. Some examples of this include the optical system, which is the main source in providing guidance to the software which will guide the user throughout the store, as well as the software which takes in this information in order to guide the user throughout the store.

To mitigate the risks as much as possible with these points of failure, both by minimizing the quantity of single sources of failures that exist throughout the project as well as by maximizing the chances that these systems work as intended by the end of the project, the group has consulted with many professors with relevant experience to the project. For example, Professor Chan was consulted about many of the electrical components and Dr. Weeks was consulted about the optical system and its interaction with the electrical systems. Through these interactions, among others, the group was made aware of several potential problems and ways they could be rectified while staying within the scope of the project, as well as potential ways certain ideas could be implemented with the least risk of failure.

In addition, the group researched existing problems and solutions for the feasibility of certain systems and any existing protocols for combining the component systems. Some examples of this include research into the Microsoft Kinect and its use in ROS2 navigation software, a component which is somewhat similar to the optical depth sensing system that is being implemented in this project.

4.3.4 Safety

Several components of this system carry the risk of causing harm, either to the user or to the group while we are building it. Some of the items which carry the most risk include the laser diode as well as the mechanical system for attaching the completed system to the grocery cart. For each of these components that cause a risk, mitigations must be put in place to ensure that both we and the user are as safe as possible while using the system.

For example, for the optical system which will contain a laser diode, mitigations include engineering and administrative controls to ensure that no one looks directly into the diode, especially without the diffraction layer. Each of the group members has or will complete the online Laser Safety Training, EHS309, offered by the University's Department of Environmental Health and Safety, which is required before gaining access to the CREOL Senior Design laboratory. Other safeguards will be put in place as necessary to ensure the safety of all participants while interacting with lasers or the optical system.

For the mechanical system, it will be ensured that all edges are smooth and do not cause a risk to the user or the assemblers' post-assembly. Similarly, for the power sub-system, there will be fuses, ventilation, and other electrical and mechanical contingencies in place as necessary to ensure that the batteries remain within a safe operating environment and do not cause a fire hazard.

Chapter 5 Comparison of ChatGPT and Other Similar Platforms

5.1 LLM Platform Comparisons

ChatGPT and other similar tools, including Google's Gemini and Meta's Llama are Large Language Models (LLMs), computer neural networks that predict the next word that is to be said. These models are trained on a wide variety of data and many can be fine-tuned with additional data by the user. Although they do contain a lot of data that they were trained on, the models do not have any reasoning capabilities, and many do not have the native ability to use the internet as additional context for their responses.

Additionally, the models do not have the ability to know when they are wrong and therefore will "hallucinate" or confidently give the wrong answer very often, especially for more complex prompts. Because of this, effort must be made to ensure that any responses are correct as it is not very easy to know otherwise. One example consisting of code that demonstrates this includes a study by NVidia in which they attempted to use LLMs to assist with Formal Verification. As seen in Figure 5.1 below, the highest likelihood of full success that was achieved was 45.6%, for a very small test case (seven lines of Verilog RTL), which is not something that can be relied upon without additional safeguards. Other examples outside of software include legal cases being hallucinated when being used by lawyers, which have caused many to be sanctioned by their local Bar associations.

Figure 5.1: Functionality Statistics of LLMs for Formal Verification

Model	Syntax	Func.	Partial Func.	BLEU
gpt-4o	0.911	**0.456**	**0.582**	0.503
gemini-1.5-pro	0.810	0.253	0.380	0.484
gemini-1.5-flash	**0.949**	0.380	0.557	0.518
Mixtral-8x22b	0.823	0.190	0.278	0.450
Llama-3.1-70b	0.861	0.291	0.354	0.464
Llama-3-70b	0.899	0.291	0.506	0.464
Llama-3.1-8b	0.835	0.203	0.304	0.525
Llama-3-8b	0.747	0.063	0.215	0.491

Because of these limitations, the models should not be treated like a search engine, no matter how they are used by the masses, unless you already know the answer to the problem or at least have enough knowledge to know when the model is hallucinating. Therefore, although the models are not very good at answering unknown problems or replacing the need for a search engine, they may still be good first steps at answering certain problems, which can then be verified elsewhere, or used to assist in generating ideas.

Although the models are normally hosted "in the cloud," some models, including Llama and Deepseek, can also be locally hosted using tools such as Ollama and Open WebUI, which together are a tool that mimics the look and feel of ChatGPT but with the ability to use local resources. This means that although your prompt history is still saved locally, the prompts are never sent to the cloud. There are many concerns of tools such as ChatGPT using your prompts for further training data which is almost completely mitigated with the use of local models.

While there are many upsides to using local models, there are also some quite major drawbacks which lead the vast majority of people to not host the models themselves. The main drawbacks include the complexity of setup - which although isn't very hard with modern resources for the tech literate, could create a problem for those with less knowledge. In addition, intensive computing costs are a large factor - as many of the most advanced models require at least one GPU with large amounts of VRAM along with a large amount of system RAM and storage space to hold the models, which can make for both a costly up front purchase as well as ongoing power and cooling costs. Finally, these open source models tend to be less capable than commercial models available through Anthropic, OpenAI, Google, and Microsoft - something which is changing as newer models seem to be releasing more often under open source licenses, allowing people to self host them in addition to providing first party services to those who don't want to do so.

As required, all prompts and responses to a Large Language Model for this project are placed in Appendix B.

5.2 Usage Examples

5.2.1 Idea Generation

As discussed in the previous section on limitations of LLM models and platforms, one major problem with using LLM for learning specifically is the concept of hallucinations. Hallucinations in this context can be described as information that an LLM will present as true that it seemingly pulls from thin air, with no foundation for its truth or existence. This phenomenon occurs increasingly frequently the more in depth you go into a subject of interest, and the more niche the area of discussion becomes. This heavily correlates with the intuition that when a LLM simply has less data to train on about a subject, it tends to fill in some of the gaps with its best guesses.

Now, the opposite side of this phenomenon is that for high-level, introductory conversations, an LLM can be extremely helpful. For instance, one of the hardest portions of learning about a new engineering field, for example, is trying to figure out popular approaches to common problems, and more generally speaking, the most popular approaches that define the field broadly. Notably, this works best the more popular the field is, but it can be crucial for an extremely accelerated learning rate of engineers, scholars, and curious people in general. Below is a case-study exemplifying this.

Looking at the response from [Prompt 1], it is apparent to see how useful this can be. Not only would person with no prior knowledge of controls engineering be introduced to common terminology that is searchable in typical search engines, but the LLM also presented the overviews of each term in order to provide high-level intuition to the learner.

5.2.2 Part Selection

While a LLM such as ChatGPT may be a helpful tool in guiding someone towards components that may be a good choice for a design need, the user must verify the information to ensure that the supplied information is accurate. Oftentimes the result may contain links to the wrong component or unsupported pages, incorrect specifications from the part, or even parts that are discontinued or do not exist. [Prompt 2] outlines a conversation in which ChatGPT is prompted to suggest laser diode driver models for the specific laser diode used in this design. The LLM is provided with the basic specifications and the name of the laser diode and requested to provide some compatible drivers. The links it provides for each driver do not lead to the driver it names; rather, they either lead to the home page of the manufacturer or supplier or link to a page that is not found. Searching some of the components on Google show that many of the listed specifications for the various components also differ from the specifications listed on their respective websites and datasheets. This indicates that it is generally a good idea to verify that a suggested part's specifications are accurate to the datasheet before incorporating it in a design. An alternative use for LLM given the inaccuracy of specific component reporting may be to suggest sources and manufacturers that supply the needed parts. Oftentimes, these sites include filters to isolate components that fit the design needs, which may be a more accurate way to determine compatible parts.

5.2.3 Research

Despite their use on common, well-documented, and easily written subjects, LLMs constantly struggle to aid in more in-depth investigations required to conduct thorough research on a subject. Intuitively, due to the sparse amount of documentation on research subjects, which are by definition niche, or else they wouldn't be very good research, the LLM has little opportunity to learn about these subjects in a way that it can effectively reproduce.

Secondly, LLMs also don't have the natural intuition required to not only interpret these texts, but to also derive their implications, connections, and broader impacts on the paper's original and connected fields. For instance, despite the ability to match plain text in titles and content of a paper and a researcher's prompt, an LLM lacks the underlying reasoning needed to truly understand what a researcher would be looking for. There is an immense amount of nuance that comes with assumptions and connotations of technical terminology, and again, due to the lack of reasoning, it is impossible for LLMs to truly understand what a researcher is looking for without the proper integration of other forms of deep learning, including reinforcement learning and hierarchical learning.

Research in the context of LLM platforms is also deeply impacted by the phenomenon of hallucinations. Again, due to the sparse nature of research, this leads to a lack of significant, quality training data for a LLM to train on, and thus when inference time is called upon in order to reference this data, it is extremely common for the LLM to fill in the gaps of its "understanding," where it has little to not confidence in the information it is providing.

5.2.4 Code Writing

Large Language Models (LLMs) are excellent tools for programming and code writing, particularly when it comes to micro-problems that have well-documented solutions, which includes implementations of common algorithms, syntax correction and debugging, and even small multi-file projects that have extremely common structures, such as in web development. They provide instant solutions to common programming problems, allowing developers to rapidly prototype ideas without needing to reference extensive documentation. By leveraging LLMs, developers can focus more on problem-solving and logic rather than getting stuck on syntax or common implementation patterns, which allows for extremely accelerated productivity when they are employed in the correct contexts.

However, when it comes to large-scale software development, LLMs fall short due to their lack of deep understanding of software architecture, maintainability, and long-term project scalability. LLMs have historically struggled with understanding highly abstracted decisions that go into system design, and can not perform the weeks, months, or sometimes years of careful planning needed to build a truly scalable, maintainable, and robust product, which goes past simply writing code. Furthermore, LLMs do not have the capacity to fully comprehend the intricate dependencies, performance trade-offs, and evolving requirements that come with large-scale systems. Additionally, they lack the ability to coordinate across teams, manage version control effectively, and enforce coding standards throughout a project's lifecycle.

While LLM platforms are great for the generation of repeated code that can be easily mistyped, they do not possess nearly the amount of intuition needed to make a great project. This is also due to many non-technical aspects of what great projects possess, which includes user-design intuition, possible breaking points, and security. All this to say, they have their pros and cons, but more often than not, they should strictly be used to write software that has been done in some way, shape, or form before, and should always be checked and tested before being deployed.

5.2.5 Navigation Tool Integration

Throughout the time we have spent writing this report and designing our system, ChatGPT has been a valuable tool for accelerating research and providing structured guidance on complex design tasks. One significant way it benefited our project was in identifying a suitable localization tool for our unique sensor suite. Since our system relied solely on a custom-built active stereo vision system without LiDAR, we needed a solution capable of mapping and localization that could function effectively under these constraints. Not only did the model help construct some of the fundamental steps of how to transform the structured light output of the IR camera into depth data that could be read by RTAB-Map, but it also gave an outline of how to integrate this RTAB-Map-based localization with more commonly used Nav2 planner Nav2. ChatGPT provided an overview of different options for localization, such as RTAB-Map and ORB-SLAM, explaining their strengths, installation procedures, and integration requirements. This saved us significant research time and ensured we selected a tool that aligned with our hardware capabilities.

Beyond just selecting a localization method, ChatGPT also helped us outline a clear roadmap for integrating localization with a planning library, specifically Navigation2 (Nav2). It provided step-by-step instructions on configuring RTAB-Map to generate a map and publish transformations that Nav2 could consume. Additionally, it highlighted necessary parameter adjustments, TF frame requirements, and potential pitfalls, helping us structure our implementation efficiently. By following this guidance, we avoided unnecessary trial and error, ensuring smoother integration and a more structured development approach.

Moving forward, we expect ChatGPT to continue playing a critical role, especially in the development and integration of these designs. Specifically, with the immense amount of documentation and literature behind the tools and concepts of the RTAB-Map and Nav2 libraries, ChatGPT is expected to aid specifically in the quick debugging and summarization of problems that would normally require hours to days of documentation review.

5.2.6 Optical Calculations

Large Language Models (LLMs) like ChatGPT have been very helpful in numerous areas of this project, such as for research or part selection comparisons. However, when used for theoretical events that involve calculations, it struggles to understand certain principles of the technologies involved in the theoretical event. The LLM also makes various assumptions when faced with a multi-component, multi-variable task.

The LLM had difficulty calculating the total light power entering the eye (as seen in Prompt 3), a necessary step in determining the maximum safe power of the project. This was because of its inability to account for several variables. The response did not consider the optics of the human eye. Incorrectly, it stated that the total light entering the eye is determined by the diameter of the pupil. Although this is technically true, the LLM forgot to consider the refractive characteristics of the cornea, which causes more light to enter through the pupil. Therefore, the LLM should have calculated the entrance pupil and continued its calculations from there.

In response to the question, ChatGPT also hallucinated the idea that the lines of the structured light projected from a DOE expand at a rate equal to the FOV that the structure expands. Although a minimal expansion of the light line occurs because of the quality of the incident beam on the DOE, the expansion occurs in the formed structure. For someone who is not knowledgeable about the topic of diffractive optics, this information provided by the LLM could have harmed that person's understanding of the topic. Consequently, well-structured, unambiguous prompts ensure well-formed responses. And the only way to provide this type of prompt is by doing our research in textbooks, articles, or research papers.

Although it is common to notice LLMs hallucinate when given very niche scientific topics, it also struggles with simple reasoning. In the prompt given, it was stated that there were 60 horizontal lines and 60 vertical lines, a total of 120 lines. But in the answer, Chat-

GPT provided that it calculated the total power distributed across 60 lines right after stating its acknowledgment that there are 60 vertical and 60 horizontal lines. We have experienced this type of incorrect assumption when trying to make scientific calculations on imaginary optical scenarios. Better results follow from dividing the problem into smaller and easier tasks suitable for ChatGPT. However, when these tasks are completed and verified, it is necessary for us to make the final integrations and calculations.

Moving forward, we expect to be using LLMs such as ChatGPT for low-level repetitive calculations where the variables and assumptions are given in the prompt. But we cannot fully trust in it performing high technical level based assumptions on technology and physics applications in order to calculate imaginary scenarios.

Chapter 6 System Hardware Design

6.1 Optical Subsystem Hardware

Figure 6.1 illustrates the optical coupling system designed to couple light from the Osram SPL TR85 edge-emitting laser diode into the SMF-28 Fiber. Due to the asymmetric divergence of the laser diode's emission along the x- and y-axes, beam shaping is necessary to ensure better coupling efficiency. The system consists of two plano-convex lenses and a pair of anamorphic prisms, arranged to collimate, reshape, and focus the beam into the fiber core. The highly divergent output from the laser diode is first collimated using a plano-convex lens with a 30 mm focal length, transforming the initially diverging beam into a more uniform collimated state. The collimated light then passes through a pair of anamorphic prisms, which reshape the beam in one axis, reducing ellipticity and achieving a more symmetric beam profile. Finally, a second plano-convex lens, also with a 30 mm focal length, focuses the shaped beam into the core of the optical fiber. Proper alignment of these optical components is crucial to minimizing insertion loss and ensuring efficient light transmission into the fiber.

Figure 6.1: Laser Diode Coupling to Fiber Optic

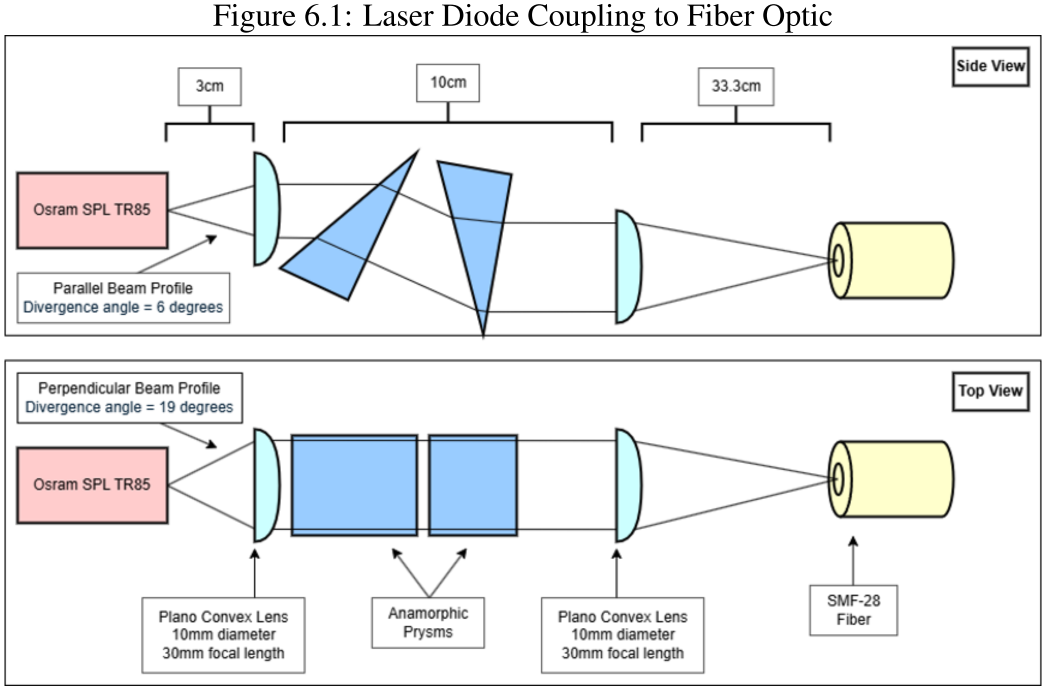

Figure 6.2 shows the optical setup designed to generate and capture structured light for depth sensing. The system starts with an SMF-28 optical fiber, which delivers the light source. Since the light emerging from the fiber is highly divergent, it first passes through a plano-convex lens (10 mm diameter, 20 mm focal length) to collimate it into a uniform beam. Once collimated, the light is transmitted through a diffractive optical element (DOE-SG60), which structures the beam into a specific pattern with a 50-degree field of view (FOV). This structured light is then projected into the environment, where it interacts with objects and reflects toward the system. The returning light is captured by an Arducam 2MP IMX462 sensor, which records the distorted pattern caused by objects in the scene. By analyzing these distortions, depth information can be extracted, allowing the system to map the environment in three dimensions.

Figure 6.2: Collimation of Light from Fiber to DOE

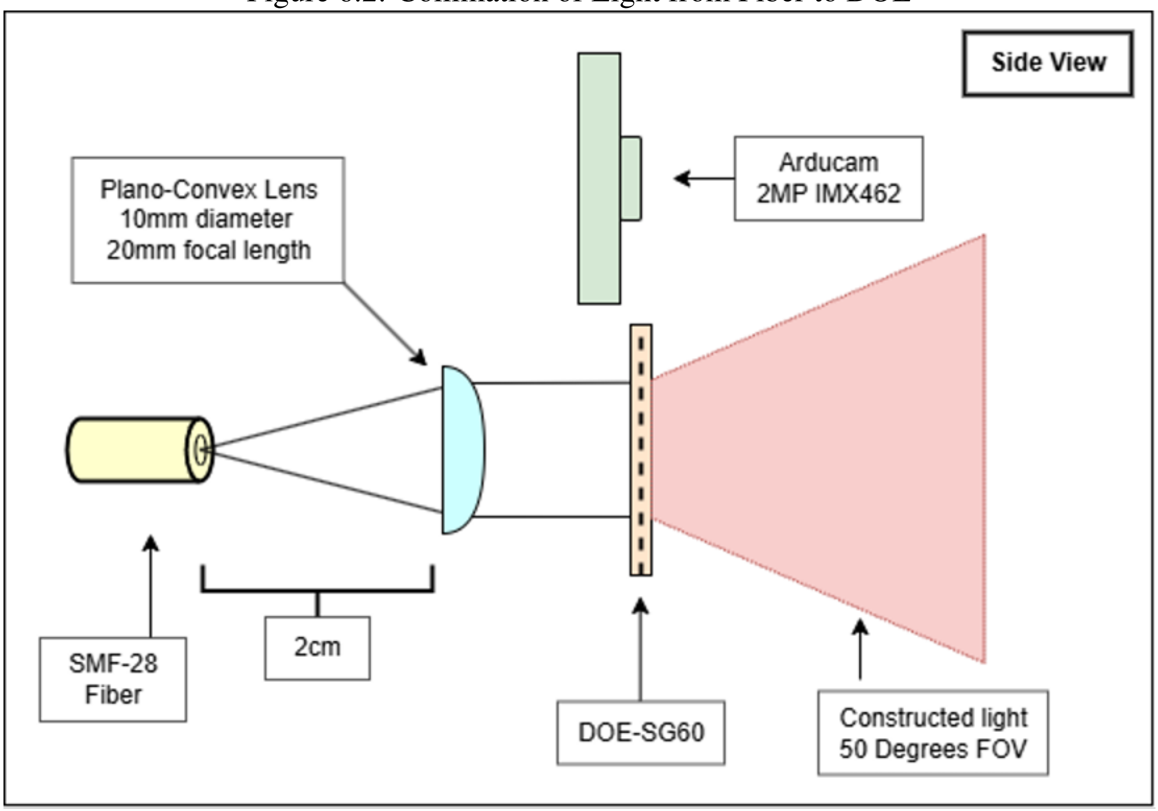

The connections between the electrical components in the optical subsystem are displayed in Figure 6.3 below. These components include the IR CMOS cameras, the laser diode driver, the laser diode, and the SBC. The SBC receives 5V and 3A from the power daughterboard specified in the following section. The SBC also has a data connection to the MCU to receive IMU sensor data and information from the application interface, which it processes with the camera data to send back to the MCU for control of the audio and haptic peripherals. The CMOS camera modules connect to the SBC's USB interface to receive power and supply camera data. The power board also supplies 5V and up to 250mA to the laser diode driver, which powers the laser diode. The driver also receives an analog data input from the MCU's DAC pin for pulsed modulation of the laser diode.

Figure 6.3: Hardware Block Diagram of the Electrical Components of the Optical Subsystem

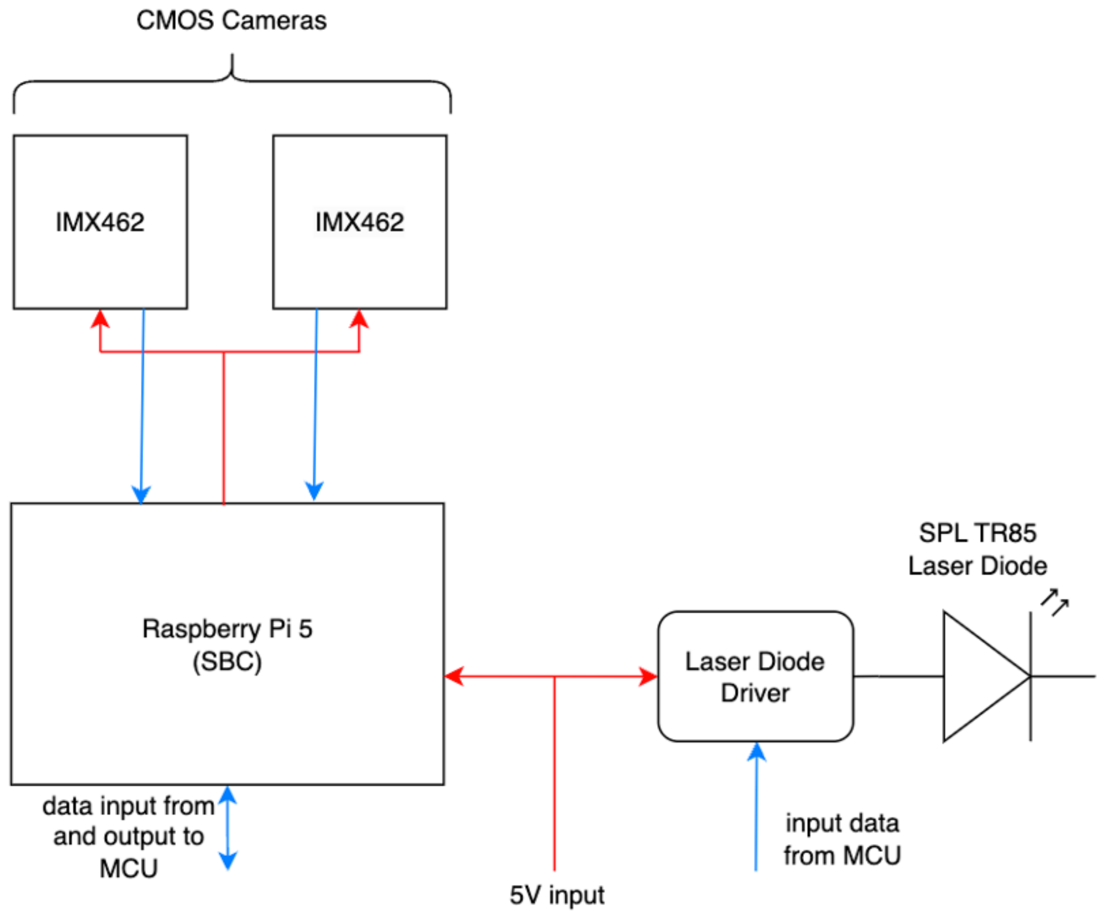

6.2 Main Board

The high-level block diagram of the main board and its associated components are shown in Figure 6.4 below. It's primary function is to connect to peripherals, which includes incoming data from the app interface to the MCU, and output cues to the speaker and haptic motors. The MCU also receives and does initial processing of data from the IMU, which his housed on the same board, and communicates this information to the SBC. It then receives information from the SBC which determines outputs to the haptic motors and speaker through the respective drivers and amplifiers. The MCU communicates wirelessly to the app interface, through I2C to the IMU and haptic motor drivers, and through a DAC pin to the speaker amplifier. The main board also receives a 3.3V power input from the power supply daughterboard, since all components on this board operate at 3.3V.

Figure 6.4: Hardware Block Diagram of the Electrical Components of the Main System

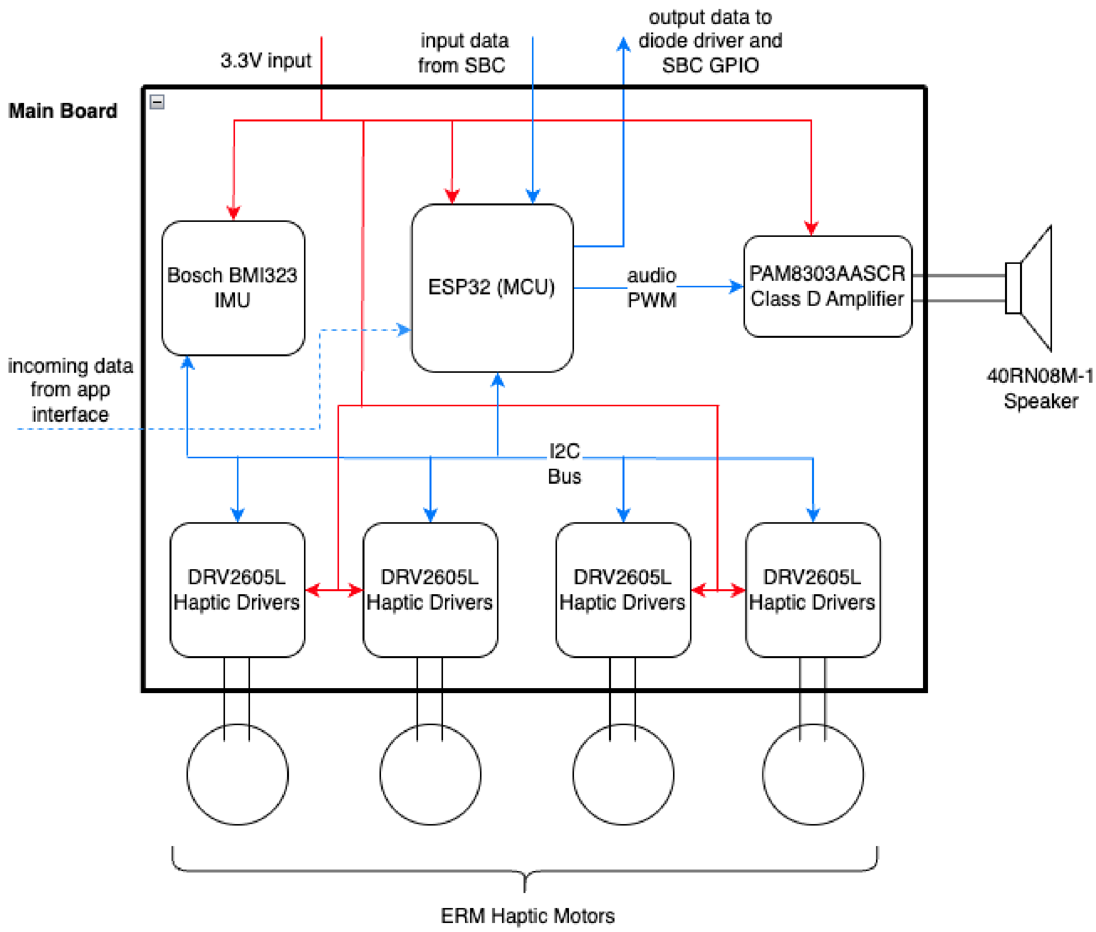

The schematic of the main board is shown below in Figure 6.5. The board receives 3.3V along with GND through the 2-pin screw terminal block connecter from the power daughterboard. The microcontroller symbol was updated to include the ESP32-WROOM-32E symbol and footprint, rather than the previously selected ESP32-WROOM-DA model. However, both IC's share the same pin layout, enabling easy migration between the two. The schematic also includes a USB to UART bridge controller to allow the MCU to be programmed through a USB Micro B port. This is done by the CP2102N IC, along with an auto-reset circuit to streamline programming and backup manual buttons for booting and resetting connected to the MCU. The remaining components, excluding the speaker driver, all communicate via I2C, which enables the SDA and SCL lines to be pulled up to the 3.3V line. For the IMU and haptic motor drivers, proper circuit design guidelines from the respective datasheets for each part are followed to choose appropriate bypass capacitors for voltage supply pins, configure the pinouts for the required operational modes, and other connections to the MCU, such as enable or interrupt pins. The haptic drivers are divided into two pairs, each sharing an enable pin for left and right haptic cues to the user. Similarly, circuit design guidelines are followed for the speaker amplifier to ensure proper supply voltage through the 3.3V line and the positive and negative input DAC control inputs. The speaker amplifier outputs to the positive and negative leads of the speaker through a 2-pin screw terminal block connecter. The haptic drivers similarly output to a combined 8-pin header for control of 4 haptic motors, which will be placed on the shopping cart handlebar.

The MCU also establishes lines for output to the laser diode driver and the input/output to the SBC. The driver output utilizes a 2-pin header with GND and a DAC pin on the MCU for modulated laser diode control. The pins to the SBC utilize the I2C SDA and SCL communication pins on the MCU.

Figure 6.5: Main Board Schematic

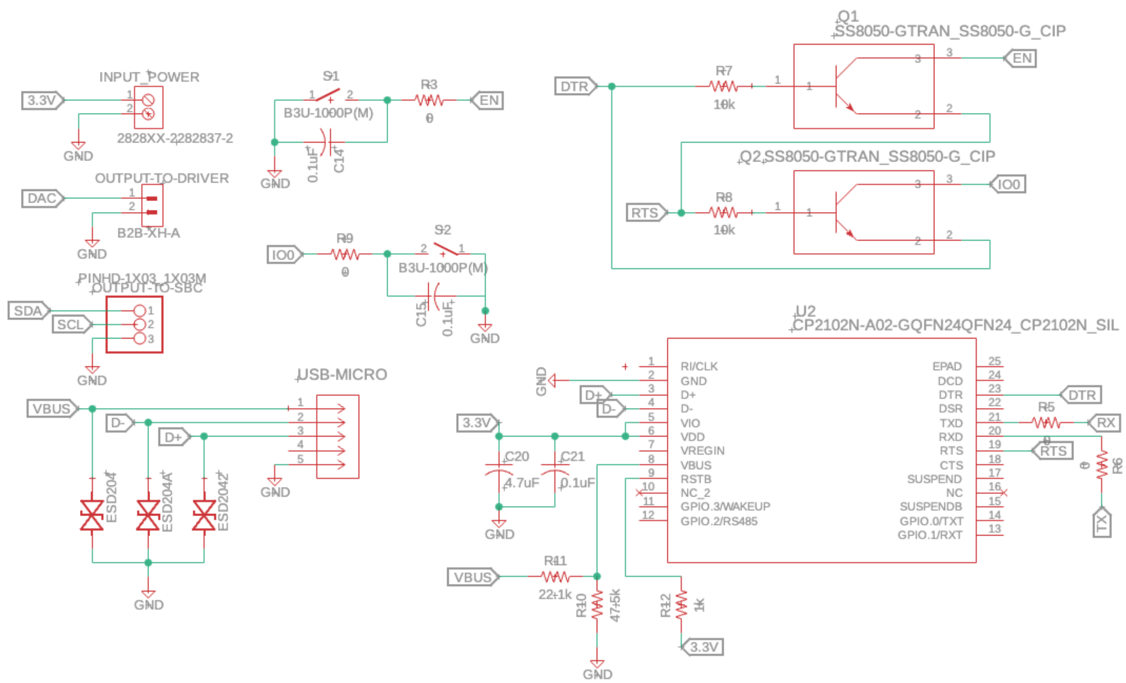

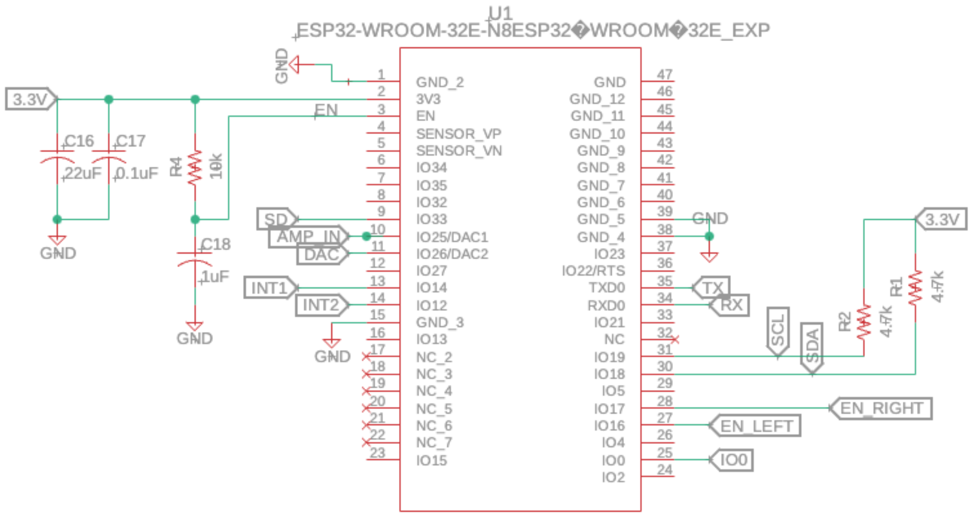
U1
ESP32-WROOM-32E-N8ESP32�WROOM�32E_EXP
3.3V
C16
22uF
C17
0.1uF
R4
10k
C18
1uF
EN
SD
AMP_IN
DAC
INT1
INT2
GND
GND_2
3V3
EN
SENSOR_VP
SENSOR_VN
IO34
IO35
IO32
IO33
IO25/DAC1
IO26/DAC2
IO27
IO14
IO12
GND_3
IO13
NC_2
NC_3
NC_4
NC_5
NC_6
NC_7
IO15
GND
GND_12
GND_11
GND_10
GND_9
GND_8
GND_7
GND_6
GND_5
GND_4
IO23
IO22/RTS
TXD0
RXD0
IO21
NC
IO19
IO18
IO5
IO17
IO16
IO4
IO0
IO2
TX
RX
SCL
SDA
R2
4.7k
R1
4.7k
EN_RIGHT
EN_LEFT
IO0

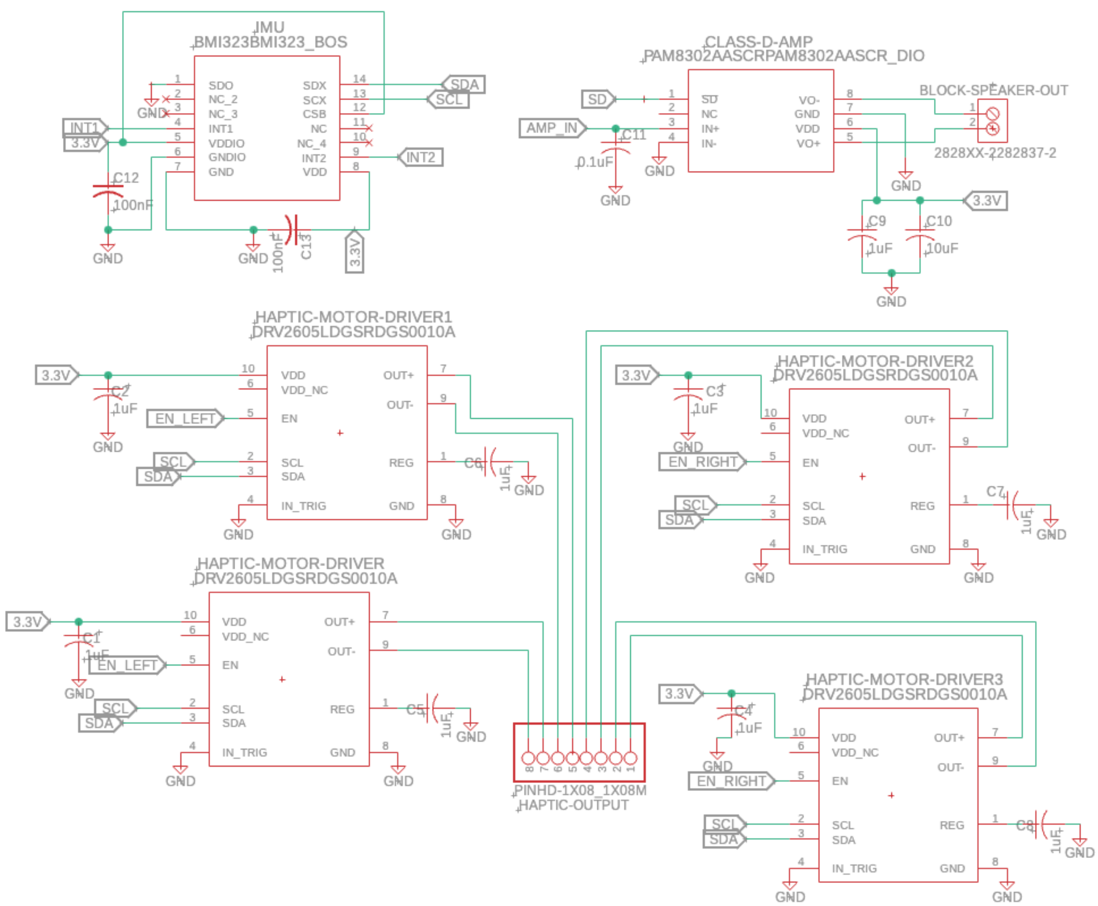
IMU
BMI323BMI323_BOS
SDO
NC_2
NC_3
INT1
VDDIO
GNDIO
GND
SDX
SCX
CSB
NC
NC_4
INT2
VDD
SDA
SCL
INT1
3.3V
INT2
C12
100nF
C13
100nF
GND
CLASS-D-AMP
PAM8302AASCRPAM8302AASCR_DIO
SD
AMP_IN
SD
NC
IN+
IN-
VO-
GND
VDD
VO+
C11
0.1uF
BLOCK-SPEAKER-OUT
2828XX-2282837-2
C9
1uF
C10
10uF
HAPTIC-MOTOR-DRIVER1
DRV2605LDGSRDGS0010A
VDD
VDD_NC
EN
SCL
SDA
IN_TRIG
OUT+
OUT-
REG
GND
C2
1uF
EN_LEFT
C6
1uF
HAPTIC-MOTOR-DRIVER2
DRV2605LDGSRDGS0010A
C3
1uF
EN_RIGHT
C7
1uF
HAPTIC-MOTOR-DRIVER
DRV2605LDGSRDGS0010A
C1
1uF
EN_LEFT
C5
1uF
PINHD-1X08_1X08M
HAPTIC-OUTPUT
HAPTIC-MOTOR-DRIVER3
DRV2605LDGSRDGS0010A
C4
1uF
EN_RIGHT
C8
1uF

6.3 Power Management and Distribution Subsystem Daughterboard

Figure 6.6 highlights the overall power management and distribution system, with the selected LiFePO4 battery input into the two 5V and one 3.3V buck converters, which output 5V and 5A to the SBC, 5V up to 2.5A to the laser diode driver, and 3.3V up to 2.5A to the main board.

Figure 6.6: Hardware Block Diagram of the Power Distribution Subsystem

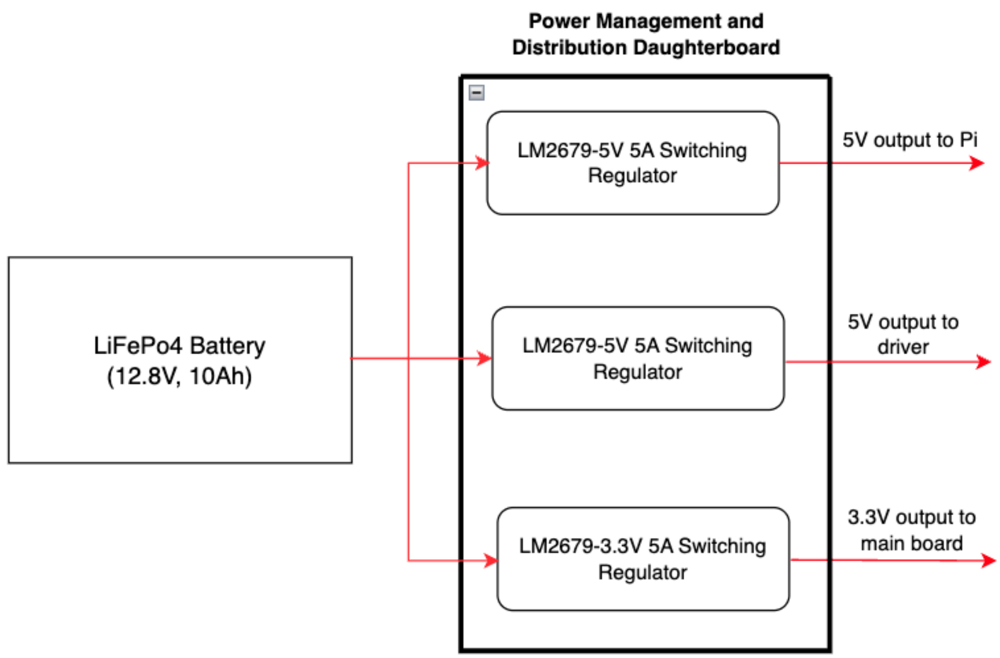

Figure 6.7 is the more detailed schematic view of the high-level block diagram represented above. It contains a 2-pin screw terminal block connecter for the 12.8V battery input supply, which is converted into both 5V and 3.3V by the chosen regulators. The regulator circuit designs were derived through both WEBENCH and datasheet input and output voltage and current specifications for the ICs. The power output to the main board, which requires 3.3V for its components, is a 2-pin JST header with 3.3V and GND. For the optical subsystem, the outputs to the driver and SBC are separated due to their different input types. For the driver, a 2-pin 5V and GND output is used. The Raspberry Pi 5 requires 5V and 5A through USB-C. The output on the power board to the SBC is a USB-C 3.1 receptacle with the CC pins pulled down to ground with a 5.1kOhm resistor to indicate to the SBC that the incoming USB-C power supply is 5V.

Figure 6.7: Power Daughterboard Schematic

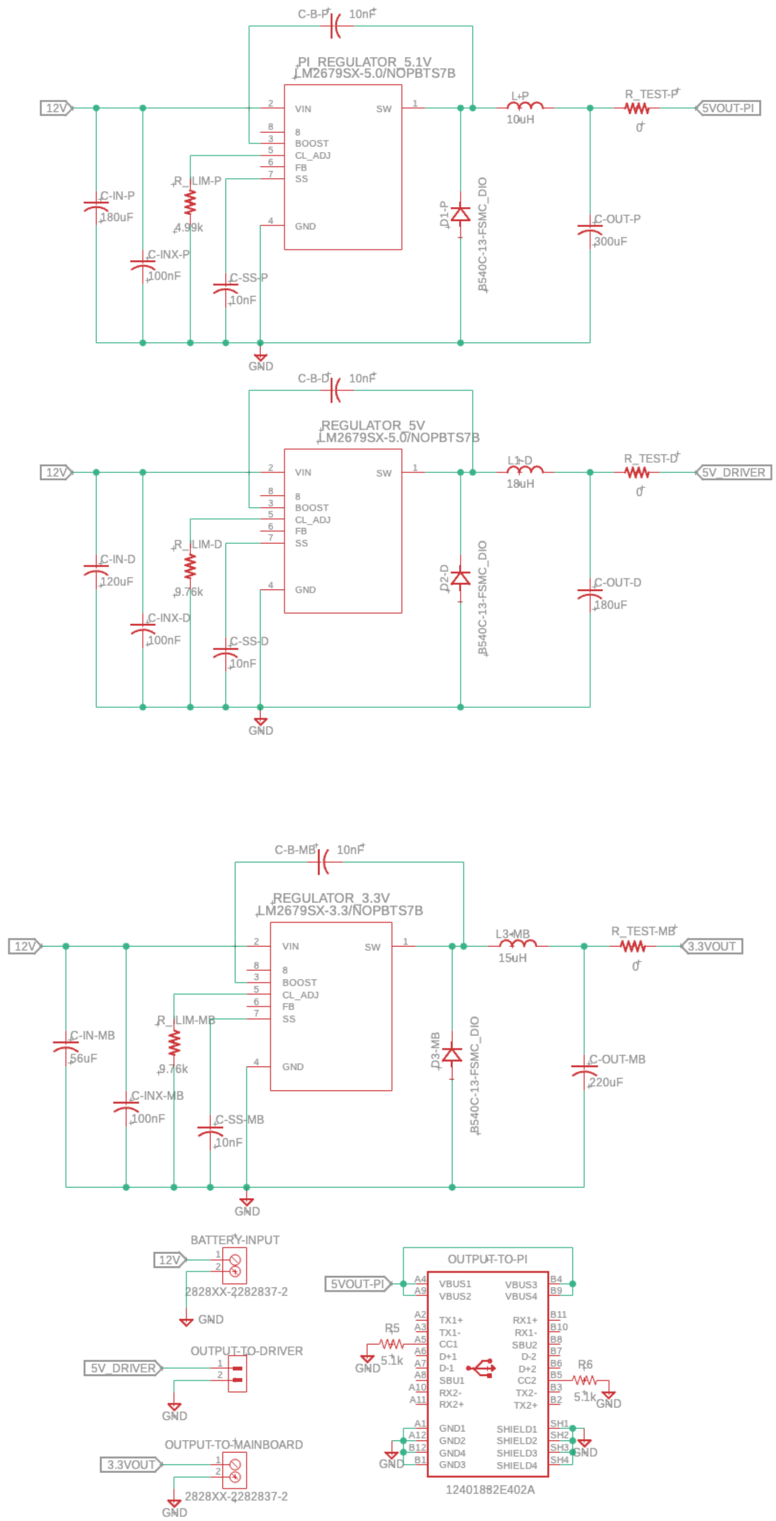

Chapter 7 Software Design

7.1 Microcontroller Programs

7.1.1 Overview

As indicated on the above hardware I/O diagram, as well as the below overview of the programs that will be ran on the microcontroller, there are a total of 4 different processing tasks that will be done directly on the microcontroller. These include the following:

- Control the output speakers and haptic motors
- Control the output of the laser diode via its driver
- Pass through IMU data to the SBC
- Host web application

For each of these, additional details describing the workflow will be found below. It should be noted that each of the programs will be idle during certain times. Some examples of this include the web application which will not be used after the user has selected the items they wish to navigate to, as well as the remainder of the programs not being used during this initial selection stage. This means that while we must account for storing all of the programs together on the MCU's EEPROM, we must only account for the clock cycles and memory needed to run the programs that are being used at any given time. Because of this, we do not believe that the use of a Real-Time Operating System will be necessary for use on the MCU.

Figure 7.1: MCU Responsibilities

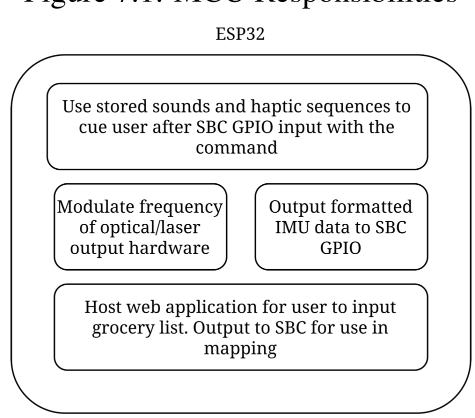

7.1.2 Output Sound and Haptics

As demonstrated above, the haptic motors and speaker outputs are used such that the user can be guided throughout the store as they are navigating it for their grocery item list entered in the web application.

The MCU will be constantly receiving a number from the SBC over GPIO, calculated using the navigation stack positioned on the SBC, which will tell the MCU which direction the user should navigate next. At the moment when it receives this input, which will be called the "direction index," it will use a lookup table to determine which way the user should move next - with both a rough direction and magnitude of any changes that the user should make to their current position to avoid obstacles that are in their way along with navigating to the next item as safely as possible.

It will then use this lookup table to load an output pattern for each of the outputs - speaker and haptic motors - to indicate to the user which direction to move. Whenever there is a new input, this will replace the previous output pattern as demonstrated from the output pattern on the speaker and motors. A diagram showing this flow can be found directly below:

Figure 7.2: Sound and Haptic Workflow

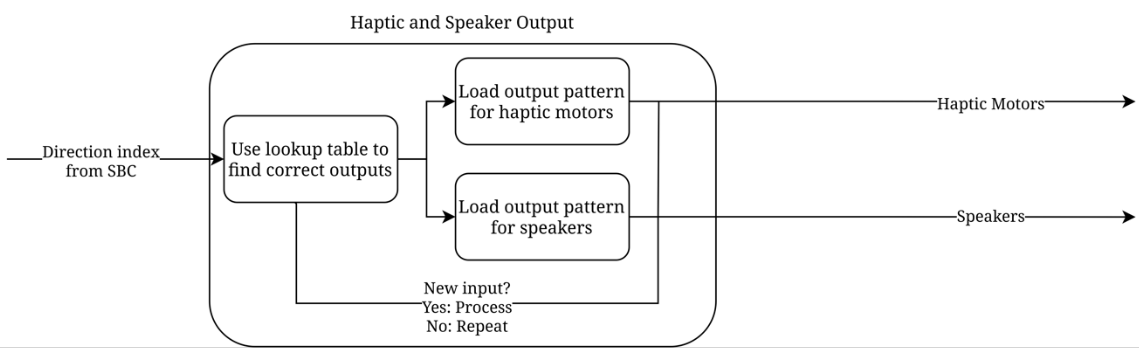

7.1.3 Laser Diode Modulation

In a standard environment such as a grocery store, there is likely to be an ample amount of IR sources, all of which we want to ignore other than those from the laser diode from our system. In order to do this, we must modulate the laser diode, via its driver, at many different frequencies, each of which must be less than half of the frame rate of the camera.

The reason for this restriction is because the software running on the SBC needs to be able to know how many times the source turns on and off in a given time window, which can only be done reliably if the frame rate is at least twice that of the modulation frequency.

Modulating the laser allows the SBC to detect the interference from other IR sources, with knowledge of the modulation frequency at any given time, to determine what part of the received signal by the camera is from the laser diode and which others must be filtered out before feeding into the navigation algorithm.

A PWM output pin will be used to output the pattern in which the laser diode driver should turn on and off the diode in order to perform these tasks as described. As shown in the below diagram, and reproduced below, first, using built in math functions, a sine wave with amplitudes between 0 and 1, inclusive are used to generate the modulation pattern. This is then passed into a formula which determines the actual clock frequency given the output from the previous sine wave. The SBC will also be privy to this information such that it can know what IR sources it can filter out from the signal input it receives from the camera.

Figure 7.3: Laser Diode Workflow

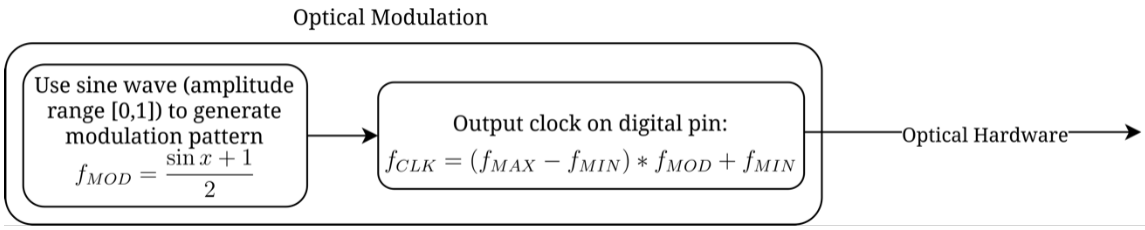

7.1.4 IMU Data

Before being ingested by the ROS software hosted on the SBC, the raw IMU data from the sensor group is used as an input to the MCU. The MCU will then lightly process the data signals coming from the IMU as to remove noise. The purpose of this extra step is to make sure the data is as accurate as possible when it is consumed by the SBC and thereafter used for navigation of the user throughout the store.

Since the data will only be minimally processed on the MCU, there is not much of a hardware processing requirement for this specific program on the MCU, with most of the hardware recourses being left available to be used by the other programs controlling the output hardware with help of the input from the SBC along with the optical modulation program.

A small control flow diagram of this program can be found directly below.

Figure 7.4: IMU Workflow

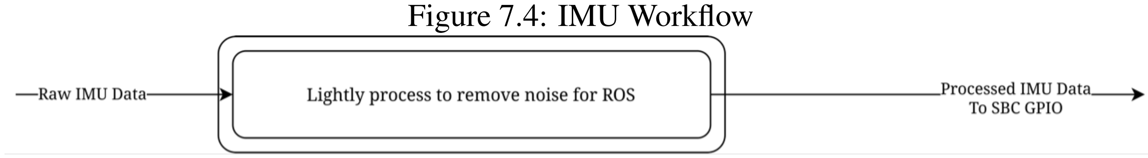

7.1.5 Web Application and Data Forwarding

The web application will, as described in the below flowchart, collect information from the user in a list interface, in which a database or similar lookup table is interacted with, about the items that the user would like to add to their cart and navigate the store to. This will be done using the WiFi controller on the microcontroller and will be handled with the WiFi direct standard. The user will first search for an item, then they will select each item that they wish to add to their cart. After they have added each item that they wish to pick up throughout the store, they will go to a final screen where they can change their cart as necessary before starting navigation throughout the store.

When the user begins navigation, the list of items will get sent from the microcontroller to the single board computer over the single board computer's GPIO pins such that the single board computer can then use its route planning software to find a route throughout the store that is most optimal. After this is complete, the ROS-based navigation stack will be enabled on the single board computer and the programs containing the localization software will be enabled on the microcontroller, respectively.

Figure 7.5: Web App Workflow

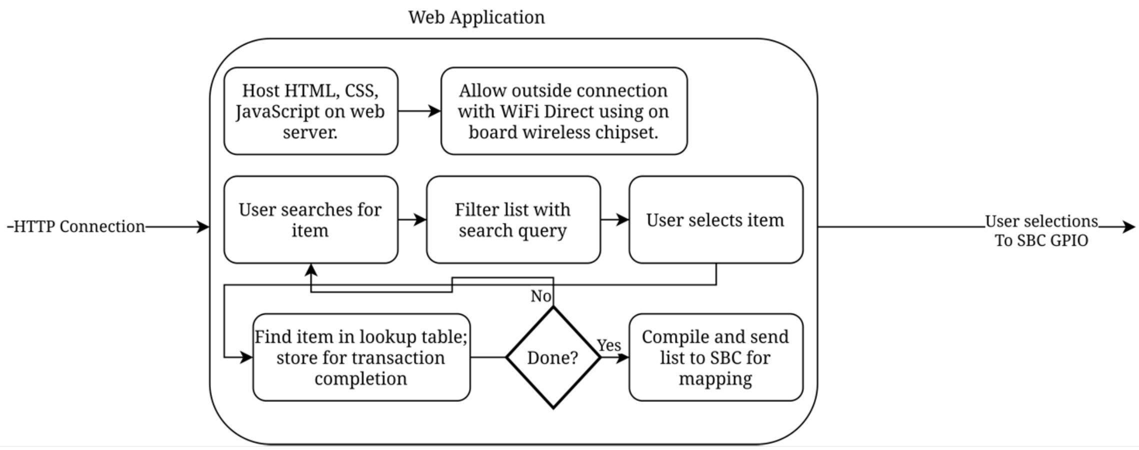

7.1.6 Web Application Mockup

In the web application, as explained just above, the user will first navigate to the main page (index.html) hosted on the MCU's web server. After this, they will be able to select the items that they would like to add to their shopping list, which will be navigated to during that portion of the usage of the cart. This can be done with or without searching for a specific item, and is done using JavaScript such that the user doesn't need to reload the webpage each time they update their search query. Each keystroke will update the query from the MCU.

The user can then remove any items that they would, after selecting, not like to navigate to, while in the shopping cart view. After they are satisfied with their list, they can click "View Cart" - shown in the top right corner in the below flowchart, which will bring them to a list of the items that they have selected as a confirmation prior to as a confirmation prior to starting navigation. In addition, this confirmation screen also contains the options to remove any items - after which they will disappear from the list - along with the options to remove these items on the final screen and the option to go back to the previous page where they can add more items as they wish. The user can continually navigate between these pages without issue as they see fit.

Once the user is satisfied with their list, they can click "Begin Navigation" to indicate that this process is complete and they are ready to begin store navigation. When this button is pressed by the user, as shown in the flowchart, the web server on the MCU will be shut down and the rest of the hardware will be enabled such that the user will be able to navigate the store with the assistance from the programs running at that time.

A complete flowchart of the program - from selection to final navigation - can be found below:

Figure 7.6: Web App Selection to Navigation Flowchart

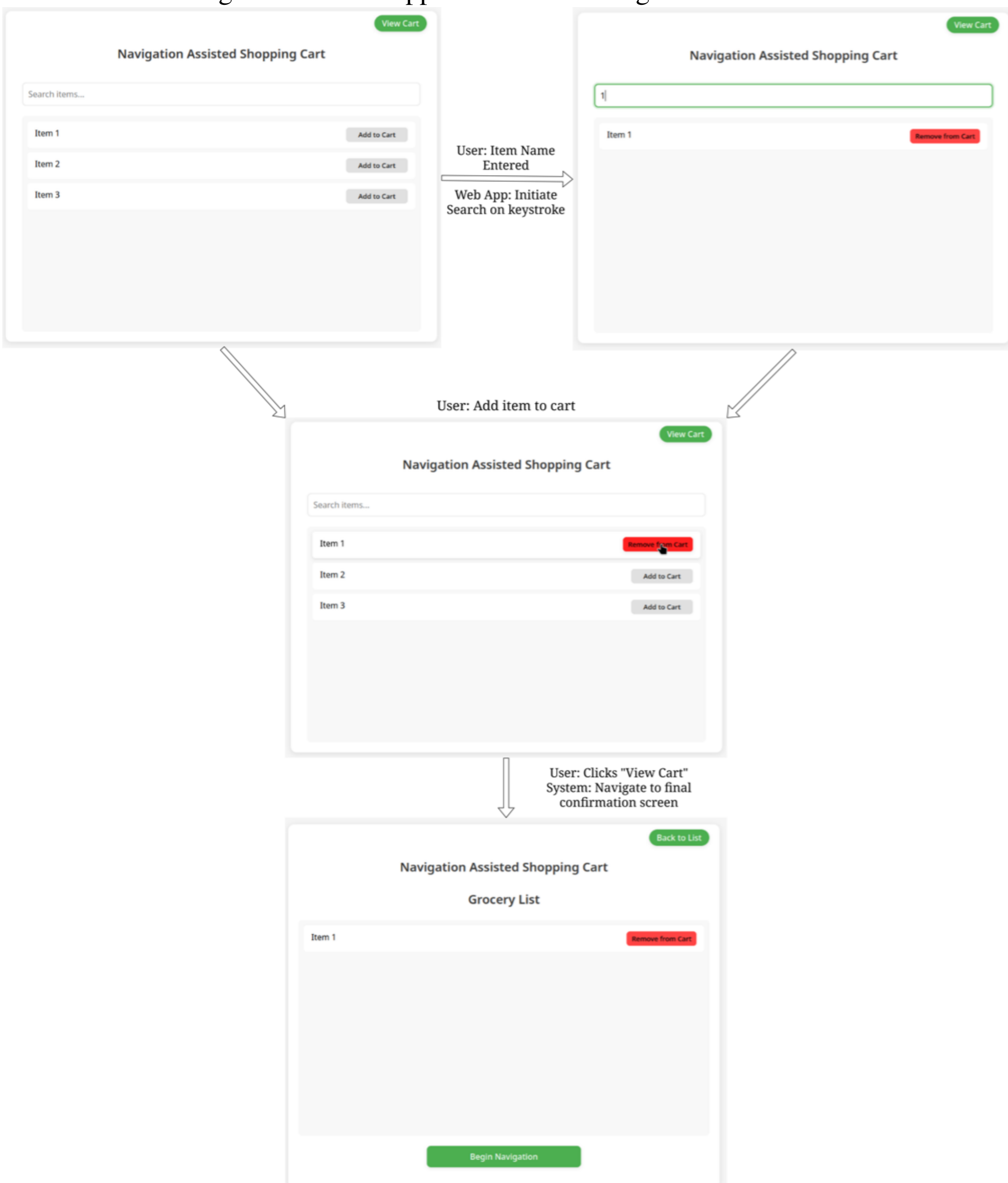

7.2 Single Board Computer Programs

Due to the real-time nature of robotics, concurrency will be playing a huge role in the development of the shopping cart. From sensor reads, to serial comms, and all the way to autonomous navigation, the shopping cart will be calculating a significant amount of data and algorithms at each clock cycle. This leads us to adopt a single-board computer (SBC) to not only aid in the computation, but to also enable the implementation of highly abstract robotics concepts inherent to autonomous navigation. Processes running on the SBC are all specifically for autonomous navigation, and include a large ROS2 graph, a localization/planning/control loop, depth image processing for our custom camera, and communication with the web server set to be developed on the MCU.

7.2.1 MCU Server Flowchart

Before navigation occurs, the cart needs to know where it's navigating to. This is going to be achieved via the construction of a WiFi connection on the ESP32 MCU. Through this connection, the MCU will be able to receive a json containing the unordered list of groceries that the shopper needs. Specifically, we are going to be using the extensively documented WiFi.h and ArduinoJSON.h libraries, which allows us to use highly abstracted functions to interact with the on-board ESP32 WiFi chip and easily interact with JSONs. This process includes the initialization of a connection via pre-loaded credentials, and the establishment of a connection with the MCU's serial monitor. The MCU will then wait for a JSON to be sent to it's IP address from the mobile app, in which it will then deserialize, extract, and output the JSON to the SBC. There will also be implementations of error handling to process parsing and connection errors.

Figure 7.7: MCU to Server Flowchart

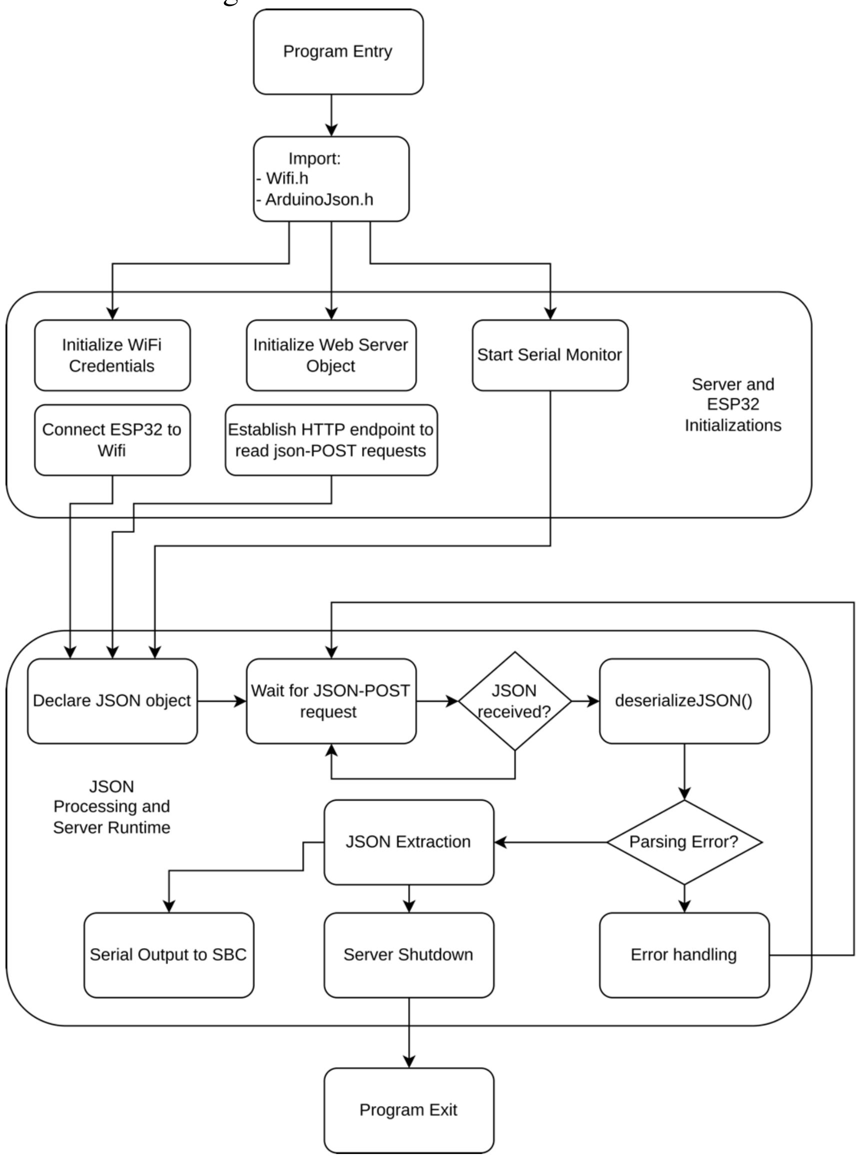

7.2.2 Autonomous Navigation Control Loop

The overarching control loop algorithm is the most important in terms of understanding the navigational aspect of the project. This includes the high-level algorithms, and the important branches leading in and out of the loop itself. Starting with the mobile app, the SBC is supplied with an unordered grocery list, which it then orders based off a discrete grid routing algorithm. Once this ordered list is supplied, the loop itself can begin, by repeatedly planning a path in the continuous space, forming a control output to send to the haptic sensors, and localizing. At each timestep, we are also checking to see if we reached the desired waypoint, e.g. a grocery item or the deli, in which we send out unique audio outputs to give more clear indications of the progress. The most important part of the loop, however, is the shopper themself, as they are the one truly turning the haptic output into movement. This dynamic is interesting from multiple stanpoints, but especially so from a control theoretic perspective.

Figure 7.8: Autonomous Navigation Control Loop Flowchart

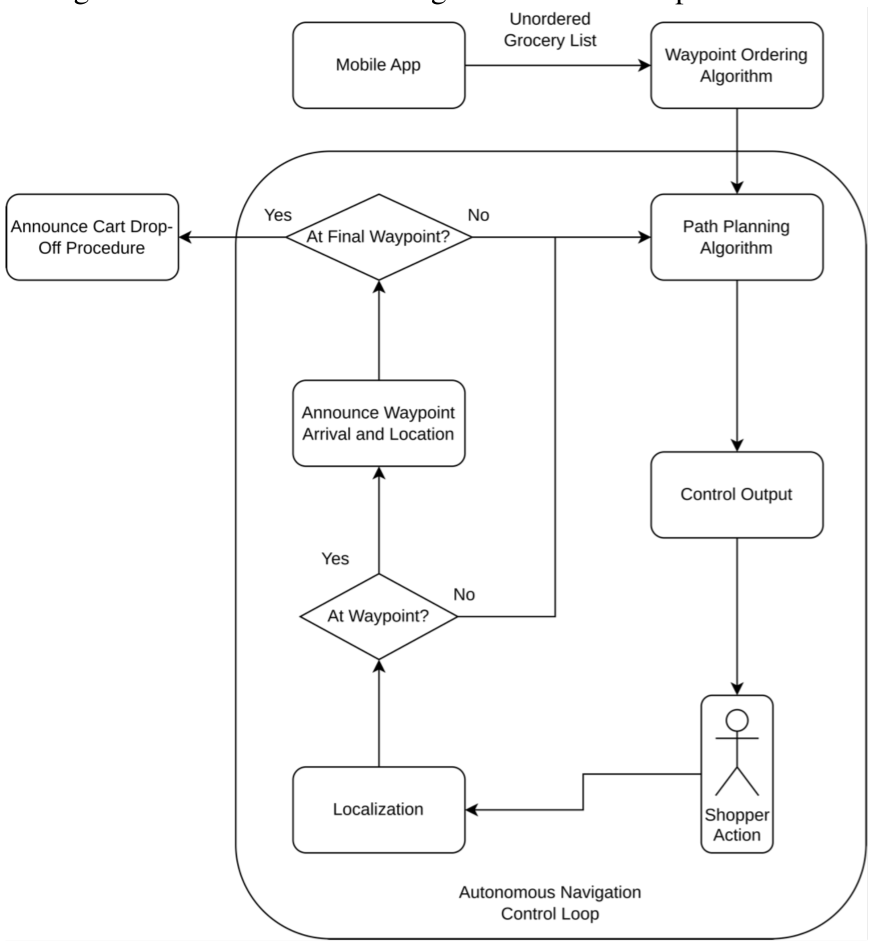

7.2.3 Depth Image Construction

The most unique aspect of our project, especially on the software side, is the implementation of a custom depth image construction algorithm. This is where we take in images from our IR cameras and convert them to ROS2-compatible depth images for localization purposes. The algorithm to construct these depth images can be seen below, but works based off a structured-light configuration. A structured light grid is cast from an IR projector, and the camera receives images based off the IR imagery that returns. With that image, we can compare the distortion per pixel to the reference structure, and thus construct depth estimates on a per-pixel basis. This is looped over for every pixel, at every frame, so we will be running a low FPS to account for the additional computational strain this is inevitably going to cause.

Figure 7.9: Depth Image Construction Flowchart

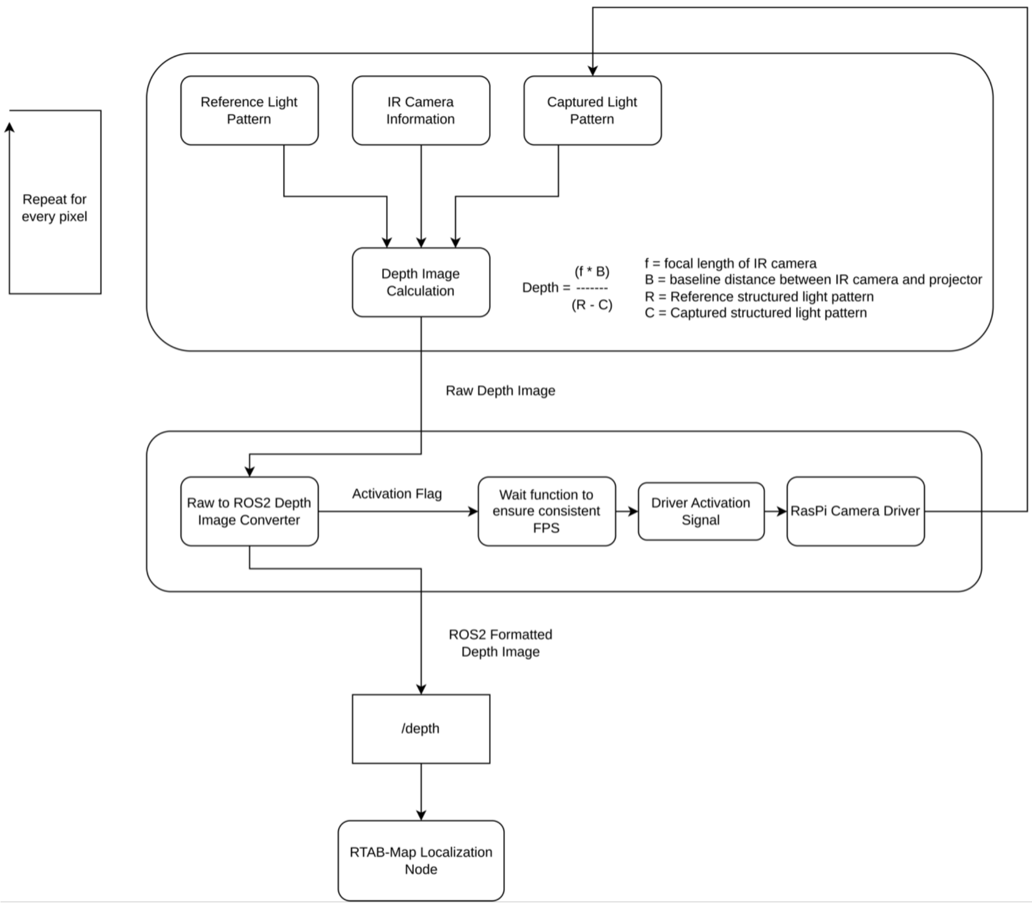

7.2.4 ROS2 System Graph

Finally, as discussed in the description of the AutoNav Control Loop, robotics normally consists of a highly concurrent environment of processes running on the high-brain board. While this can be achieved extremely efficiently through custom implementations of a DDS, e.g. in C++ or Rust, the easiest way to implement this concurrency is the ROS2 ecosystem. This includes the use of custom ROS2 nodes made for autonomous navigation, such as the use of RTAB-MAP for localization and mapping, and Nav2 for path planning in continuous domains. For our implementation, this also includes custom nodes for depth image construction, serial communication for sensor input and command output, and odometry calculations for localization node input. A full view of the nodes, the topics they communicate over, and the entire graph can be seen below.

Figure 7.10: ROS2 Communication Flowchart

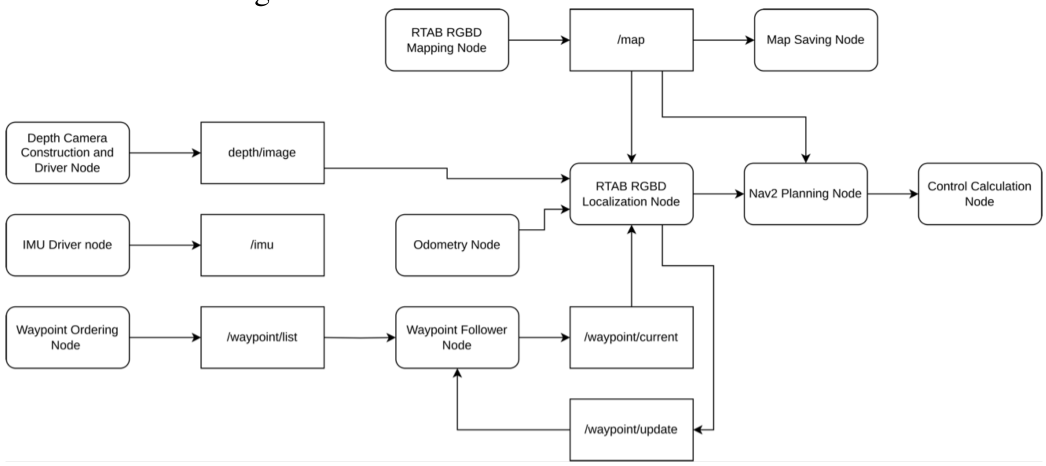

Chapter 8 System Fabrication/Prototype Construction

8.1 PCB

The printed circuit board (PCB) for the system was designed using Autodesk Fusion, which provides an integrated environment for both schematic capture and PCB layout. The design process begins in the schematic editor, where circuit connections are defined. Components are selected from Fusion's built-in libraries and placed according to logical signal paths and voltage domain groupings. For specialized components not included in the default libraries, models were imported from Ultra Librarian as .lbr files, which include both schematic symbols and associated PCB footprints.

Once all components are wired and labeled according to their respective datasheets and recommended application circuits, an electrical rules check (ERC) is performed to identify any design violations or incomplete connections. The design is then transitioned into the PCB layout workspace, where component placement is optimized to minimize trace lengths and reduce noise. Passive components such as decoupling capacitors and resistors are grouped closely with their corresponding ICs or power inputs to maintain signal integrity, as per datasheet recommendations.

Autodesk Fusion allows for user-defined design rules, which were configured to reflect manufacturing constraints and expected current loads. These include minimum and preferred trace widths, via sizes, and clearances. For initial routing, the autorouter tool was used to generate trace paths based on net connections and rule constraints. In cases where the autorouter was unable to complete certain connections, typically due to complex routing constraints or tight component spacing, manual routing was employed to complete the layout.

A custom board outline was created to minimize unused space, and mounting holes were added to allow mechanical integration with the rest of the system. Copper pours were used to establish ground planes, improving both thermal management and EMI performance. A final design rules check (DRC) was run to ensure compliance with all layout constraints. An initial PCB layout is shown in Figure 8.1 for the Main Board and Figure 8.2 for the Power Daughterboard. Fusion also allows users to view a 3D model of the designed PCB, which can be used when designing enclosures or housing to ensure the PCB meets size requirements.

Once the PCB layout is finalized, the design is exported as a set of Gerber and drill files, which are used by PCB manufacturers to fabricate the board. The design files will be reviewed against multiple fabrication vendors to determine the most suitable option based on cost, lead time, and quality assurances. Some commonly used manufacturers include JLCPCB, PCBWay, and OSH Park. The manufacturer will be selected based on a comparison of their capabilities, pricing tiers, shipping timelines, and support for additional services such as stencil fabrication or board assembly.

Figure 8.1: Preliminary PCB of the Main Board

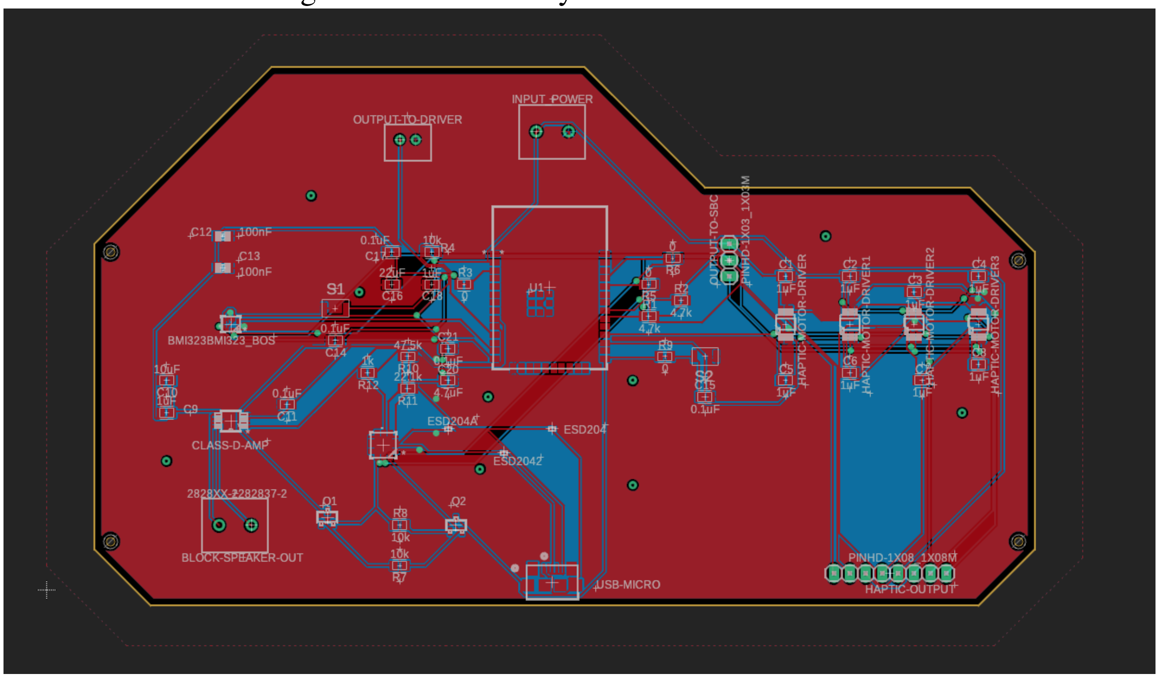

Figure 8.2: Preliminary PCB of the Power Daughterboard

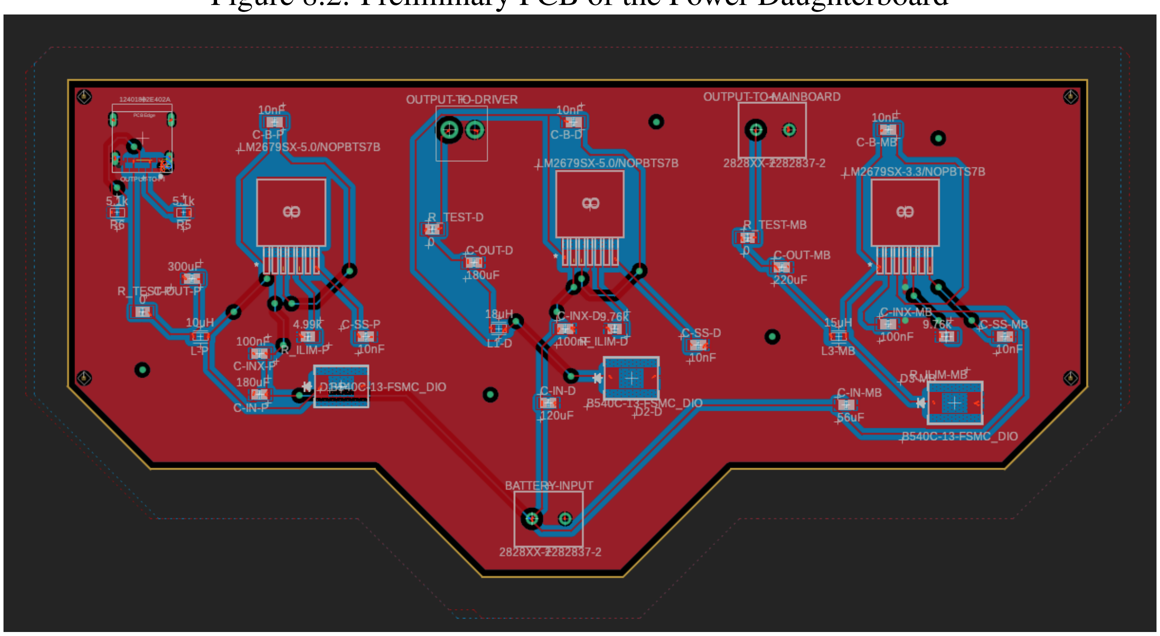

8.2 Battery and Electronics Enclosure

To house and organize the system's electronic components, a custom CAD enclosure was designed. The enclosure accommodates the LiFePO4 battery, two PCBs (the power regulation daughterboard and the main control board), and a Raspberry Pi 5, all arranged in a tiered configuration to optimize internal space and cable routing. This layered structure separates the power and logic domains while maintaining accessibility for debugging, upgrades, and thermal management.

The enclosure features strategically placed through-holes to support interconnections between subsystems. These include openings for power and signal routing between the battery and the two PCBs, as well as external output paths for USB camera modules, haptic motor leads, and speaker wiring. The holes are dimensioned to accommodate standard connector sizes and to allow strain relief as needed during assembly and transport. The CAD view of the enclosure is shown below in Figure 8.3.

Figure 8.3: Enclosure Prototype for Battery and Logic Boards

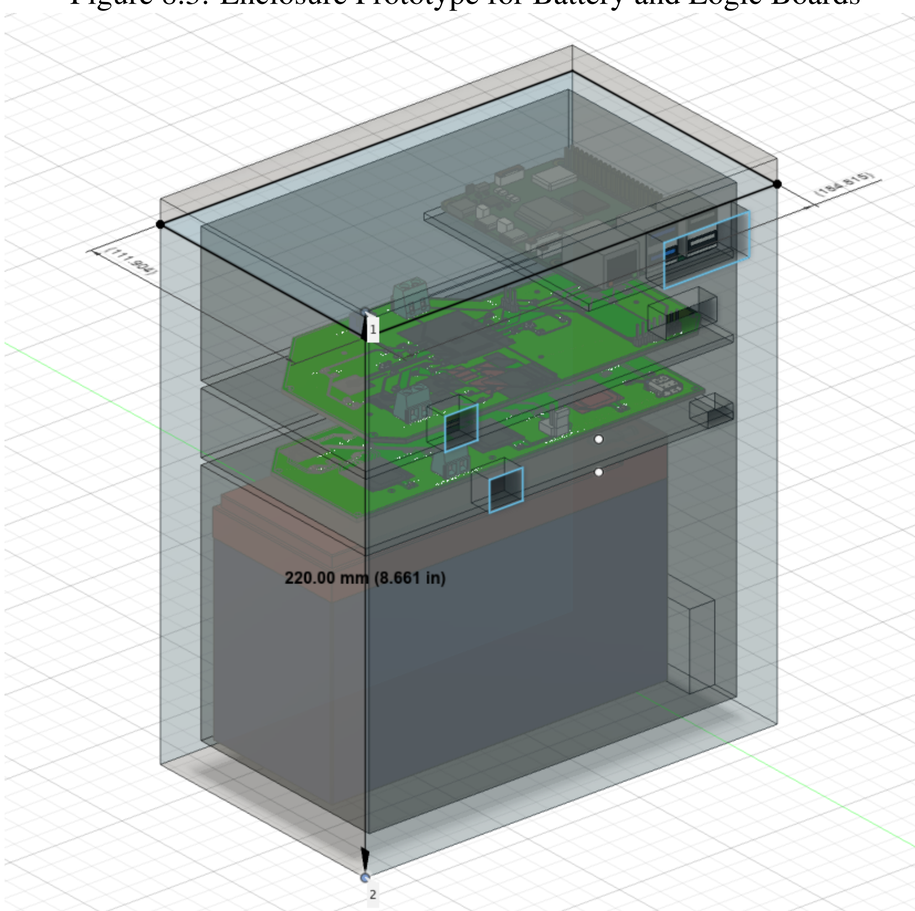

An important design constraint for the enclosure was its ability to fit comfortably within a standard shopping cart, as the system is intended for portable use in grocery store environments. The enclosure was therefore modeled to be both compact and lightweight, with smooth outer surfaces and accessible ports for ease of handling and user interaction.

Future revisions may include rotating PCBs, consolidating connectors, or introducing snap-fit structures to eliminate unnecessary internal volume and simplify assembly. These considerations aim to make the system more portable, user-friendly, and production-ready in subsequent design iterations.

8.3 Haptics and Speaker Shopping Cart Interface

To deliver tactile and auditory feedback to the user, a custom snap-fit interface was designed to mount directly onto a standard shopping cart handlebar. This interface houses the haptic motor modules and speaker unit, positioning them ergonomically along the handle to ensure consistent contact with the user's hands and unobstructed sound projection. Making the interface snap-fit allows for quick installation and removal without the need for tools or fasteners.

The interface is composed of three distinct sections: two haptic modules, positioned on the left and right sides of the handlebar, and a central speaker housing. Each haptic module contains two embedded vibration motors, positioned to align with the user's palm when grasping the handle. This configuration enables the system to convey directional or intensity-based feedback independently to each hand, improving the clarity and intuitiveness of haptic cues. The speaker module is integrated into the central section of the handlebar mount and is oriented to face outward, directing sound toward the user. The speaker is mounted via four screws to threaded inserts extruded from the interface. The overall interface is displayed below in Figure 8.4, where the blue bar represents the handlebar that the white modules are attached to.

Figure 8.4: Haptics and Speaker Interface Prototype with Shopping Cart Handle

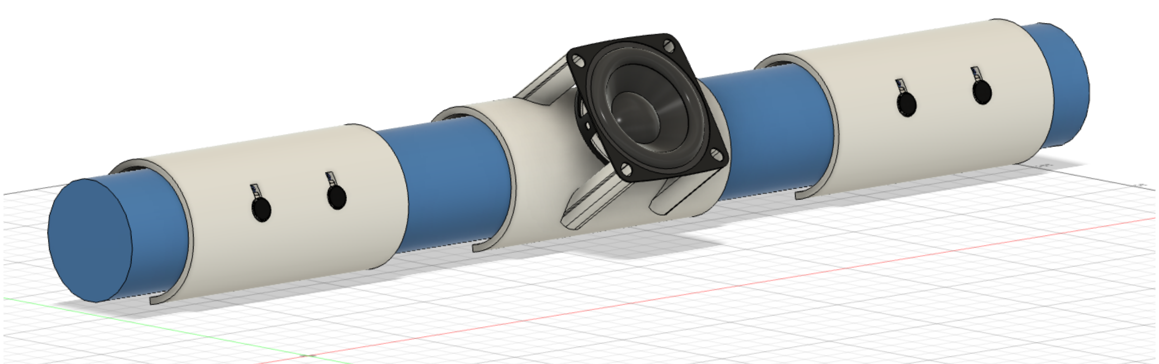

The module lengths and spacing were verified against the dimensions of standard commercial shopping carts to ensure a proper fit across various models. Since the modules are snap-fit, the user may also place them at preferred locations along the handlebar. Initial prototyping will be followed by testing across different cart types to refine the design and validate the consistency of vibrational and audio feedback delivery.

Chapter 9 System Testing and Evaluation

9.1 Hardware Testing

The hardware testing phase focused on evaluating the key components integrated into the system. These components included the MPU-9250 inertial measurement unit (IMU), the DRV2605L haptic motor driver, and the PAM8302A Class D audio amplifier. Each of these modules was tested individually to verify functionality, signal communication with the microcontroller, and compatibility with system-level requirements. Additionally, a HiLetgo 5V 20mA 632nm 5mW Red Dot Laser Diode was evaluated for feasibility in modulating the laser diode for low frequencies.

An ESP32-WROOM-32 development board served as the central microcontroller platform for hardware testing. Its built-in support for I²C, PWM, and analog output made it well-suited for interfacing with all peripheral modules. All firmware development and testing were conducted using the Arduino IDE, which allowed for rapid prototyping and debugging during the integration process.

The following subsections provide detailed descriptions of the testing procedures and validation results for each hardware interface: MCU to IMU, MCU to Speaker, MCU to Haptic, and Laser Diode Modulation. The software for the microcontroller driven tests can be found in Appendix D.

9.1.1 Laser Diode Modulation

To verify the feasibility of externally modulating a red laser diode for pulsed optical output, a hardware test was conducted using a function generator, DC power supply, and a P2N2222A NPN transistor. The red dot laser diode module, rated at 5V and less than 20mA operating current, was powered directly by a regulated 5V DC supply. The function generator was configured to output a 30Hz square wave (0–5V) and connected to the base of the P2N2222A through a 1kOhm resistor.

The transistor was configured in a low-side switching setup, with the collector connected to the laser's ground terminal and the emitter connected to system ground. When the base received a HIGH signal (5V), the transistor entered saturation and allowed current to flow through the laser, successfully turning it on. When the signal was LOW, the transistor turned off, breaking the current path and turning the laser off.

The result was a clearly visible modulated laser output at approximately 30Hz, demonstrating successful optical pulsing using external control. Changing the set frequency on the function generator also allowed us to vary the laser diode pulse rate. No noticeable delay or flickering was observed, and the waveform integrity was confirmed through visual inspection and oscilloscope verification at the base and collector terminals. This validated the laser's compatibility with low-frequency digital modulation using a discrete transistor switch.

Figure 9.1: Laser Diode Modulation Test Setup with Function Generator and DC Power Supply

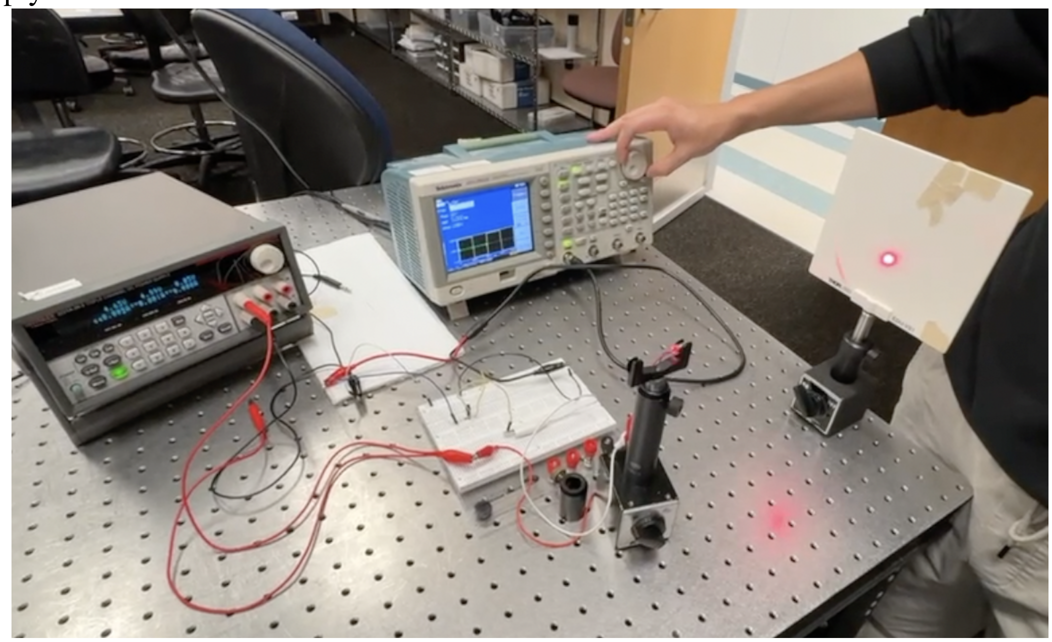

9.1.2 Active Stereo Vision

To verify the feasibility of using a active stereo system for depth imaging, We used the modulated laser diode and two thorlabs cameras with lens modules for our emission and detection systems. For a simulated environment we used a black paper wall mounted on the optical table 1 meter away from the camera and emission system, then for our object we used a small 10cm by 5cm piece of white carboard held by a post in the center of the black background. The balck background was useed in order to test the efficacy of the camera detecting low reflections from low reflecting objects of black color.

Figure 9.2: Active stereo vision system setup

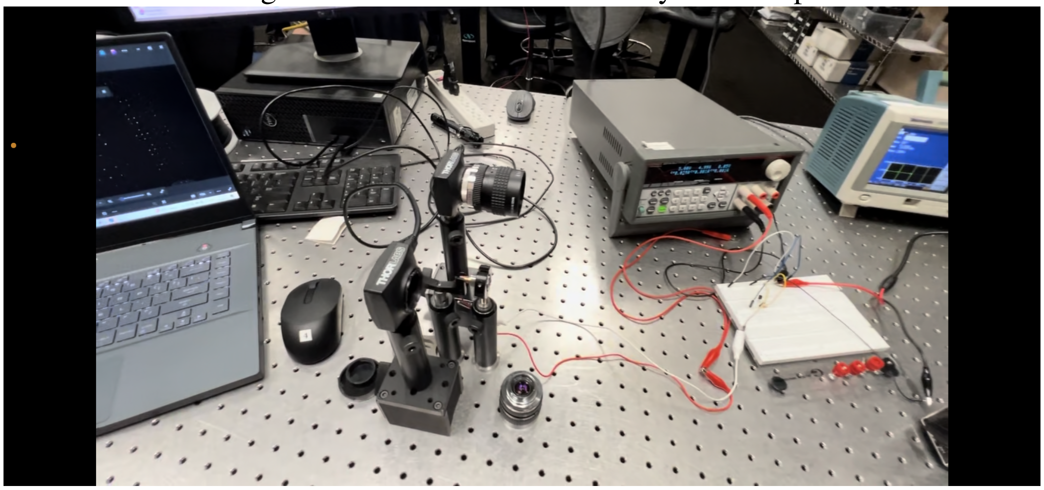

Figure 9.3: Ambient Simulation Setup

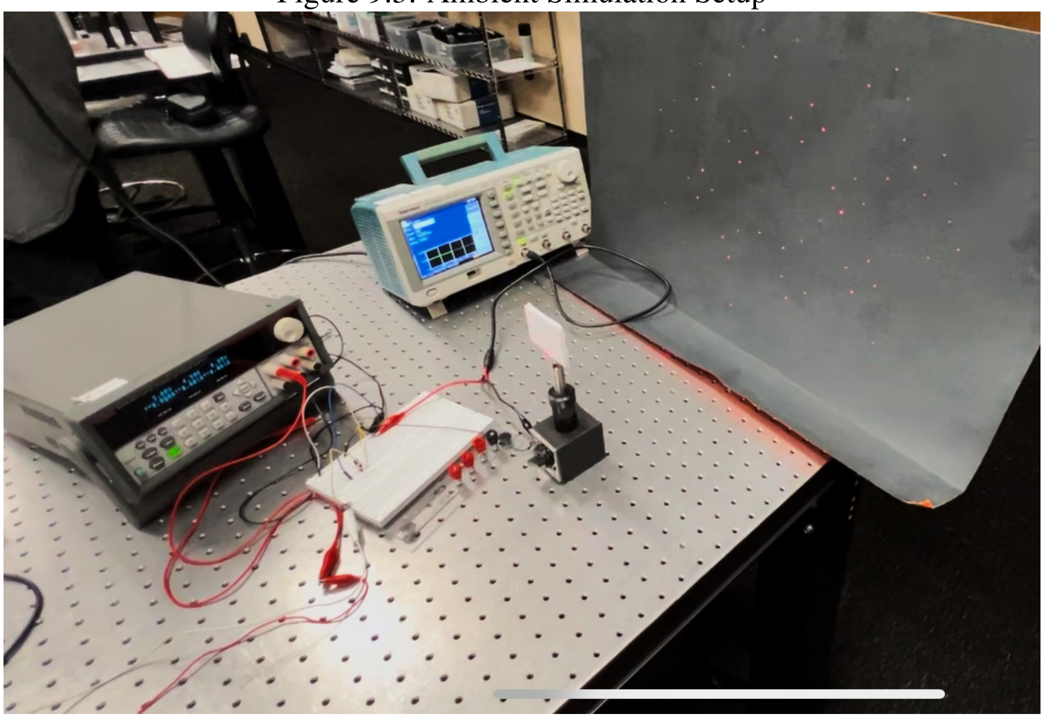

The output from this cameras was collected and analysed, but mainly we wanted to verify that we could pick up most of the projected light. We achieved to capture most of the projected light with the camera and also detected by the matlab imaging. Since active stereo vision relies on disparity calculations, ensured that the projected light in the object had greater location shift between the two images than the projected light on the background.

Figure 9.4: Ambient Simulation Setup

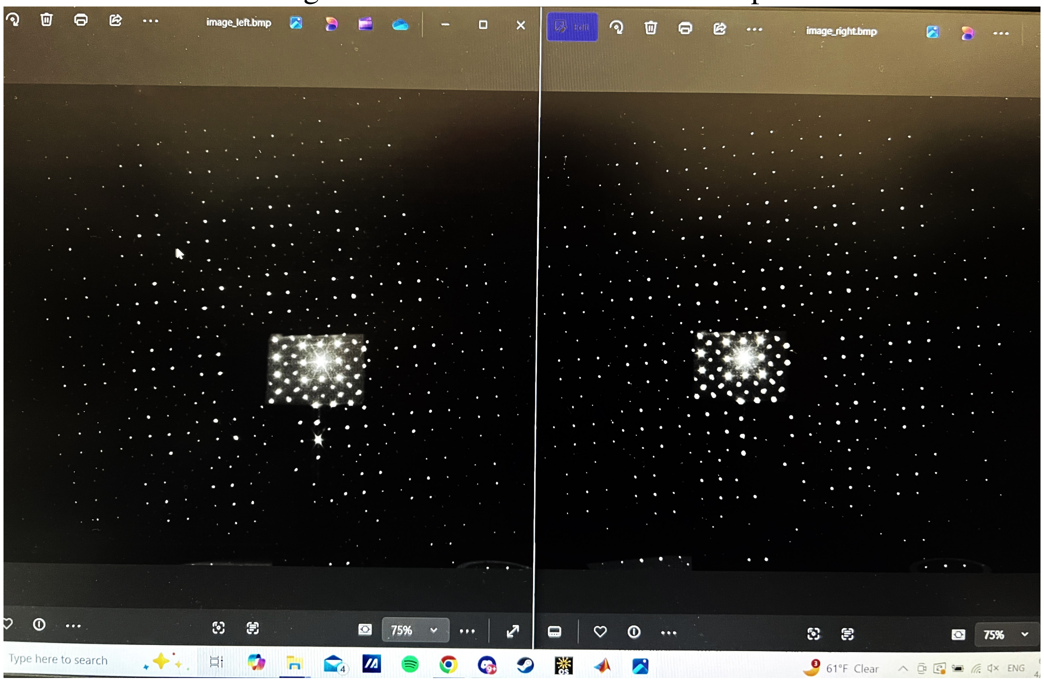

9.1.3 MCU to IMU

To validate communication between the ESP32 microcontroller and the MPU-9250 IMU, the I²C protocol was used. The ESP32 was configured as an I²C master, with the IMU connected via the standard SDA and SCL lines. Initial testing involved writing a basic script to scan the I²C bus and confirm detection of the IMU's address. Once communication was confirmed, the Arduino MPU9250 library was used to initialize the sensor and read real-time data for roll, pitch, and yaw.

The raw sensor outputs were printed to the serial monitor and verified for responsiveness to physical motion. The IMU consistently provided data across all axes with expected ranges and stability, demonstrating successful hardware integration and functional sensor output. This confirmed that the ESP32 could reliably collect motion data from the IMU for future use in system-level processing or feedback loops.

Figure 9.5: Breadboard IMU Test Displaying Motion Data on the Serial Monitor

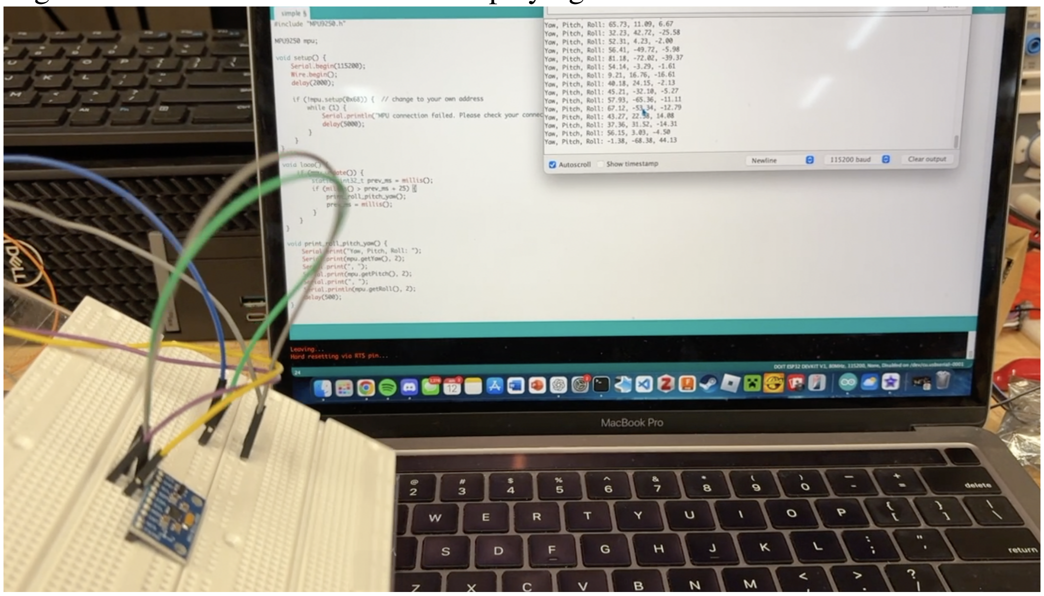

9.1.4 MCU to Speaker

The PAM8302A Class D amplifier was tested to evaluate audio output capability from the ESP32. A DAC-capable GPIO pin (GPIO25) on the ESP32 was used to output analog audio signals. Test code was written to generate sine wave tones using dacWrite() at varying frequencies, simulating simple audio playback. The amplifier's input was connected to the ESP32's DAC pin, and its output was connected to an 8-ohm speaker.

Upon powering the system and running the test script, a series of audible tones were successfully produced by the speaker, confirming signal amplification and correct signal routing. The volume and clarity of the tones demonstrated that the ESP32 could provide a sufficiently strong signal for the PAM8302A to drive a standard speaker. Additionally, the code was written to allow the programmer to change the output volume, which will be adapted for the final product setup. This test validated the audio output path from the microcontroller to the end speaker through the class D amplifier.

Future work for the speaker subsystem will focus on testing the playback of voice signals through the ESP32's DAC output. This involves converting pre-recorded .wav audio files into a raw byte format compatible with the ESP32's built-in DAC. This testing will validate the system's ability to deliver intelligible audio cues or feedback signals, enabling more natural auditory interaction in the final application.

Figure 9.6: Connections between the ESP32, Class D Amplifier, and 8-Ohm Speaker

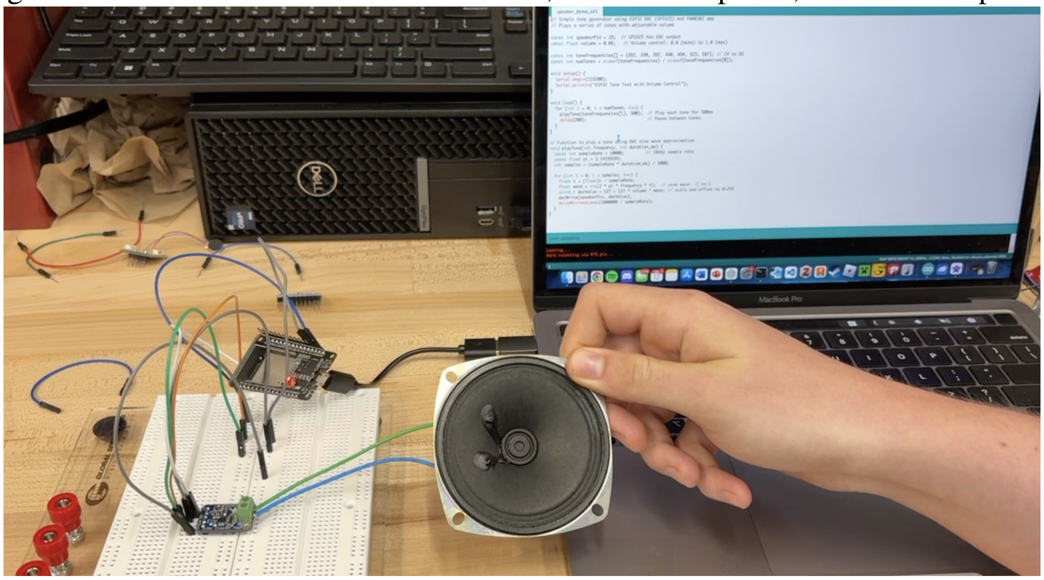

9.1.5 MCU to Haptic

The DRV2605L haptic motor driver was tested to verify its ability to produce vibration effects when controlled by the ESP32. Communication was established using the I²C protocol, with the ESP32 as the master. After confirming device detection via I²C scanning, the Adafruit DRV2605 Arduino library was used to configure the driver and send predefined waveform commands.

A vibration motor was connected to the DRV2605L output, and various waveform effects from the onboard library were triggered programmatically. The motor responded with the correct intensity and duration, corresponding to the selected waveform IDs. This demonstrated successful I²C control, waveform selection, and haptic actuation, confirming that the microcontroller could interface with and control the haptic feedback system as intended.

Next steps will involve testing the signal intensity required on a shopping cart handlebar to ensure that the users can accurately perceive the cues. Differently signal types will be experimented with to deliver specific cues to the user, and the haptic output will be divided into left and right zones for directional communication.

Figure 9.7: Connections between the ESP32, Haptic Driver, and ERM Haptic Motor

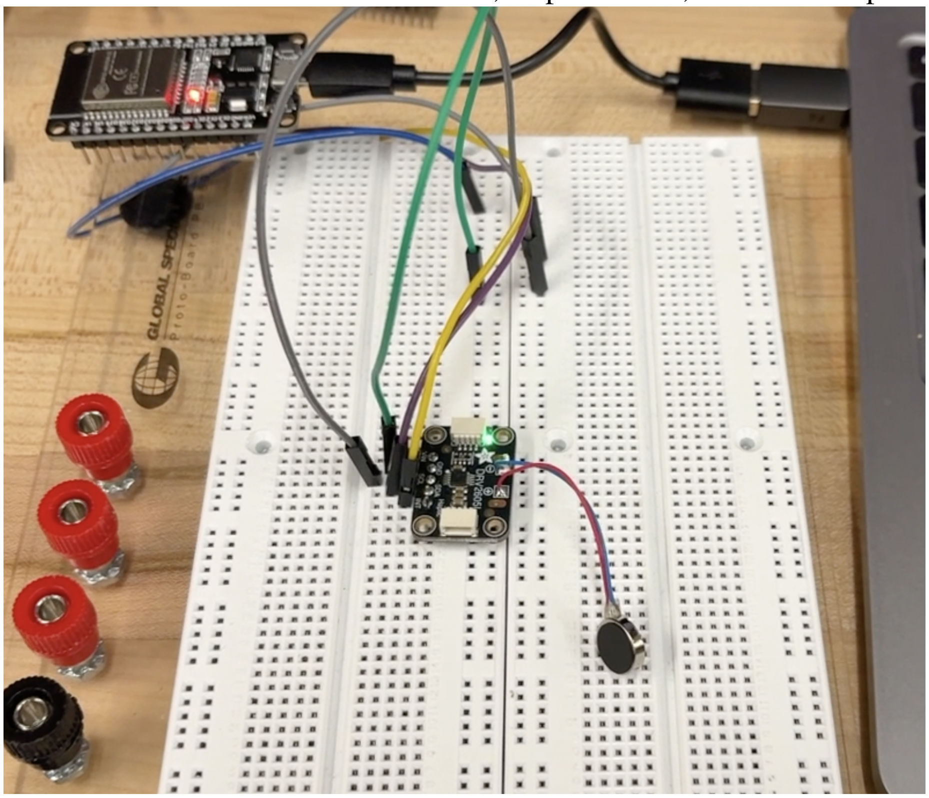

9.2 Software Testing

The software testing phase focused on validating the embedded communication protocols and control logic that enable external interaction with the ESP32. Two primary areas were tested: I²C-based communication between the ESP32 and a Raspberry Pi, and web server-based GPIO control hosted on the ESP32.

Together, these tests verified the ESP32's capability to support both wired and wireless communication interfaces, providing a flexible software foundation for remote monitoring, control, and integration with higher-level computing platforms. The software for the evaluations performed here can be found in Appendix D.

9.2.1 SBC to/from MCU Communication

To enable data exchange between the ESP32 microcontroller unit (MCU) and a Raspberry Pi single-board computer (SBC), the I²C protocol was implemented with the ESP32 configured as an I²C slave and the Raspberry Pi as the master. This configuration supports bidirectional communication, allowing the Pi to both send control messages and request data from the ESP32.

The software implementation on the ESP32 utilized the Wire library. The Wire.onReceive() function was used to handle incoming transmissions from the Raspberry Pi, while Wire.onRequest() was used to respond with outgoing messages when requested by the master. String-based communication was implemented, with messages stored and parsed as String objects. Outgoing messages were converted to byte arrays and sent using Wire.write() along with the appropriate message length.

On the Raspberry Pi side, Python and the smbus2 library were used to write strings to the ESP32 and read back its responses. The communication was tested by sending structured messages such as command strings or identifiers from the Pi to the ESP32. The ESP32 was able to store and print the received messages to the serial monitor in real time. In return, the Pi successfully read a predefined message ("Hello from ESP32!") from the ESP32, which was dynamically sent as a string of bytes upon request.

This test confirmed that string-based, bidirectional communication between the ESP32 and Raspberry Pi via I²C was both functional and stable. The approach demonstrates that the system can reliably handle text-based commands and responses, which is useful for debugging, coordination, or future protocol extensions between the microcontroller and the SBC.

9.2.2 MCU-hosted Web Server

To facilitate remote control of the ESP32's GPIO pins via a web interface, a lightweight HTTP server was implemented directly on the microcontroller. This setup allows users to interact with the ESP32 through a standard web browser, enabling real-time control of connected peripherals such as LEDs or relays.

The implementation was guided by the tutorial "ESP32 Web Server – Arduino IDE" by Rui Santos [90]. The ESP32 was programmed using the Arduino IDE, using the WiFi.h and WebServer.h libraries to establish Wi-Fi connectivity and handle HTTP requests, respectively.

In the setup phase, the ESP32 connects to a specified Wi-Fi network and initializes the web server on port 80. Specific GPIO pins, such as GPIO 26 and GPIO 27, are configured as outputs and set to a default LOW state. The web server defines routes corresponding to different control actions; for instance, accessing /26/on sets GPIO 26 to HIGH, turning on the connected LED, while /26/off sets it back to LOW.

Upon uploading the code and connecting the ESP32 to the network, the device's IP address is displayed in the serial monitor. Navigating to this IP address in a web browser presents a simple interface with buttons to control the state of the GPIO pins. User interactions are handled by the server, which parses the HTTP requests and toggles the GPIO states accordingly.

This setup was tested by connecting LEDs to the designated GPIO pins and observing their response to web-based controls. The LEDs reliably turned on and off in response to the corresponding button presses in the web interface, confirming the successful integration of web server functionality with GPIO control on the ESP32.

This implementation demonstrates the ESP32's capability to serve as a standalone web server for real-time hardware control, providing a foundation for more complex IoT applications involving remote monitoring and actuation.

Figure 9.8: Web Server Communicating to ESP32 to Control GPIO LEDs

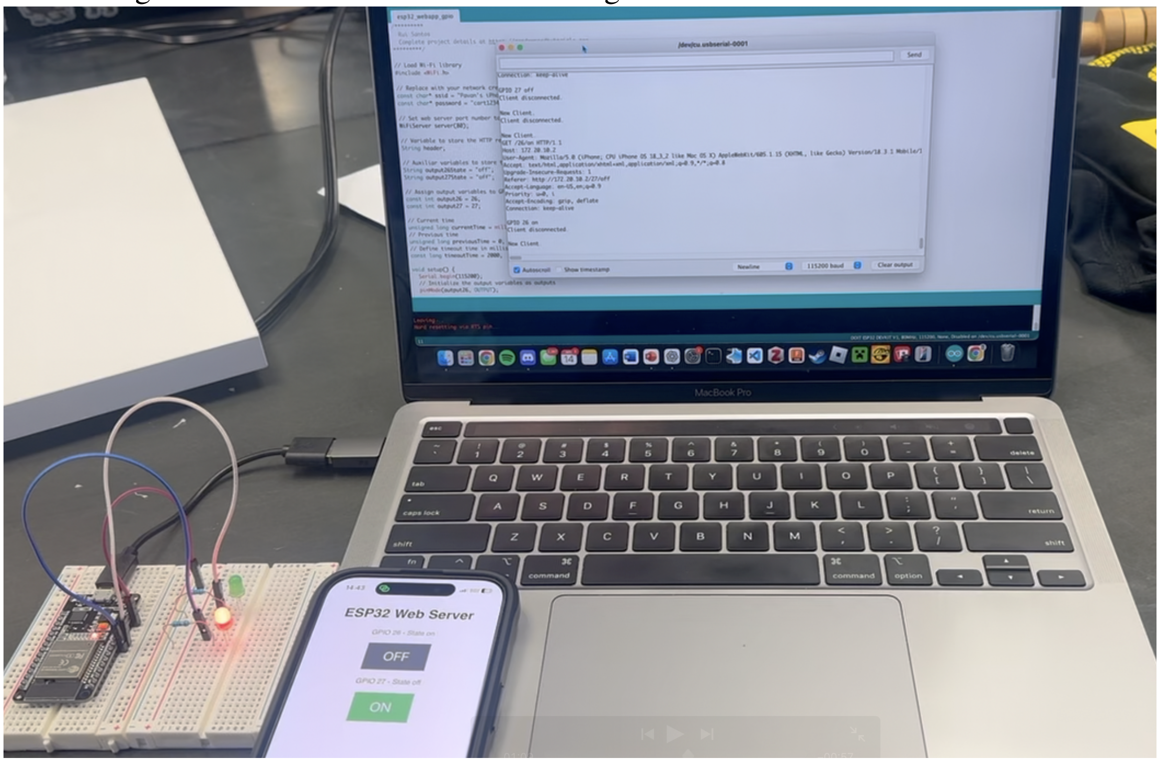

9.3 MPE Calculations and Laser Classification

To evaluate the safety classification of the structured light laser system, the distributed power exposure was analyzed relative to the Maximum Permissible Exposure (MPE) limits specified by ANSI Z136.1. The laser diode used in the system emits 200 mW of power at a wavelength of 850 nm, placing it under Class 3B when collimated. However, with a Diffractive Optical Element (DOE) expanding the emission into a 30×30 grid of lines across a $50^\circ \times 50^\circ$ field of view (FOV), the energy is distributed spatially across a large area.

The power per individual line is calculated using:

$$P_{\text{line}} = \frac{P_{\text{total}}}{N_{\text{lines}}} = \frac{200 \text{ mW}}{900} \approx 0.222 \text{ mW}$$

At an observation distance d (in cm), the length of each line due to FOV expansion is:

$$L_{\text{line}} = 2d \tan\left(\frac{\theta}{2}\right), \quad \text{where } \theta = 50^\circ$$

For example, at $d = 10$ cm:

$$L_{\text{line}} \approx 2 \cdot 10 \cdot \tan(25^\circ) \approx 9.3 \text{ cm}$$

The power density along a line is:

$$P_{\text{cm}} = \frac{P_{\text{line}}}{L_{\text{line}}} = \frac{0.222 \text{ mW}}{9.3 \text{ cm}} \approx 0.0239 \text{ mW/cm}$$

Assuming a 3 mm pupil diameter ($r_{\text{pupil}} = 0.15$ cm), the portion of the line that enters the eye is:

$$L_{\text{eye}} = 2d \cdot \tan^{-1}\left(\frac{r_{\text{pupil}}}{d}\right)$$

This value evaluates to approximately 0.3 cm and remains nearly constant for all reasonable viewing distances.

The total power entering the eye is then:

$$P_{\text{eye}} = P_{\text{cm}} \cdot L_{\text{eye}} = 0.0239 \text{ mW/cm} \cdot 0.3 \text{ cm} \approx 7.17 \times 10^{-3} \text{ mW} = 7.17\ \mu\text{W}$$

The ANSI Z136.1 MPE for 850 nm light at a 0.1 s exposure is:

$$\text{MPE} = 10.1 \text{ W/m}^2 = 1.01 \text{ mW/cm}^2$$

Since $P_{\text{eye}} = 7.17\ \mu\text{W} < 1.01 \text{ mW/cm}^2$, this exposure level is considered safe beyond 10 cm. At distances shorter than 10 cm, P_{eye} exceeds the MPE threshold, maintaining a Class 3B hazard. Beyond 10 cm, the system can be considered Class 1 for normal viewing conditions.

These findings support the conclusion that while the source diode is Class 3B, the full system can operate safely without eye protection beyond a 10 cm viewing distance due to the optical power redistribution introduced by the DOE.

9.4 Integration Steps & Further Plans

As we move into the assembly of this project, the integration of the various subsystems is integral for a timely demonstration. The first two parallel steps of this plan is the construction of an electronics testbed and a simulated ROS2 graph on PC. The electronics testbed will be made to establish all of the connections power and communication connections between the power supplies, sensors, and compute boards, and give software a test-bench to work with. This testbench can then be used to integrate all relevant hardware drivers and communication protocols, in order to be ready for ROS2 integration.

Simultaneously, the ROS2 system graph will be constructed to run on simulation on a separate PC to establish all of the digital connections between nodes in the graph. This simulation will interact with digital hardware emulators in order to provide a proof of concept that the graph works generally, before trying to implement it onto a resource constrained platform such as an SBC. One key component of this simulation is the development and implementation of the depth image constructor, as without it none of the localization, and thus navigation will work. This can be done using simulated cameras.

Once both the electronics testbed and the ROS2 system are working separately, the ROS2 system will then be transferred onto the RaspberyPi, and will be altered to work with the hardware drivers rather than software emulators. This step is vital to show that the graph can run on the RaspberryPi at all, and that the all hardware-software interfaces are fully functional.

Once this is finished, mechanical integration will come last, where the team will physically transfer the electronics testbed onto the grocery cart. This will include the use of longer cables and other slight variations, so we are expecting minor debugging to occur. Finally, once physically integrated, the team will spend the rest of the time tuning the localization, control, and navigation algorithms, while making whatever needed quality of life changes that are necessary.

Chapter 10 Administrative Content

10.1 Budget

The budget for this project shall be around 1000 USD, which should be enough for the team to complete a successful project while keeping costs minimal for everyone involved. The goal of the members is to keep costs within this budget as to reduce the amount of personal expenses incurred by the individual members.

Higher complexity components, such as the optical system and single board computer, are allocated a larger proportion of the budget as shown below. On the other hand, smaller items aren't allocated nearly as much since although we may require more of them, they are relatively inexpensive in total.

Table 10.1: Expected Budget Table

Sub-system	**Amount**
Optics	$300
Power	$200
Control Electronics	$400
Mechanical Components	$100
Total	**$1000**

10.2 Bill of Materials

Table 10.2: Bill of Materials

Item	Subsystem	Unit Price	Qty	Total Price
Raspberry Pi 5 8GB	Electrical	\$80.00	1	\$80.00
Micro SD Card (Raspberry Pi)	Electrical	\$9.95	1	\$9.95
ESP-32-WROOM-DA	Electrical	\$6.95	1	\$6.95
Speaker	Electrical	\$1.95	1	\$1.95
Haptic Motor	Electrical	\$1.54	4	\$6.16
Class D Amplifier	Electrical	\$1.05	1	\$1.05
DRV2605L Haptic Motor Driver	Electrical	\$2.52	4	\$10.08
IMU	Electrical	\$3.23	1	\$3.23
Li-ion Battery	Electrical	\$37.99	1	\$37.99
5V Regulator	Electrical	\$5.59	1	\$5.59
3.3V Regulator	Electrical	\$5.59	1	\$5.59
CMOS Camera	Optical	\$39.99	2	\$79.98
Laser Diode	Optical	\$65	1	\$65
Laser Diode Driver	Optical	\$60	1	\$60
DOE	Optical	\$80	2	\$160
FBT Splitter	Optical	\$28.49	1	\$28.49
Bandpass Filter	Optical	\$5	2	\$10
PLA (3-D Printer)	Mechanical	n/a	n/a	\$10.00
Misc. (jumpers, resistors, capacitors, inductors, diodes)	Electrical	n/a	n/a	\$10.00

10.3 Distribution of Works

The tables below detail the distribution of work that has been decided collectively among the group members. Although each member might be assigned a specific task, it is expected that they will have assistance in completing some parts if needed from other members. In addition, the members must work together to ensure that each component works with the others of the completed system and meets the overall system requirements as outlined in Chapter 2. Members are expected to provide regular updates on the progress of the tasks that they are individually assigned during group meetings.

Major: Photonics Science and Engineering	**Responsibilities**
Matias Barzallo	IR Depth Camera Optical Design and Development
	IR Depth Camera Electrical Integration
Major: Computer Engineering, VLSI Track	**Responsibilities**
Michael Castiglia	Microcontroller Software Integration
	Sensor Driver Integration
	Mobile App Design and Development
	High Brain - Low Brain Board Communications
Major: Computer Engineering, Comprehensive Track	**Responsibilities**
Aden McKinney	Autonomous Navigation Stack Design and Development
	Mobile App Design and Development
	Control Output Software Development
Major: Electrical Engineering, Comprehensive Track	**Responsibilities**
Pavan Senthil	Power System Design and Implementation
	PCB Design
	Sensor Hardware Integration
	Control Output Hardware Integration

10.4 Milestones

Table 10.3: Project Initialization Timeline Table

Project Initialization				
Planned Begin Date	**Planned End Date**	**Required End Date**	**Task**	**Description**
7/5/24	7/15/24	1/14/25	Team Formation	Form team with 4 known members for Spring and Summer
7/15/24	9/1/24	1/24/25	Idea Generation	Discuss and decide on final project idea
9/1/24	12/1/24	1/24/25	Divide and Conquer Document	Chapters 2, 10, and relevant appendices
12/1/24	1/24/25	–	Chapter 3	Implementation Research
1/24/25	2/7/25	3/24/25	60-Page Milestone	Chapters 2-5, and 10
2/7/25	2/28/25	4/22/25	Final Paper (120 pages)	Final Document as Submitted

The team has met and will continue to meet several times outside of those indicated above, both without others and with assistance from the review committee, advisors, and others, to complete the milestones within the given tie limit. This project's research started well before the beginning of the Senior Design 1 semester as an attempt to get ahead of deadlines, mainly in Senior Design 2 which would be more compressed due to the nature of completing it in the Summer C section.

Table 10.4: Project Fabrication Timeline Table

Project Fabrication				
Planned Begin Date	**Planned End Date**	**Required End Date**	**Task**	**Description**
1/1/24	1/24/25	3/24/25	Component Selection	Selecting components for each part of the project.
1/15/25	2/21/25	3/24/25	Software Design	Design the software stack
1/15/25	2/21/25	3/24/25	Optical Design	Design for the optical subsystem
1/15/25	2/21/25	3/24/25	Other Hardware Design	Design for the PCB, power, and other hardware.
2/21/25	3/15/25	4/22/25	Manufacturing and Integration	Making the prototype and integrating the individual components together.
2/21/25	3/15/25	4/22/25	Testing	Test the assembled prototype and fix any issues that may arise.
2/14/25	3/15/25	4/22/25	First Prototype Completion	Final demo video for website of the breadboarded sample proposal for SD1

Due to the nature of this project and the complexity contained within, as well as deadlines for demonstrations of a small prototype inside of Senior Design 1 to the review committee, several of the tasks overlap between the two stages.

Chapter 11 Conclusion

In conclusion, through the use of many technologies, including but not limited to structured light projections along with mapping and navigation algorithms, the NAVIS project has the opportunity to demonstrably increase the freedom for many people who struggle with visual impairments while they are grocery shopping or doing other similar tasks. As explained in each of the previous chapters, but especially in Chapters 1-3 (Executive Summary, Project Description, and Research, respectively), the main goal of this project is to assist those who are visually impaired, but not completely blind, to be able to make a shopping list and thereafter be able to navigate a grocery store to find the items placed on their list without assistance from others. This is achieved by using aforementioned algorithms to guide the user on where to move next, based on their current location, next desired item, and any obstacles that may be in the way of the user so they can easily avoid them.

The two major components of this project are the optical and compute sub-systems, mainly realized through the use of the structured light projections and sensors along with the aforementioned algorithms, respectively. These two systems, along with the power distribution and data transmissions handled mainly by the main board which contains a microcontroller and other technologies to interact with the peripherals to interact with the outside environment by collecting data and by alerting the user on where to move next. In this configuration, the structured light sensor, along with an IMU, allow the compute system to know where it is within the store relative to the destination, along with any obstacles that may be in the way of the user while they move to their destination. This is them communicated back to the microcontroller to be alert the user using both haptic motors and speakers, which will be embedded within the system. Prior to navigation, the user will utilize their existing mobile device to select the items that they wish to navigate to. The mapping algorithm contained within the Single Board Computer will then construct an optimal route for the selected items. All together, the integration of these two systems, which includes everything from creating custom software drivers for the optical system to creating a modular way to drive the laser diode from the main board, is likely the most critical step of the combined system.

The design of the overall system, which will allow it to be attached to a standard store's grocery cart with ease, additionally helps to make the use of the system even easier for those who are visually impaired. By combining this relatively portable system with the grocery carts already standard at grocery stored across the country, the system is more useful for those who may otherwise have trouble setting up a more bulky, fully self-contained system, like if the system would be permanently attached to the grocery cart. In addition, such a solution would inevitably be harder to store and transport for the end user.

This document serves as a full and complete record of the design process for the NAVIS project, which is a Capstone Senior Design project for the following courses at the University of Central Florida's College of Engineering and Computer Science for each of the primary authors: EEL 4914 and EEL 4915L, along with OSE 4951 and OSE 4952 at CREOL, The College of Optics and Photonics for Matias Barzallo, a student in the Photonics Science and Engineering degree program. Contained within this document include all of the procedures and underlying research relating to project selection and definition, fundamental theories and technologies for each of the project's individual parts, part selection for each of the hardware components and software libraries, standards and constraints for each part of the project, administrative processes, and finally implementation of each of the prior stated processes into a final project. The student's planning and execution of the various components of this project, along with the guidance from the advisors and review committee have helped to ensure that this project is successful in its goal of assisting those with visual impairments.

Appendix A References List

[1] WHO. *World report on vision*. en. Oct. 2019. URL: https://www.who.int/publications/i/item/9789241516570 (visited on 01/23/2025).

[2] Centers for Disease Control and Prevention. *Fast Facts: Vision Loss*. en-us. May 2024. URL: https://www.cdc.gov/vision-health/data-research/vision-loss-facts/index.html (visited on 01/23/2025).

[3] Centers for Disease Control and Prevention. *VEHSS Modeled Estimates for Vision Loss and Blindness*. en-us. Nov. 2024. URL: https://www.cdc.gov/vision-health-data/prevalence-estimates/vision-loss-prevalence.html (visited on 01/23/2025).

[4] National Eye Institute. *Low Vision*. Dec. 2024. URL: https://www.nei.nih.gov/learn-about-eye-health/eye-conditions-and-diseases/low-vision (visited on 01/23/2025).

[5] Peter Ackland, Serge Resnikoff, and Rupert Bourne. "World blindness and visual impairment: despite many successes, the problem is growing". In: *Community Eye Health* 30.100 (2017), pp. 71–73. ISSN: 0953-6833. URL: https://www.ncbi.nlm.nih.gov/pmc/articles/PMC5820628/ (visited on 01/23/2025).

[6] Lalit Dandona and Rakhi Dandona. "Revision of visual impairment definitions in the International Statistical Classification of Diseases". In: *BMC Medicine* 4 (Mar. 2006), p. 7. ISSN: 1741-7015. DOI: 10.1186/1741-7015-4-7. URL: https://www.ncbi.nlm.nih.gov/pmc/articles/PMC1435919/ (visited on 01/23/2025).

[7] Chantal Keller and Dario Schafroth. *VIRAS: Visually Impaired Robot-Assisted Shopping — Project*. en. URL: https://www.ost.ch/en/details/projects/viras-visually-impaired-robot-assisted-shopping-1842 (visited on 01/23/2025).

[8] Patrick Slade, Arjun Tambe, and Mykel J. Kochenderfer. "Multimodal sensing and intuitive steering assistance improve navigation and mobility for people with impaired vision". In: *Science Robotics* 6.59 (Oct. 2021). Publisher: American Association for the Advancement of Science, eabg6594. DOI: 10.1126/scirobotics.abg6594. URL: https://www.science.org/doi/10.1126/scirobotics.abg6594 (visited on 01/23/2025).

[9] Mikko Kytö, Mikko Nuutinen, and Pirkko Oittinen. "Method for measuring stereo camera depth accuracy based on stereoscopic vision". In: Proc.SPIE. Vol. 7864. Jan. 27, 2011, p. 78640I. DOI: 10.1117/12.872015. URL: https://doi.org/10.1117/12.872015.

[10] Andrew O' Riordan et al. *Stereo Vision Sensing: Review of existing systems*. Dec. 4, 2018. DOI: 10.1109/ICSensT.2018.8603605.

[11] Andrew Hogue and Michael Jenkin. "Active Stereo Vision". In: *Computer Vision: A Reference Guide*. Ed. by Katsushi Ikeuchi. Cham: Springer International Publishing, 2021, pp. 27–32. ISBN: 978-3-030-63416-2. DOI: 10.1007/978-3-030-63416-2_282. URL: https://doi.org/10.1007/978-3-030-63416-2_282.

[12] Mingyu Jang et al. "A Comparison and Evaluation of Stereo Matching on Active Stereo Images". In: *Sensors* 22.9 (2022). ISSN: 1424-8220. DOI: 10.3390/s22093332. URL: https://www.mdpi.com/1424-8220/22/9/3332.

[13] Mikko Kytö, Mikko Nuutinen, and Pirkko Oittinen. *Method for measuring stereo camera depth accuracy based on stereoscopic vision*. Vol. 7864. Jan. 23, 2011. 78640I pp. DOI: 10.1117/12.872015.

[14] YongCan Shuang and ZhenZhou Wang. "Active stereo vision three-dimensional reconstruction by RGB dot pattern projection and ray intersection". In: *Measurement* 167 (Jan. 1, 2021), p. 108195. ISSN: 0263-2241. DOI: 10.1016/j.measurement.2020.108195. URL: https://www.sciencedirect.com/science/article/pii/S0263224120307338.

[15] Daniel Scharstein and R. Szeliski. *High-accuracy stereo depth maps using structured light*. Vol. 1. July 18, 2003. I pp. ISBN: 0-7695-1900-8. DOI: 10.1109/CVPR.2003.1211354.

[16] Ifeanyi F. Ezebili and Kristiaan Schreve. "Depth Factor and Sensitivity Coefficient in Active Stereo-Camera Imaging". In: *Journal of Sensors* 2024.1 (2024), p. 6034943. DOI: https://doi.org/10.1155/2024/6034943. URL: https://onlinelibrary.wiley.com/doi/abs/10.1155/2024/6034943.

[17] Jason Geng. "Structured-light 3D surface imaging: a tutorial". In: *Adv. Opt. Photon.* 3.2 (June 2011), pp. 128–160. DOI: 10.1364/AOP.3.000128. URL: https://opg.optica.org/aop/abstract.cfm?URI=aop-3-2-128.

[18] Zhenzhou Wang, Qi Zhou, and YongCan Shuang. "Three-dimensional reconstruction with single-shot structured light dot pattern and analytic solutions". In: *Measurement* 151 (Feb. 1, 2020), p. 107114. ISSN: 0263-2241. DOI: 10.1016/j.measurement.2019.107114. URL: https://www.sciencedirect.com/science/article/pii/S0263224119309807.

[19] Ryo Furukawa, Ryusuke Sagawa, and Hiroshi Kawasaki. "Depth Estimation Using Structured Light Flow — Analysis of Projected Pattern Flow on an Object's Surface". In: *2017 IEEE International Conference on Computer Vision (ICCV)*. Venice: IEEE, Oct. 2017, pp. 4650–4658. ISBN: 978-1-5386-1032-9. DOI: 10.1109/ICCV.2017.497. URL: http://ieeexplore.ieee.org/document/8237759/ (visited on 01/31/2025).

[20] Lindsay Kleeman and Roman Kuc. "Sonar Sensing". In: Jan. 1, 2008, pp. 491–519. ISBN: 9783540239574. DOI: 10.1007/978-3-540-30301-5_22.

[21] International Hydrographic Organization. "Depth Determination". In: *Manual on Hydrography*. Monaco: International Hydrographic Bureau, 2010, pp. 119–197. URL: https://iho.int/uploads/user/pubs/cb/c-13/C-13.pdf.

[22] Paul F. McManamon. *LiDAR technologies and systems*. Bellingham, Washington, USA: SPIE Press, 2019. 504 pp. ISBN: 9781510625396.

[23] Ilya Poberezhskiy et al. "Flash lidar performance testing: configuration and results". In: Proc.SPIE. Vol. 8379. May 14, 2012, p. 837905. DOI: 10.1117/12.920326. URL: https://doi.org/10.1117/12.920326.

[24] *Absorbed Solar Radiation*. URL: https://www.engineeringtoolbox.com/solar-radiation-absorbed-materials-d_1568.html (visited on 04/19/2025).

[25] *Materials - Light Reflecting Factors*. URL: https://www.engineeringtoolbox.com/light-material-reflecting-factor-d_1842.html (visited on 04/19/2025).

[26] *Molecular Expressions: Science, Optics, and You: Light and Color - Primary Colors*. URL: https://micro.magnet.fsu.edu/optics/lightandcolor/primary.html (visited on 04/19/2025).

[27] P. M. Ripley. "The physics of diode lasers". In: *Lasers In Medical Science* 11.2 (June 1996), pp. 71–78. ISSN: 0268-8921, 1435-604X. DOI: 10.1007/BF02133204. URL: http://link.springer.com/10.1007/BF02133204 (visited on 04/19/2025).

[28] *Laser Light Characteristics*. URL: https://www.newport.com/n/laser-light-characteristics (visited on 04/19/2025).

[29] Bruno Gayral. "LEDs for lighting: Basic physics and prospects for energy savings". In: *Demain l'énergie* 18.7 (Sept. 1, 2017), pp. 453–461. ISSN: 1631-0705. DOI: 10.1016/j.crhy.2017.09.001. URL: https://www.sciencedirect.com/science/article/pii/S163107051730052X.

[30] Sohel Uddin et al. "LEDs as energy efficient lighting systems: A detail review". In: *2011 IEEE Student Conference on Research and Development*. 2011, pp. 468–472. DOI: 10.1109/SCOReD.2011.6148785.

[31] Angelo V. Arecchi, R. John Koshel, and Tahar Messadi. *Field guide to illumination*. SPIE field guides FG11. OCLC: ocn164570409. Bellingham, Wash: SPIE, 2007. 137 pp. ISBN: 9780819467683.

[32] Takahiro Numai. *Fundamentals of semiconductor lasers*. 2nd edition. Springer series in optical sciences Volume 93. Tokyo New York: Springer, 2015. ISBN: 9784431551485.

[33] D Garbuzov et al. “High Power 1300 nm Fabry-Perot and DFB Ridge Waveguide Lasers”. In: *Proceedings of SPIE* 4651 (Jan. 1, 2002).

[34] Paul C. *How Does Temperature Affect the Wavelengths of Lasers?* Arroyo Instruments. July 1, 2022. URL: https://www.arroyoinstruments.com/blog/how-does-temperature-affect-the-wavelengths-of-lasers/ (visited on 04/19/2025).

[35] Rainer Michalzik and Karl Ebeling. “Operating Principles of VCSELs”. In: (Jan. 1, 2003). ISSN: 978-3-642-08743-1. DOI: 10.1007/978-3-662-05263-1_3.

[36] *i-Quu Labs — Blog Post*. URL: https://i-quu.com/blogpost_1.html (visited on 04/19/2025).

[37] Mohammed Fadhali et al. “Mode matching for efficient laser diode to single mode fiber coupling”. In: *Proc. of SPIE Vol* 6793 (Jan. 1, 2008), 67930G–1. DOI: 10.1117/12.799264.

[38] Sonam Berwal and Neha Khatri. “Design and comparative analysis of fiber-coupled laser diode system using ball, cylindrical, and toroidal lens”. In: Proc.SPIE. Vol. 11777. Apr. 18, 2021, 117770U. DOI: 10.1117/12.2592529. URL: https://doi.org/10.1117/12.2592529.

[39] M. Maeda et al. “Hybrid laser-to-fiber coupler with a cylindrical lens”. In: *Appl. Opt.* 16.7 (July 1977), pp. 1966–1970. DOI: 10.1364/AO.16.001966. URL: https://opg.optica.org/ao/abstract.cfm?URI=ao-16-7-1966.

[40] *Anamorphic Prism Pairs*. URL: https://www.thorlabs.com (visited on 04/19/2025).

[41] Joseph C. Palais. *Fiber optic communications*. 3rd ed. Englewood Cliffs, NJ: Prentice Hall, 1992. 335 pp. ISBN: 9780134735542.

[42] *Coaxial Pigtail High Power Laser Diode 850nm - Buy Red Laser 850nm,High Power 850nm,High Power 850nm Product on Alibaba.com*. www.alibaba.com. URL: https://www.alibaba.com/product-detail/Coaxial-pigtail-High-Power-Laser-Diode_60094342963.html (visited on 04/19/2025).

[43] *850nm 50mW/80mW IR Pigtail Laser 5um SM Fiber Coupled Laser Diode*. URL: https://www.civillaser.com/index.php?main_page=product_info&products_id=5017 (visited on 04/19/2025).

[44] *LASER TREE 850nm 100mW Infrared Fiber Coupled Laser Diode*. LASER TREE. URL: https://lasertree.com/products/laser-tree-850nm-100mw-infrared-fiber-coupled-laser-diode (visited on 04/19/2025).

[45] *[Hot Item] High Output Power PF Long Wavelength Pulsed Conditions 850nm Pulsed Laser for OTDR*. Made-in-China.com. URL: https://shengshioptical.en.made-in-china.com/product/LCvmBdODwFhQ/China-High-Output-Power-PF-Long-Wavelength-Pulsed-Conditions-850nm-Pulsed-Laser-for-OTDR.html (visited on 04/19/2025).

[46] Qiang Zhang et al. “Diffractive optical elements 75 years on: from micro-optics to metasurfaces”. In: *Photonics Insights* 2.4 (Dec. 1, 2023), R09. DOI: 10.3788/PI.2023.R09. URL: https://doi.org/10.3788/PI.2023.R09.

[47] Svetlana N. Khonina et al. “Advancements and Applications of Diffractive Optical Elements in Contemporary Optics: A Comprehensive Overview”. In: *Advanced Materials Technologies* 10.4 (Feb. 2025), p. 2401028. ISSN: 2365-709X, 2365-709X. DOI: 10.1002/admt.202401028. URL: https://advanced.onlinelibrary.wiley.com/doi/10.1002/admt.202401028 (visited on 04/19/2025).

[48] S.N. Khonina, N.L. Kazanskiy, and M.A. Butt. “Exploring Diffractive Optical Elements and Their Potential in Free Space Optics and imaging- A Comprehensive Review”. In: *Laser & Photonics Reviews* 18.12 (Dec. 2024), p. 2400377. ISSN: 1863-8880, 1863-8899. DOI: 10.1002/lpor.202400377. URL: https://onlinelibrary.wiley.com/doi/10.1002/lpor.202400377 (visited on 04/19/2025).

[49] R. Gale. “Principles and applications of the digital micromirror device in projection displays”. In: *1999 IEEE LEOS Annual Meeting Conference Proceedings. LEOS’99. 12th Annual Meeting. IEEE Lasers and Electro-Optics Society 1999 Annual Meeting (Cat. No.99CH37009)*. Vol. 1. 1999, 212–213 vol.1. DOI: 10.1109/LEOS.1999.813554.

[50] *Digital Micromirror Device*. URL: https://www.asme.org/About-ASME/Engineering-History/Landmarks/243-Digital-Micromirror-Device (visited on 04/19/2025).

[51] Zichen Zhang, Zheng You, and Daping Chu. “Fundamentals of phase-only liquid crystal on silicon (LCOS) devices”. In: *Light: Science & Applications* 3.10 (Oct. 24, 2014), e213–e213. ISSN: 2047-7538. DOI: 10.1038/lsa.2014.94. URL: https://www.nature.com/articles/lsa201494 (visited on 04/19/2025).

[52] Xizheng Ke. “Liquid-Crystal Spatial Light Modulators and Their Applications”. In: *Handbook of Optical Wireless Communication*. Singapore: Springer Nature Singapore, 2024, pp. 1015–1063. ISBN: 9789819715213. DOI: 10.1007/978-981-97-1522-0_28. URL: https://link.springer.com/10.1007/978-981-97-1522-0_28 (visited on 04/19/2025).

[53] J. Fabian Villa-Manriquez et al. *Laser Scanning and Speckle Pattern Projection for Speed-Adaptive Robotic Pipeline Monitoring*. 2025. DOI: 10.2139/ssrn.5081773. URL: https://www.ssrn.com/abstract=5081773 (visited on 04/19/2025).

[54] Rongqian Yang et al. “Robust and Accurate Surface Measurement Using Structured Light”. In: *IEEE Transactions on Instrumentation and Measurement* 57.6 (June 2008), pp. 1275–1280. ISSN: 0018-9456, 1557-9662. DOI: 10.1109/TIM.2007.915103. URL: http://ieeexplore.ieee.org/document/4444774/ (visited on 04/19/2025).

[55] *DE-R 256 - HOLOEYE Photonics AG*. URL: https://holoeye.com/product/de-r-256/ (visited on 04/19/2025).

[56] *Laserland DOE Diffractive Optical Elements Lens DG Grating Lens Diffraction Gratings for Lasers Laser Light Pattern Projection Stage Star Lighting Effect - Optical Lens*. URL: https://store.laserland.com/optical-lens/doe-diffractive-optical-elements-lens-dg-grating-lens-diffraction-gratings-for-lasers-laser-light-pattern-projection-stage-star-lighting-effect.html (visited on 04/19/2025).

[57] *Diffractive Optical Element, Diffractive Optics, Diffractive Lens - Digigram DOE Diffractive Grating Diffuser Laser Beam Shaping*. URL: https://www.digigram.com.tw/en/prd/public_diffraction_element (visited on 04/19/2025).

[58] *DOE-SG60 - Diffractive Optical Element, Grid 60x60, 30° at 650nm — Lasermate Group, Inc.* https://lasermate.com/. URL: https://lasermate.com/optics/diffractive-optical-element/grid/doe-sg60/ (visited on 04/19/2025).

[59] Gerald C. Holst and Terrence S. Lomheim. "CMOS Fundamentals". In: *CMOS/CCD Sensors and Camera Systems, Second Edition*. SPIE, Apr. 29, 2011. ISBN: 9780819486530. DOI: 10.1117/3.2524677.ch4. URL: https://www.spiedigitallibrary.org/eBooks/PM/CMOSCCD-Sensors-and-Camera-Systems-Second-Edition/Chapter4/CMOS-Fundamentals/10.1117/3.2524677.ch4 (visited on 04/19/2025).

[60] *Introduction to CMOS Image Sensors*. URL: https://evidentscientific.com/en/microscope-resource/knowledge-hub/digital-imaging/cmosimagesensors (visited on 04/19/2025).

[61] Yonggang Chen. "CMOS Stress Sensor Circuits". In: (Dec. 15, 2006). URL: https://etd.auburn.edu//handle/10415/608 (visited on 04/19/2025).

[62] *Arducam PiVariety Camera, 2.2MP Mira220 MONO Global Shutter Camera Module*. URL: https://www.arducam.com/arducam-pivariety-camera-2-2mp-mira220-mono-global-shutter-camera-module.html (visited on 04/19/2025).

[63] *Arducam OV9281 1MP Monochrome Global Shutter Camera Module with M12 Mount lens for Raspberry Pi 5/4/3B+/3*. URL: https://www.arducam.com/ov9281-mipi-1mp-monochrome-global-shutter-camera-module-m12-mount-lens-raspberry-pi.html (visited on 04/19/2025).

[64] *Thorlabs - CS165MU Zelux® 1.6 MP Monochrome CMOS Camera, 1/4*. URL: https://www.thorlabs.com (visited on 04/19/2025).

[65] *2MP IMX462 Color Ultra Low Light STARVIS Camera Module with 141°(H) Wide-Angle M12 Lens for Raspberry Pi*. URL: https://www.arducam.com/2mp-imx462-color-ultra-low-light-starvis-camera-module-with-141h-wide-angle-m12-lens-for-raspberry-pi.html (visited on 04/19/2025).

[66] *How does an interference filter work?* Delta Optical Thin Film. URL: https://deltaopticalthinfilm.com/knowledge/tech-notes-and-papers/how-does-an-interference-filter-work/ (visited on 04/19/2025).

[67] G. Domingo, R. S. Itoga, and C. R. Kannewurf. "Fundamental Optical Absorption in Sn S 2 and Sn Se 2". In: *Physical Review* 143.2 (Mar. 11, 1966), pp. 536–541. ISSN: 0031-899X. DOI: 10.1103/PhysRev.143.536. URL: https://link.aps.org/doi/10.1103/PhysRev.143.536 (visited on 04/19/2025).

[68] Charles Richard et al. "An integrated hybrid interference and absorption filter for fluorescence detection in lab-on-a-chip devices". In: *Lab on a Chip* 9.10 (2009), p. 1371. ISSN: 1473-0197, 1473-0189. DOI: 10.1039/b819080a. URL: https://xlink.rsc.org/?DOI=b819080a (visited on 04/19/2025).

[69] *[Hot Item] Industrial Camera Filter 850nm 940nm Narrow Band Pass Filter*. Made-in-China.com. URL: https://optics.en.made-in-china.com/product/nFQEmOPAuHcU/China-Industrial-Camera-Filter-850nm-940nm-Narrow-Band-Pass-Filter.html (visited on 04/19/2025).

[70] *[Hot Item] IR Cut Filter Optical Bandpass Filter with 650nm, 850nm, 940nm Infrared Customizable and Coated Filter*. Made-in-China.com. URL: https://ybtoptics.en.made-in-china.com/product/fdCayecVElWQ/China-IR-Cut-Filter-Optical-Bandpass-Filter-with-650nm-850nm-940nm-Infrared-Customizable-and-Coated-Filter.html (visited on 04/19/2025).

[71] *Everix Ultra-Thin OD 2 Bandpass Filter, 850nm, 12.5mm Dia.* Edmund. URL: https://www.edmundoptics.com/p/everix-ultra-thin-od-2-bandpass-filter-850nm-125mm-dia/48726/.

[72] *Thorlabs - FBH850-40 Hard-Coated Bandpass Filter, Ø25 mm, CWL = 850 nm, FWHM = 40 nm*. URL: https://www.thorlabs.com (visited on 04/19/2025).

[73] "Fibre Optical Splitters". In: *International Research Journal of Modernization in Engineering Technology and Science* (Sept. 5, 2023). ISSN: 25825208. DOI: 10.56726/IRJMETS44418. URL: https://www.irjmets.com/uploadedfiles/paper//issue_9_september_2023/44418/final/fin_irjmets1693667503.pdf (visited on 04/19/2025).

[74] kinglong. *FBT vs PLC Splitters: A Comprehensive Comparison of Fiber Optic Splitting Technologies – Share Knowledge*. Mar. 30, 2025. URL: https://blogs.bu.edu/kinglong/fiber/fbt-vs-plc-splitters-a-comprehensive-comparison-of-fiber-optic-splitting-technologies/ (visited on 04/19/2025).

[75] *Thorlabs - TG625R5F1A 1x2 MM Dual-Window Fiber Coupler, Ø62.5 Core, 0.275 NA, 50:50 Split, FC/PC*. URL: https://www.thorlabs.com (visited on 04/19/2025).

[76] *Multimode 1X2 coupler / tap, OM1 62.5/125um fiber, 850nm, 50/50 split ratio, 1m fiber long, 3mm type, Packaging: Box 90 x 16 x 9mm*. go4fiber. URL: https://www.go4fiber.com/multimode-1x2-coupler-tap-om1-62-5-125um-fiber-850nm-50-50-split-ratio-1m-fiber-long-3mm-type-packaging-box-90-x-16-x-9mm.

[77] Nicholas E. M. Pasquini. "NRL Charters Navy's Quantum Inertial Navigation Path To Reduce Drift". In: *NRL News & Press Releases* (Apr. 2024). URL: https://www.nrl.navy.mil/Media/News/Article/3732862/nrl-charters-navys-quantum-inertial-navigation-path-to-reduce-drift/.

[78] Richard B. Thompson. "Global Positioning System: The Mathematics of GPS Receivers". en. In: *Mathematics Magazine* 71.4 (Oct. 1998), pp. 260–269. ISSN: 0025-570X, 1930-0980. DOI: 10.1080/0025570X.1998.11996650. URL: https://www.tandfonline.com/doi/full/10.1080/0025570X.1998.11996650 (visited on 01/31/2025).

[79] *What are the Different Types of Audio Amplifier Classes? — audioholics.com*. URL: https://www.audioholics.com/audio-amplifier/amplifier-classes.

[80] Michael Motola-Barnes. *Haptic Actuators: Comparing Piezo to ERM and LRA — blog.piezo.com*. URL: https://blog.piezo.com/haptic-actuators-comparing-piezo-erm-lra.

[81] Rebekka Hoffmann et al. "Measuring relative vibrotactile spatial acuity: effects of tactor type, anchor points and tactile anisotropy". en. In: *Experimental Brain Research* 236.12 (Dec. 2018), pp. 3405–3416. ISSN: 0014-4819, 1432-1106. DOI: 10.1007/s00221-018-5387-z. URL: http://link.springer.com/10.1007/s00221-018-5387-z (visited on 02/16/2025).

[82] Espressif, Inc. *ESP32-WROOM-DA Datasheet*. URL: https://www.espressif.com/sites/default/files/documentation/esp32-wroom-da_datasheet_en.pdf.

[83] Raspberry Pi Foundation. *Raspberry Pi 5 Product Brief*. Jan. 2025. URL: https://datasheets.raspberrypi.com/rpi5/raspberry-pi-5-product-brief.pdf.

[84] Xuerui Yi, Caroline Kirk, and Neil Robertson. "Nickel hydroxide-based energy storage devices: nickel-metal hydride batteries vs. nickel hydroxide hybrid supercapacitors". en. In: *Carbon Neutrality* 3.1 (Dec. 2024), p. 39. ISSN: 2788-8614, 2731-3948. DOI: 10.1007/s43979-024-00114-7. URL: https://link.springer.com/10.1007/s43979-024-00114-7 (visited on 02/16/2025).

[85] Antti Väyrynen and Justin Salminen. "Lithium ion battery production". en. In: *The Journal of Chemical Thermodynamics* 46 (Mar. 2012), pp. 80–85. ISSN: 00219614. DOI: 10.1016/j.jct.2011.09.005. URL: https://linkinghub.elsevier.com/retrieve/pii/S0021961411003090 (visited on 02/16/2025).

[86] MaxAmps. *LiPo vs Lithium Ion Batteries for Unmanned & Robotics Applications — Unmanned Systems Technology — unmannedsystemstechnology.com*. URL: https://www.unmannedsystemstechnology.com/feature/lipo-vs-lithium-ion-batteries-for-unmanned-robotics-applications/.

[87] *Top 5 Differences Between Lithium-ion And Lithium-polymer Batteries — — blog.nitecorestore.com*. URL: https://blog.nitecorestore.com/lithiumion-and-lithiumpoly-batteries.html.

[88] Bioenno Tech LLC. *Battery Life Showdown: Nickel-Metal Hydride vs. Lithium Ion vs. Lithium Iron — bioennopower.com*. URL: https://www.bioennopower.com/blogs/news/battery-life-comparison-nimh-li-ion-lifepo4.

[89] *Voltage Regulator Types and Working Principles — monolithicpower.com*. URL: https://www.monolithicpower.com/en/learning/resources/voltage-regulator-types.

[90] Rui Santos. *ESP32 Web Server – Arduino IDE*. https://randomnerdtutorials.com/esp32-web-server-arduino-ide/. Accessed: Apr. 18, 2025.

Appendix B Content Permission Requests

Figure B.1: Request for Figure - Removed due to no response

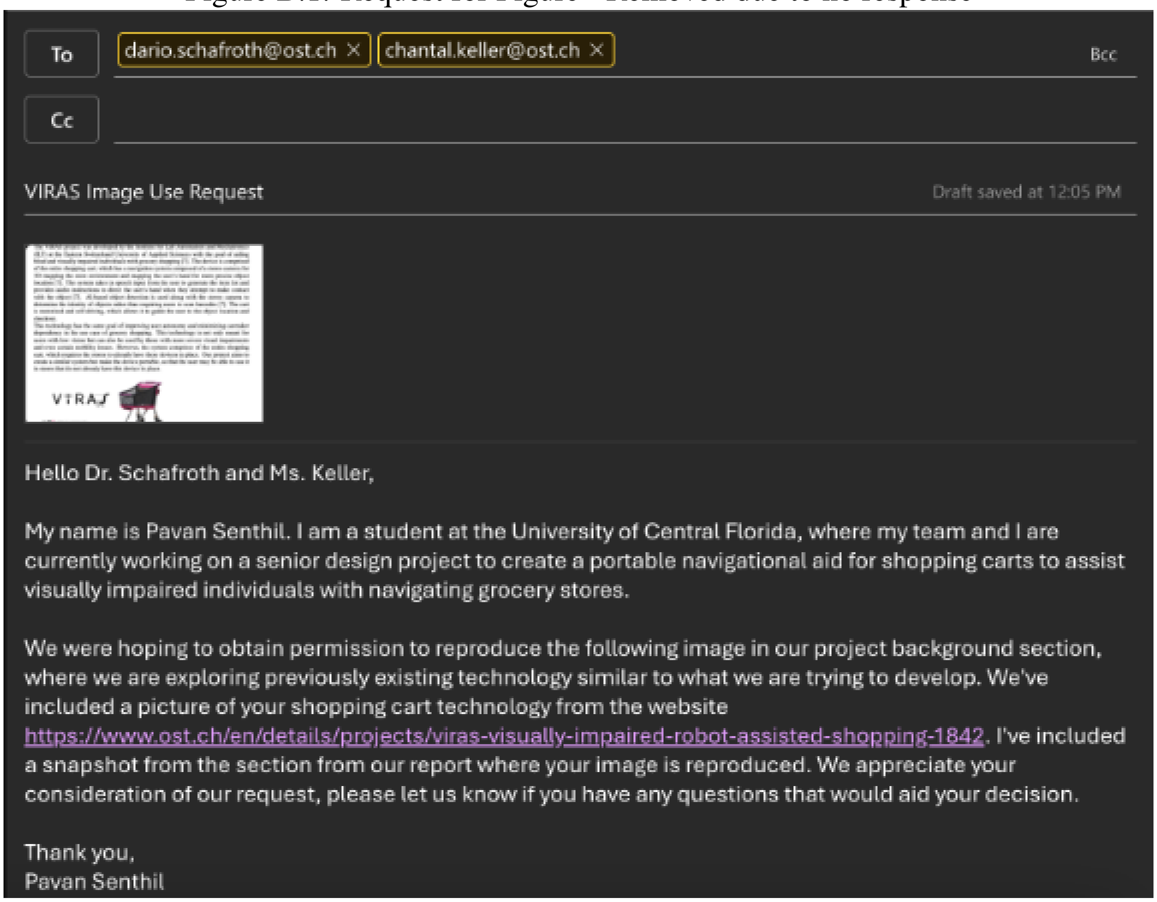

To dario.schafroth@ost.ch chantal.keller@ost.ch Bcc

Cc

VIRAS Image Use Request Draft saved at 12:05 PM

Hello Dr. Schafroth and Ms. Keller,

My name is Pavan Senthil. I am a student at the University of Central Florida, where my team and I are currently working on a senior design project to create a portable navigational aid for shopping carts to assist visually impaired individuals with navigating grocery stores.

We were hoping to obtain permission to reproduce the following image in our project background section, where we are exploring previously existing technology similar to what we are trying to develop. We've included a picture of your shopping cart technology from the website https://www.ost.ch/en/details/projects/viras-visually-impaired-robot-assisted-shopping-1842. I've included a snapshot from the section from our report where your image is reproduced. We appreciate your consideration of our request, please let us know if you have any questions that would aid your decision.

Thank you,
Pavan Senthil

Figure B.2: Request for Figure - Removed due to no response

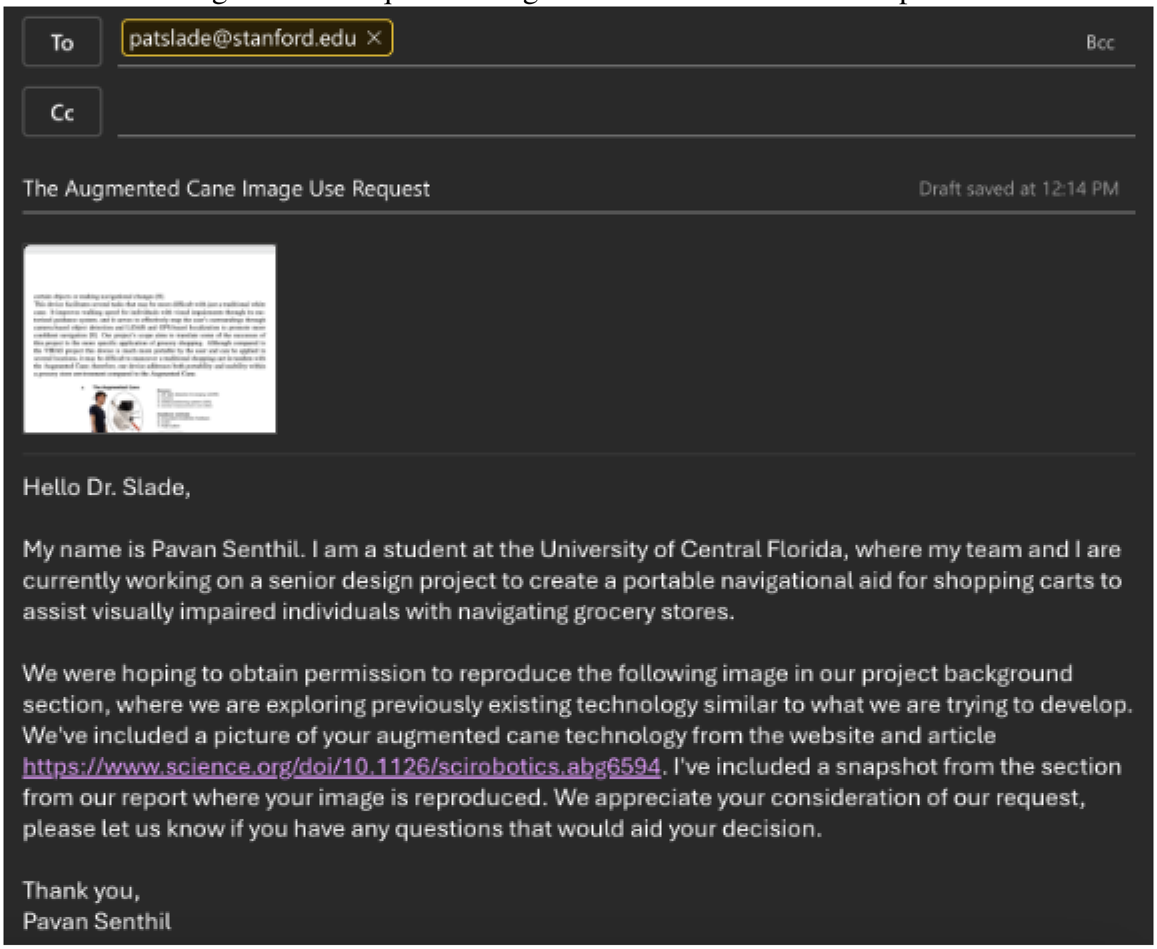

To patslade@stanford.edu

Bcc

Cc

The Augmented Cane Image Use Request

Draft saved at 12:14 PM

Hello Dr. Slade,

My name is Pavan Senthil. I am a student at the University of Central Florida, where my team and I are currently working on a senior design project to create a portable navigational aid for shopping carts to assist visually impaired individuals with navigating grocery stores.

We were hoping to obtain permission to reproduce the following image in our project background section, where we are exploring previously existing technology similar to what we are trying to develop. We've included a picture of your augmented cane technology from the website and article https://www.science.org/doi/10.1126/scirobotics.abg6594. I've included a snapshot from the section from our report where your image is reproduced. We appreciate your consideration of our request, please let us know if you have any questions that would aid your decision.

Thank you,
Pavan Senthil

Appendix C Large Language Model Prompts

Prompt 1:
What are the best topics to investigate in order to be introduced to basic controls engineering for robotics?

Response (Using ChatGPT 4o):
If you're looking for an introduction to basic controls engineering for robotics, here are some of the best topics to explore:

1. Mathematical Foundations
   - Linear Algebra - Matrices, eigenvalues/eigenvectors, and transformations.
   - Differential Equations - Essential for modeling dynamic systems.
   - Laplace Transforms - Helps analyze systems in the frequency domain.
   - Fourier Analysis - Useful for understanding signal processing in control.
2. Classical Control Theory
   - System Modeling - Representing robotic dynamics with differential equations.
   - Transfer Functions - Describes system response in the Laplace domain.
   - Stability Analysis - Bounded-input bounded-output (BIBO) stability, Routh-Hurwitz criterion.
   - Root Locus, Bode, and Nyquist Plots - Graphical methods for control system design.
3. Feedback Control
   - Proportional-Integral-Derivative (PID) Control - The most common control technique.
   - State-Space Representation - A more generalized control framework.
   - Observers (e.g., Kalman Filter, Luenberger Observer) - Estimating unobservable states.
4. Modern Control Theory
   - Pole Placement - Designing controllers via state feedback.

- Optimal Control (LQR) - Designing controllers that optimize a given cost function.
- Model Predictive Control (MPC) - Useful for advanced robotic applications.

5. Nonlinear Control
    - Lyapunov Stability Theory - Ensuring stability in nonlinear systems.
    - Feedback Linearization - Transforming nonlinear systems into linear ones.
    - Sliding Mode Control - Robust control technique for uncertain environments.
6. Robot-Specific Control Techniques
    - Inverse Kinematics and Dynamics - Controlling robotic arms and mobile robots.
    - Trajectory Generation - Planning smooth and stable paths.
    - Impedance and Admittance Control - Interaction control for force-sensitive applications.
    - Hybrid Position-Force Control - Used for manipulation tasks.
7. Learning-Based Control
    - Adaptive Control - Adjusting controllers in real time based on changes in system dynamics.
    - Reinforcement Learning for Control - Policy-based and value-based learning.
    - Neural Network-Based Control - Using deep learning for nonlinear systems.
8. Practical Implementation
    - ROS (Robot Operating System) - Hands-on implementation of control algorithms.
    - Gazebo/Simulink for Simulation - Simulating robotic dynamics and controllers.
    - Embedded Systems for Control (Arduino, Raspberry Pi, STM32, etc.) - Running real-time controllers on hardware.

Would you like recommendations for textbooks or online resources?
END PROMPT

Prompt 2:
Can you suggest some laser diode drivers for the OSRAM SPL TR85 Laser Diode? I anticipate running the diode through a pulsed current configuration, and the diode has a peak output power of 200mW and a wavelength of 850nm.

Response (Using ChatGPT 4o):

For the OSRAM SPL TR85 laser diode, which operates at 850nm with a peak output power of 200mW and a typical forward current of 225mA, you will need a pulsed laser diode driver that can provide controlled, short-duration pulses at the correct current level.
Recommended Pulsed Laser Diode Drivers

1. **Thorlabs LDP-V 1010**
   - **Current Output:** Up to 1A
   - **Pulse Width:** 1ns - 1ms
   - **Repetition Rate:** Up to 1MHz
   - **Pros:** High-speed pulsing capability, adjustable parameters
   - **Cons:** Bulkier and more expensive, lab-oriented
2. **Analog Modules 766 Series**
   - **Current Output:** 100mA - 1A
   - **Pulse Width:** Adjustable in the ns range
   - **Repetition Rate:** Up to 5MHz
   - **Pros:** High-precision pulse control, good thermal handling
   - **Cons:** Requires additional external circuitry for triggering
3. **Laser Components LDP-CW 14 100-20**
   - **Current Output:** Adjustable up to 1A
   - **Pulse Width:** Nanosecond-scale
   - **Repetition Rate:** Up to 2MHz
   - **Pros:** Compact, designed for pulsed laser diodes
   - **Cons:** Limited voltage range, requires careful thermal management
4. **IC-Haus iC-HB**
   - **Current Output:** 200mA - 2A
   - **Pulse Width:** 10ns - Continuous
   - **Repetition Rate:** Adjustable, high-speed capable
   - **Pros:** Small form factor, integrated pulse shaping
   - **Cons:** Requires additional external components for fine control

Key Considerations for Selection

- **Pulse Duration & Frequency:** Match with your application (e.g., short bursts or continuous pulsing).
- **Current Drive Capability:** Should match or exceed 225mA peak current requirement.
- **Voltage Supply Compatibility:** Ensure it operates within your system's voltage range.
- **Thermal Management:** Ensure proper heat dissipation to avoid diode damage.

Would you like help in designing a triggering circuit for the laser pulses?
END PROMPT

Prompt 3:
Imagine a laser diode of 850nm wavelength and 50mW power is shined into a DOE where light is reshaped into 60 vertical lines and 60 horizontal lines creating a grid structure that expands at a FOV of 50 degrees by 50 degrees. Calculate the total power concentrated in the eye of a person if this person is looking directly at one of these lines for 1 second. Do this for a distance between the eye and emission of 0.1m to 3m with intervals of 0.1m

Response (Using ChatGPT 4o):
To determine the total power concentrated in the eye, we need to follow these steps:

1. **Determine the Power per Line**
   - The laser power is 50 mW.
   - The DOE splits the light into 60×60 grid lines, totaling 3600 intersections.
   - Assuming uniform distribution, the power per line is:

$$P_{\text{line}} = \frac{50 \text{ mW}}{60} \approx 0.8333 \text{ mW}$$

2. **Compute the Irradiance of a Line**
   - The $50^\circ \times 50^\circ$ field of view (FOV) expands as distance increases.
   - The angular width of each line is:

$$\frac{50^\circ}{60} \approx 0.8333^\circ$$

   - At a distance d, the width of the line in meters is:

$$w_{\text{line}} = 2d \tan(0.8333^\circ/2)$$

- Assuming uniform intensity along the line, the irradiance (power per unit length) is:

$$I = \frac{P_{\text{line}}}{w_{\text{line}}}$$

3. **Determine Power Entering the Eye**

   - The human pupil diameter is typically 7 mm (0.007 m) in dark conditions.
   - If the eye collects light across this pupil diameter, the fraction of power captured is:

$$P_{\text{eye}} = I \times 0.007$$

Now, let's compute this for distances from 0.1 m to 3 m in intervals of 0.1 m.
Here are the calculated power values entering the eye for various distances:

Distance (m)	**Power in Eye (µW)**
0.1	4.01
0.2	2.01
0.3	1.34
0.4	1.00
0.5	0.80
0.6	0.67
0.7	0.57
0.8	0.50
0.9	0.45
1.0	0.40
...	...
3.0	$\sim$0.13

END PROMPT

Prompt 4:
can you find any resources on the reflectivity of 635nm light from common objects and surfaces

Response (Using ChatGPT 4o):
Yes, there are several resources detailing the reflectivity of 635nm light from various common materials. Here's a summary of key findings:

Table C.1: Reflectivity of Common Materials at 635 nm

Material	Reflectance at 635 nm	Notes
Spectralon	˜99%	Highly diffuse reflector, used as a calibration standard .
Polished Aluminum	65–87%	Reflectance varies with surface finish .
Polished Copper	70–75%	High reflectivity in the red spectrum .
Chrome (Polished)	60–70%	Reflectance depends on surface quality .
Concrete (Rough)	20–30%	Reflectance varies with texture and composition .
Red Brick	10–15%	Low reflectance due to pigmentation .
Granite	20–25%	Reflectance influenced by mineral content .
Vegetation (Crops)	15–24%	Reflectance affected by chlorophyll content .
Forests	7–14%	Dense canopy leads to lower reflectance .
Ice	32–38%	Reflectance can vary with purity and surface conditions .

Additional Resources

- **USGS Spectral Library Version 7**: Provides detailed spectral reflectance data for a wide range of materials, including minerals, soils, vegetation, and man-made substances. This resource is invaluable for obtaining precise reflectance values at specific wavelengths like 635 nm.
- **NIST Spectral Reflectance Standards**: Offers standardized measurements of spectral reflectance, which are useful for calibration and comparison purposes.

END PROMPT

Appendix D Software Code

D.1 MCU to IMU

```
#include "MPU9250.h"

MPU9250 mpu;

void setup() {
    Serial.begin(115200);
    Wire.begin();
    delay(2000);

    if (!mpu.setup(0x68)) {  // change to your own address
        while (1) {
            Serial.println("MPU connection failed. Please check
               your connection with connection_check example.");
            delay(5000);
        }
    }
}

void loop() {
    if (mpu.update()) {
        static uint32_t prev_ms = millis();
        if (millis() > prev_ms + 25) {
            print_roll_pitch_yaw();
            prev_ms = millis();
        }
    }
}

void print_roll_pitch_yaw() {
    Serial.print("Yaw, Pitch, Roll: ");
    Serial.print(mpu.getYaw(), 2);
    Serial.print(", ");
    Serial.print(mpu.getPitch(), 2);
    Serial.print(", ");
    Serial.println(mpu.getRoll(), 2);
```

```
}
```

D.2 MCU to Speaker

```
// Simple tone generator using ESP32 DAC (GPIO25) and PAM8302 amp
// Plays a series of tones with adjustable volume

const int speakerPin = 25;  // GPIO25 has DAC output
const float volume = 0.05;   // Volume control: 0.0 (mute) to 1.0 (max)

const int toneFrequencies[] = {262, 330, 392, 440, 494, 523, 587}; // C4 to D5
const int numTones = sizeof(toneFrequencies) / sizeof(toneFrequencies[0]);

void setup() {
  Serial.begin(115200);
  Serial.println("ESP32 Tone Test with Volume Control");
}

void loop() {
  for (int i = 0; i < numTones; i++) {
    playTone(toneFrequencies[i], 500);  // Play each tone for 500 ms
    delay(200);                         // Pause between tones
  }
}

// Function to play a tone using DAC sine wave approximation
void playTone(int frequency, int duration_ms) {
  const int sampleRate = 10000;         // 10kHz sample rate
  const float pi = 3.14159265;
  int samples = (sampleRate * duration_ms) / 1000;

  for (int i = 0; i < samples; i++) {
    float t = (float)i / sampleRate;
    float wave = sin(2 * pi * frequency * t);  // sine wave: -1 to 1
    uint8_t dacValue = 127 + 127 * volume * wave; // scale and offset to 0-255
    dacWrite(speakerPin, dacValue);
    delayMicroseconds(1000000 / sampleRate);
  }
}
```

D.3 MCU to Haptics

```
#include <Wire.h>
#include "Adafruit_DRV2605.h"

Adafruit_DRV2605 drv;

void setup() {
  Serial.begin(9600);
  Serial.println("Adafruit DRV2605 Basic test");
  if (! drv.begin()) {
    Serial.println("Could not find DRV2605");
    while (1) delay(10);
  }

  drv.selectLibrary(1);

  // I2C trigger by sending 'go' command
  // default, internal trigger when sending GO command
  drv.setMode(DRV2605_MODE_INTTRIG);
}

uint8_t effect = 1;

void loop() {
//  Serial.print("Effect #"); Serial.println(effect);

   if (effect == 1) {
    Serial.println("11.2 Waveform Library Effects List");
  }

  if (effect == 1) {
    Serial.println(F("1 - Strong Click - 100%"));
  }
  if (effect == 2) {
    Serial.println(F("2 - Strong Click - 60%"));
  }
  if (effect == 3) {
    Serial.println(F("3 - Strong Click - 30%"));
  }
  if (effect == 4) {
    Serial.println(F("4 - Sharp Click - 100%"));
  }
  if (effect == 5) {
    Serial.println(F("5 - Sharp Click - 60%"));
  }

```

```
  // set the effect to play
  drv.setWaveform(0, effect);  // play effect
  drv.setWaveform(1, 0);       // end waveform

  // play the effect!
  drv.go();

  // wait a bit
  delay(500);

  effect++;
  if (effect > 5) effect = 1;
}
```

D.4 MCU to SBC

```
#include <Wire.h>

#define I2C_SLAVE_ADDR 0x08  // Must match Pi code
String incomingMessage = "";
String outgoingMessage = "Hello from ESP32!";

void receiveEvent(int len) {
  incomingMessage = "";
  while (Wire.available()) {
    char c = Wire.read();
    incomingMessage += c;
  }
  Serial.print("Received from Pi: ");
  Serial.println(incomingMessage);
}

void requestEvent() {
  Wire.write((const uint8_t *)outgoingMessage.c_str(),
     outgoingMessage.length());
  Serial.println("Sent to Pi: " + outgoingMessage);
}

void setup() {
  Serial.begin(115200);
  Wire.begin(0x08);  // Set ESP32 as I2C slave at address 0x08
  Wire.onReceive(receiveEvent);
  Wire.onRequest(requestEvent);
  Serial.println("ESP32 ready as I2C slave...");
}

```

```
void loop() {
  // You can update outgoingMessage here dynamically
  delay(100);
}
```

D.5 SBC to MCU

```
import smbus2
import time

I2C_ADDR = 0x08
bus = smbus2.SMBus(1)  # I2C bus 1 on Pi

def write_to_esp32(message):
    data = [ord(c) for c in message]
    bus.write_i2c_block_data(I2C_ADDR, 0, data)
    print(f"Sent: {message}")

def read_from_esp32(length=32):
    data = bus.read_i2c_block_data(I2C_ADDR, 0, length)
    text = ''.join([chr(b) for b in data if b != 0])
    print(f"Received: {text}")

try:
    while True:
        write_to_esp32("Hello from Pi!")
        time.sleep(1)
        read_from_esp32()
        time.sleep(2)

except KeyboardInterrupt:
    print("Stopped")
```

D.6 MCU-hosted Web Server

```
/*********
  Rui Santos
  Complete project details at https://randomnerdtutorials.com
*********/

// Load Wi-Fi library
#include <WiFi.h>

// Replace with your network credentials
```

```
const char* ssid = "Pavan’s iPhone";
const char* password = "cart1234";

// Set web server port number to 80
WiFiServer server(80);

// Variable to store the HTTP request
String header;

// Auxiliar variables to store the current output state
String output26State = "off";
String output27State = "off";

// Assign output variables to GPIO pins
const int output26 = 26;
const int output27 = 27;

// Current time
unsigned long currentTime = millis();
// Previous time
unsigned long previousTime = 0;
// Define timeout time in milliseconds (example: 2000ms = 2s)
const long timeoutTime = 2000;

void setup() {
  Serial.begin(115200);
  // Initialize the output variables as outputs
  pinMode(output26, OUTPUT);
  pinMode(output27, OUTPUT);
  // Set outputs to LOW
  digitalWrite(output26, LOW);
  digitalWrite(output27, LOW);

  // Connect to Wi-Fi network with SSID and password
  Serial.print("Connecting to ");
  Serial.println(ssid);
  WiFi.begin(ssid, password);
  while (WiFi.status() != WL_CONNECTED) {
    delay(500);
    Serial.print(".");
  }
  // Print local IP address and start web server
  Serial.println("");
  Serial.println("WiFi connected.");
  Serial.println("IP address: ");
  Serial.println(WiFi.localIP());
  server.begin();
```

```
}

void loop(){
  WiFiClient client = server.available();   // Listen for incoming clients

  if (client) {                             // If a new client connects,
    currentTime = millis();
    previousTime = currentTime;
    Serial.println("New Client.");          // print a message out in the serial port
    String currentLine = "";                // make a String to hold incoming data from the client
    while (client.connected() && currentTime - previousTime <= timeoutTime) {  // loop while the client's connected
      currentTime = millis();
      if (client.available()) {             // if there's bytes to read from the client,
        char c = client.read();             // read a byte, then
        Serial.write(c);                    // print it out the serial monitor
        header += c;
        if (c == '\n') {                    // if the byte is a newline character
          // if the current line is blank, you got two newline characters in a row.
          // that's the end of the client HTTP request, so send a response:
          if (currentLine.length() == 0) {
            // HTTP headers always start with a response code (e.g. HTTP/1.1 200 OK)
            // and a content-type so the client knows what's coming, then a blank line:
            client.println("HTTP/1.1 200 OK");
            client.println("Content-type:text/html");
            client.println("Connection: close");
            client.println();

            // turns the GPIOs on and off
            if (header.indexOf("GET /26/on") >= 0) {
              Serial.println("GPIO 26 on");
              output26State = "on";
              digitalWrite(output26, HIGH);
            } else if (header.indexOf("GET /26/off") >= 0) {
              Serial.println("GPIO 26 off");
              output26State = "off";
```

```
              digitalWrite(output26, LOW);
            } else if (header.indexOf("GET /27/on") >= 0) {
              Serial.println("GPIO 27 on");
              output27State = "on";
              digitalWrite(output27, HIGH);
            } else if (header.indexOf("GET /27/off") >= 0) {
              Serial.println("GPIO 27 off");
              output27State = "off";
              digitalWrite(output27, LOW);
            }

            // Display the HTML web page
            client.println("<!DOCTYPE html><html>");
            client.println("<head><meta name=\"viewport\" content=\"width=device-width, initial-scale=1\">");
            client.println("<link rel=\"icon\" href=\"data:,\">");
            // CSS to style the on/off buttons
            // Feel free to change the background-color and font-size attributes to fit your preferences
            client.println("<style>html { font-family: Helvetica; display: inline-block; margin: 0px auto; text-align: center;}");
            client.println(".button { background-color: #4CAF50; border: none; color: white; padding: 16px 40px;");
            client.println("text-decoration: none; font-size: 30px; margin: 2px; cursor: pointer;}");
            client.println(".button2 {background-color: #555555;}</style></head>");

            // Web Page Heading
            client.println("<body><h1>ESP32 Web Server</h1>");

            // Display current state, and ON/OFF buttons for GPIO 26
            client.println("<p>GPIO 26 - State " + output26State + "</p>");
            // If the output26State is off, it displays the ON button
            if (output26State=="off") {
              client.println("<p><a href=\"/26/on\"><button class=\"button\">ON</button></a></p>");
            } else {
              client.println("<p><a href=\"/26/off\"><button class=\"button button2\">OFF</button></a></p>");
            }

```

```
            // Display current state, and ON/OFF buttons for GPIO 27
            client.println("<p>GPIO 27 - State " + output27State + "</p>");
            // If the output27State is off, it displays the ON button
            if (output27State=="off") {
              client.println("<p><a href=\"/27/on\"><button class=\"button\">ON</button></a></p>");
            } else {
              client.println("<p><a href=\"/27/off\"><button class=\"button button2\">OFF</button></a></p>");
            }
            client.println("</body></html>");

            // The HTTP response ends with another blank line
            client.println();
            // Break out of the while loop
            break;
          } else { // if you got a newline, then clear currentLine
            currentLine = "";
          }
        } else if (c != '\r') {  // if you got anything else but a carriage return character,
          currentLine += c;      // add it to the end of the currentLine
        }
      }
    }
    // Clear the header variable
    header = "";
    // Close the connection
    client.stop();
    Serial.println("Client disconnected.");
    Serial.println("");
  }
}
```